The world's largest worm lizard - a new giant trogonophid (Squamata, Amphisbaenia) with extreme dental adaptations from the Eocene of Chambi, Tunisia

Georgios L Georgalis, Krister T. Smith, Laurent Marivaux, Anthony Herrel, El Mabrouk Essid, Hayet Khayati Ammar, Wissem Marzougui, Rim Temani, Rodolphe Tabuce

Zoological Journal of the Linnean Society (https://doi.org/10.1093/zoolinnean/zlae133)

The world's largest worm lizard - a new giant trogonophid (Squamata, Amphisbaenia) with extreme dental adaptations from the Eocene of Chambi, Tunisia

Georgios L. Georgalis[1,*], Krister T. Smith[2,3], Laurent Marivaux[4], Anthony Herrel[5,6,7,8], El Mabrouk Essid[9], Hayet Khayati Ammar[9], Wissem Marzougui[9], Rim Temani[9] and Rodolphe Tabuce[4]

[1] Institute of Systematics and Evolution of Animals, Polish Academy of Sciences, Sławkowska 17, 31-016 Kraków, Poland;

[2] Department of Messel Research and Mammalogy, Senckenberg Research Institute and Natural History Museum, Senckenberganlage 25, 60325 Frankfurt am Main, Germany;

[3] Faculty of Biosciences, Goethe University, Max-von-Laue-Straße 13, 60438 Frankfurt am Main, Germany;

[4] Institut des Sciences de l'Évolution de Montpellier (ISE-M, UMR 5554, CNRS/UM/IRD/EPHE), Université de Montpellier, 34095 Montpellier Cedex 5, France;

[5] Mécanismes Adaptatifs et Evolution, UMR 7179, Muséum national d'Histoire naturelle CNRS, Paris, France;

[6] Department of Biology, Evolutionary Morphology of Vertebrates, Ghent University, Ghent, Belgium;

[7] Department of Biology, University of Antwerp, Wilrijk, Belgium;

[8] Naturhistorisches Museum Bern, Bern, Switzerland;

[9] Office National des Mines (ONM), 24 rue 8601, 2035 La Charguia, Tunis, Tunisia.

ZooBank LSID: urn:lsid:zoobank.org:pub:6DF599A3-0A7B-4A76-AA28-81147F6733FF

Running Title: New giant amphisbaenian from the Eocene of Tunisia

[*] Corresponding author. Institute of Systematics and Evolution of Animals, Polish Academy of Sciences, Sławkowska 17, 31-016 Kraków, Poland.

E-mail: georgalis@isez.pan.krakow.pl

ABSTRACT

We here describe *Terastiodontosaurus marcelosanchezi*, a new amphisbaenian genus and species from the Eocene of Chambi, Tunisia. Using micro-computed tomography (µCT), we document the peculiar anatomy of the new taxon, which is characterized by extreme dental morphology, including one massive tooth on the maxilla and dentary, flat cheek teeth, and an array of other diagnostic features that readily differentiate it from all other amphisbaenians. We also redescribe the oldest named African amphisbaenian, *Todrasaurus gheerbranti*, from the late Paleocene of Morocco, using µCT. Phylogenetic analysis recovers *Terastiodontosaurus* and *Todrasaurus* as sister-taxa and provides strong support for a sister-group relationship of those two large-toothed amphisbaenians with extant *Trogonophis*. Accordingly, *Todrasaurus* shows that the divergence of crown Trogonophidae occurred much earlier than currently thought. Our survey of µCT scans reveals that *Terastiodontosaurus*, *Todrasaurus*, and *Trogonophis* are characterized by a great enamel thickness on their teeth, a feature that is absent in other examined amphisbaenians. Size estimates show that *Terastiodontosaurus* was the largest known amphisbaenian to have ever lived, with an estimated skull length > 5 cm. Based on novel muscle data of *Trogonophis*, we estimate very high bite forces for *Terastiodontosaurus*, which would allow it to crush a wide variety of snails.

Additional keywords: new genus and species; Paleogene; North Africa; phylogenetic analysis; bite force; size; autecology.

INTRODUCTION

Amphisbaenians are a charismatic group of fossorial squamates, with bizarre morphological features and extreme anatomical modifications (Zangerl 1944, 1945, Gans 1969, 1978, Montero and Gans 1999, Kearney 2003, Gans and Montero 2008). Particularly their unique skeletal anatomy has attracted and puzzled researchers already since the 19th century (e.g., Müller 1831, Wagner 1841, Gervais 1853, Bedriaga 1884). Prior to the advent and broad acceptance of phylogenetic systematics, amphisbaenians were considered as the third major group of Squamata, together with Serpentes and the paraphyletic "Lacertilia" (Zangerl 1944, Hoffstetter 1955, 1962, Kuhn 1960, 1966, Müller 1968, Gans 1969, 1978, Estes 1983). Recent phylogenetic analyses, however, have placed them as the sister group of lacertid lizards, a topology that has been supported by both molecular and combined morphological and molecular evidence (Townsend *et al.* 2004, Vidal and Hedges 2009, Müller *et al.* 2011, Jones *et al.* 2013, Pyron *et al.* 2013, Hipsley and Müller 2014, Čerňanský *et al.* 2015a, Zheng and Wiens 2016, Pyron 2017, Streicher and Wiens 2017, Simões *et al.* 2018, Burbrink *et al.* 2020, Singhal *et al.* 2021, Tałanda *et al.* 2022, Brownstein *et al.* 2023); a name, Lacertibaenia Vidal & Hedges, 2009, was even proposed for the clade Amphisbaenia + Lacertidae.

Amphisbaenians have a relatively rich fossil record across the Cenozoic of Europe (Roček 1984, Schleich 1988, Augé and Rage 1995, Delfino 2003, Augé 2005, 2012, Blain *et al.* 2007, Blain 2009, Delfino *et al.* 2011, Folie *et al.* 2013, Bolet *et al.* 2014, Vianey-Liaud *et al.* 2014, Čerňanský *et al.* 2015a, 2015b, 2016a, 2020, Georgalis *et al.* 2016, 2018b, 2024, Ivanov *et al.* 2020, Syromyatnikova *et al.* 2021, Čerňanský 2023) and North America (Loomis 1919, Gilmore 1928, 1942, Taylor 1951, MacDonald 1970, Berman 1973, 1977, Estes 1983, Sullivan 1985, Kearney *et al.* 2005, Smith 2006, 2009, Hembree 2007, Smith and Gauthier 2013, Jiménez-Hidalgo *et al.* 2015, Longrich *et al.* 2015, Stocker and Kirk 2016), coupled with a few Neogene and Quaternary occurrences from South America (Gans and Montero 1998, Scanferla *et al.* 2006, Camolez and Zaher 2010, Brizuela and Albino 2012), a few Paleogene, Neogene, and Quaternary occurrences from Africa (Rage 1976, Charig and Gans 1990, Bailon 2000, Augé and Rage 2006, Rage *et al.* 2013, 2021, Stoetzel *et al.* 2008, Saidani *et al.* 2016, El-Hares *et al.* 2022), a very few Neogene occurrences from the Arabian Peninsula (Rage 1982, Head and Müller 2022), plus only a very few occurrences from the Neogene of southwestern Asia (Georgalis *et al.* 2018a, Syromyatnikova *et al.* 2019). In addition, the Late Cretaceous (Campanian) *Slavoia* Sulimski, 1984, from Mongolia has been re-interpreted as a stem-amphisbaenian by Tałanda (2016, 2017), and if such identification is correct, it would then push back substantially the origin of the group.

Trogonophidae is a rather distinctive group of amphisbaenians that is today distributed in northern and north-central Africa (including Socotra Island, Yemen) and the Middle East (Gans 1960, 2005). Four extant genera are currently recognized, i.e., *Agamodon* Peters, 1882, *Diplometopon* Nikolski, 1907, *Pachycalamus* Günther, 1881, and the type genus, *Trogonophis* Kaup, 1830 (Gans 1960, 2005, Gans and Montero 2008). The most distinctive feature of trogonophids is their acrodont dentition (Gans 1960, El-Assy and Al-Nassar 1976, Maisano *et al.* 2006, Gans and Montero 2008), a feature that, within squamates, is otherwise present solely in the iguanian group Acrodonta (Estes 1983, Smith 2011, 2020, Smith *et al.* 2011, Georgalis *et al.* 2023). Trogonophids possess also other unique features among amphisbaenians, including locomotion and burrowing patterns, shoulder girdle or hemipenial morphology, chromosomes, vertebral arrangement, the absence of caudal autotomy, and a triangular body in cross section (Lee 1998; Gans and Montero 2008).

Recent fieldwork in Eocene levels of the Natural Park of Djebel Chambi, Tunisia, joining French palaeontologists (*Institut des Sciences de l'Évolution de Montpellier*) and geologists (*Géosciences Montpellier*) with Tunisian geologists (*Office National des Mines*, *Tunis*), has led to the discovery of one of the oldest records of Amphisbaenia in Afro-Arabia. Specimens originate from the Chambi-1 (CBI-1) fossil-bearing locality, dating from the late early – early middle Eocene (e.g., Hartenberger *et al.* 2001, Ravel *et al.* 2016). Fossils consist of craniodental and vertebral remains whose morphology is so unusual that it has led us to describe here a new genus and species. Using micro-computed tomography (µCT), we assess microanatomical features of the dentition of the new taxon and compare them with other amphisbaenians. In addition, we conduct phylogenetic analysis in order to highlight the affinities of the new Tunisian taxon, as well as of the oldest amphisbaenian from Africa, *Todrasaurus gheerbranti* Augé & Rage, 2006, from the late Paleocene of Adrar-Mgorn 1, Morocco, which we also re-describe here using µCT imaging. With proxies such as the maxilla length and comparisons with skeletons of *Trogonophis wiegmanni* Kaup, 1830, we provide size estimates for the new taxon. Also, using novel muscle data of the extant *Trogonophis*, we conduct a bite force estimation for the new Tunisian taxon. Finally, biogeographic implications about the origins and evolution of trogonophids are proposed, as well as implications about the functional morphology of the new taxon with these unique dental adaptations.

LOCALITY

The Djebel Chambi National Park is situated in the Kasserine area, in the Central Western part of Tunisia (Fig. 1). The material of this study comes from a fossil-bearing site (Chambi locus 1: CBI-1), which consists of fluvio-lacustrine deposits situated at

the base of the continental sequence of Chambi (e.g., Ravel *et al.* 2016). These localities have yielded a diverse assemblage of aquatic and terrestrial vertebrates including fishes, amphibians, turtles, crocodiles, squamates, birds (Mourer-Chauviré *et al.* 2013, 2016) and mammals such as bats, primates, eulipotyphlans, hyaenodonts, hyracoids, an elephant shrew, a marsupial, a rodent, and a sirenian (Hartenberger 1986, Crochet 1986, Sigé 1991, Court and Hartenberger 1992, 1993, Hartenberger and Marandat 1992, Vianey-Liaud *et al.* 1994, Hartenberger *et al.* 1997, 2001 Gheerbrant and Hartenberger 1999, Tabuce *et al.* 2007, 2011, Ravel *et al.* 2011, 2012, 2015, 2016; Benoit *et al.* 2013a, 2013b, 2013c, Marivaux *et al.* 2013, 2015, Solé *et al.* 2016, Tabuce 2017). Although abundant, no remains of amphibians and reptiles from Chambi have been described to date. They were initially being studied by Jean-Claude Rage (MNHN, Paris), but unfortunately, he was unable to complete his study (Rage†, 1943–2018); amphibians were only briefly mentioned in Gardner and Rage (2016). As a first step in the publication of the diversity of the herpetofauna from Chambi, and as a continuation of Rage's preliminary work, we report here the identification of a new trogonophid amphisbaenian.

MATERIAL AND METHODS

All fossil specimens of the new taxon described herein originate from recent field campaigns in the fossil bearing locality of Chambi-1 (CBI-1). The fossil specimens were found after several rounds of acid processing and screen-washings of the indurated calcareous matrix of Chambi-1. All fossil material described herein from Chambi is curated at the collections of the *Office National des Mines* (ONM) of Tunis, Tunisia. The holotype (UM THR 407) of *Todrasaurus gheerbranti* from the late Paleocene (Thanetian) of Adrar-Mgorn 1, Morocco, is permanently curated in the collections of the *Université de Montpellier* (UM). Abundant comparative material of extant amphisbaenians was studied at the collections of ISEZ, MGPT-MDHC, MNCN, NHMC, and SMF-PH. In addition, we studied µCT scans of the extant amphisbaenians *Geocalamus acutus* Sternfeld, 1912, *Monopeltis capensis* Smith, 1848, and *Zygaspis quadrifrons* (Peters, 1862), all from the collection of one of us (A.H.), plus the following specimens from the online repository of Morphosource (https://www.morphosource.org): *Geocalamus modestus* Günther, 1880 (MCZ:Herp:R-18294 [Media 000472154; ark:/87602/m4/472154]); *Monopeltis leonhardi* Werner, 1910 (MCZ:Herp:R-150042 [Media 00472731; ark:/87602/m4/472731]); *Pachycalamus brevis* Günther, 1881 (MVZ:Herp:236445 [Media 000066461; ark:/87602/m4/M66461]); *Trogonophis wiegmanni* (FMNH 109462 [Media 000098610, ark:/87602/m4/M98610]; MVZ:Herp:250710 [Media 000070546, ark:/87602/m4/M70546]; YPM HERR 6903 [Media 000073996;

ark:/87602/m4/M73996]), and one specimen of *Amphisbaena alba* Linnaeus, 1758 (FMNH 195924), available at Digimorph (http://www.digimorph.org/).

Anatomical terminology follows Gans (1960) and Gans and Montero (2008). Taxonomy of extant trogonophids follows Gans and Montero (2008). Authorships and original spellings of taxa were also checked directly in the primary references of Linnaeus (1758), Oppel (1811), Kaup (1830), Bonaparte (1838a), Gray (1844), Smith (1848), Baird (1858), Günther (1880, 1881), Peters (1862, 1882), Boulenger (1890), Peracca (1903), Nikolski (1907), Werner (1910), Sternfeld (1912), Dickerson (1916), Loomis (1919), Gilmore (1942), MacDonald (1970), Berman (1973, 1977), Sulimski (1984), Charig and Gans (1990), Bailon (2000), Augé and Rage (2006), Vidal and Hedges (2009), Müller *et al.* (2011), and Čerňanský *et al.* (2015a).

Micro-computed tomography (µCT)

µCT scanning of several fossil specimens of the new taxon from Chambi and the holotype of *Todrasaurus gheerbranti*, was conducted using a µCT-scanning station EasyTom 150 / Rx Solutions (Montpellier RIO Imaging [MRI], ISE-M, Montpellier, France). Specimen ONM CBI-1-648 was damaged during µCT scanning and the 3D model of the mesh file appears therefore more incomplete than the photograph.

The 3D virtual restoration was performed with MorphoDig software (v. 1.5.3; Lebrun 2018), Avizo.Lite 2019.4 (Visualization Sciences Group) software, 3D Slicer (Fedorov *et al.* 2012), and VG Studio MAX (v. 2023.1). 3D model files of the fossil specimens are deposited in MorphoMuseuM (Georgalis *et al.* 2024).

Phylogenetic analysis

In order to assess the phylogenetic relationships of the Chambi taxon, we used the character-taxon matrix of Longrich *et al.* (2015). A revision of this matrix is in development, and for the present, our changes were minimal. We deleted their character 308 (geographic distribution) and made some further corrections, as detailed in the list of characters (see Supporting Information, Supplementary Text), which is otherwise taken from Longrich *et al.* (2015). Furthermore, we added three characters that we discovered during our study of Trogonophidae: #308 (hypertrophy of dentary tooth), #309 (thickness of enamel on tooth crowns), and #310 (premaxillary diastema / lateral tooth "twinning". We also excluded a substantial number of highly fragmentary taxa in order to focus on the relationships of the better-known taxa. In total, we included 38 taxa and 310 characters.

We analysed the resulting character-taxon matrix (Supporting Information, Supplementary Text) in TNT v1.5 (Goloboff *et al.* 2003, 2008, Goloboff and Catalano 2016) with a parsimony ratchet and with additive characters ordered, at first without

any topological constraints. For our main analysis, we enforced two minimal monophyletic groupings as indicated by molecular phylogenies (e.g., Longrich *et al.* 2015), i.e., Afrobaenia (of Longrich *et al.* 2015) and *Amphisbaena* + *Leposternon*, specifically letting the new Chambi taxon, *Todrasaurus gheerbranti*, *Listromycter leakeyi*, and the unnamed "Adrar-Mgorn 1 amphisbaenian" float. As these results differ from recent molecular studies with respect to higher-level relationships within Afrobaenia (Graboski *et al.* 2022), we also conducted a separate analysis with constraints compatible with said studies: (Trogonophidae (*Chirindia* clade (*Monopeltis* clade, South American Amphisbaenidae))). Other fossil amphisbaenians – members of Rhineuridae, Blanidae, Bipedidae – have not been considered to be part of Afrobaenia, so their exclusion from that clade is not of consequence. We calculated a strict consensus and assessed the level of Bremer support and of bootstrap support (BS) for clades in it using 100 replications.

Bite force estimation

A specimen of *Trogonophis wiegmanni* from the collections of MNHN (MNHN-RA-1987.1895) was used for dissection. The jaw adductors were removed sequentially and their three-dimensional coordinates of origin and insertion were recorded. Muscles were subsequently weighed using a precision balance (Mettler AE100, precision ± 0.0001 g) and fibre lengths were measured using nitric acid digestion. In brief, we submerged the muscles in a 30% aqueous nitric acid solution for 24–48 h. After digestion of the connective tissue, fibres were teased apart and the nitric acid was replaced by a 50% aqueous glycerol solution to stop further digestion. Fibres were photographed and measured using Image J (Schneider *et al.* 2012). For each muscle bundle the physiological cross-sectional area was calculated assuming a muscle density of 1.06 gcm-1 (Mendez and Keys 1960, Leonard *et al.* 2021), and used as input for a static bite force model (Herrel *et al.* 1998). Model output was validated with in vivo data recorded using a Kistler force transducer (Herrel *et al.* 1999, Baeckens *et al.* 2017). Based on the orientation of the force vectors (which were derived from the anatomical features of the fossil) and assuming isometric scaling of each muscle bundle and muscle force, we then calculated the bite force of the fossil trogonophid from Chambi using the mandible of the paratype (ONM CBI-1-646).

Nomenclatural acts

The electronic edition of this article conforms to the requirements of the amended International Code of Zoological Nomenclature (ICZN), and hence the new names contained herein are available under that Code from the electronic edition of this article. This published work and the nomenclatural acts it contains have been registered in ZooBank, the official registry of zoological nomenclature for the ICZN.

The ZooBank LSIDs (Life Science Identifiers) can be resolved and the associated information viewed through any standard web browser by appending the LSID to the prefix 'https://zoobank.org/'.

The LSID for this publication is:

urn:lsid:zoobank.org:pub:6DF599A3-0A7B-4A76-AA28-81147F6733FF

The LSID for the new genus *Terastiodontosaurus* is:

urn:lsid:zoobank.org:act:DC23B781-B109-4EFB-9C0B-DA42DC09B838

The LSID for the new species *Terastiodontosaurus marcelosanchezi* is:

urn:lsid:zoobank.org:act:881978AE-4954-4D2C-8D6E-12CD56CB4C20

Institutional abbreviations

FMNH, Herpetology collection, Field Museum of Natural History, Chicago, USA; ISE-M, *Institut des Sciences de l'Évolution de Montpellier*, France; ISEZ, Institute of Systematics and Evolution of Animals, Polish Academy of Sciences, Krakow, Poland; MCZ, Herpetology collection, Museum of Comparative Zoology, Harvard University, Cambridge, USA; MGPT-MDHC, Massimo Delfino Herpetological Collection, University of Torino, Torino, Italy; MNCN, *Museo Nacional de Ciencias Naturales*, Madrid, Spain; MNHN, *Muséum national d'Histoire naturelle*, Paris, France; MVZ, Herpetology collection, Museum of Vertebrate Zoology, University of California, Berkeley, California, USA; NHMC, Natural History Museum and University of Crete, Herakleion, Greece; NHMUK, Natural History Museum, London, United Kingdom; ONM, Palaeontological collections of the Museum of the *Office National des Mines*, Tunis, Tunisia; SMF-PH, Palaeoherpetology collection, Senckenberg Forschungsinstitut und Naturmuseum, Frankfurt am Main, Germany; UM, *Université de Montpellier*, Montpellier, France; YPM, Herpetology collection, Yale Peabody Museum of Natural History, New Haven, Connecticut, USA.

SYSTEMATIC PALAEONTOLOGY

Squamata Oppel, 1811

Amphisbaenia Gray, 1844

Trogonophidae Bonaparte, 1838a

Terastiodontosaurus Georgalis & Smith gen. nov.

Zoobank registration. urn:lsid:zoobank.org:act:DC23B781-B109-4EFB-9C0B-DA42DC09B838.

Etymology. The genus name derives from the Greek words "τεράστιος" ("*terastios*"), meaning "huge" / "enormous", "ὁδούς" (in genitive: "ὁδόντος" ["*odontos*"]), meaning "tooth", and "σαύρα" ("*saura*"), meaning "lizard". The gender of the new genus name is masculine.

Type and only known species. *Terastiodontosaurus marcelosanchezi* Georgalis & Smith gen. et sp. nov.

Diagnosis. As for the type and only known species.

Note on the proper authorship and spelling of Trogonophidae. Although authorship of Trogonophidae is generally attributed to Gray (1865) (e.g., Estes 1983, Bailon 2000, Kearney 2003), it should be noted that versions of that name had also appeared earlier. These are the Trogonophidina of Bonaparte (1838a), Trogonophina of Bonaparte (1838b, 1839, 1840a, 1840b), Trogonophidæ of Gray (1840), and Trogonophes of Fitzinger (1843). Even within the works of Gray, that author earlier misspelled this group as Trigonophes and Trigonophidae (Gray 1844), with Kuhn (1966, 1967) subsequently assigning authorship to Gray (1844). Vanzolini (1951) supposedly created Trogonophinae as a new subfamily, however, obviously this cannot be the case following the Principle of Coordination of ICZN (1999: Article 36), which dictates that "A name established for a taxon at any rank in the family group is deemed to have been simultaneously established for nominal taxa at all other ranks in the family group". These being said, it so appears that Trogonophidina of Bonaparte (1838a: 392) is the first introduction of the name, even though it was not accompanied by a diagnosis or an explicit mention of a type genus. The same applies to the second usage of the name, again by the same author and again the same year, Trogonophina of Bonaparte (1838b: 124), which also was not accompanied by a diagnosis or a type genus. The following year, Bonaparte (1839: 10) applied for the first time a (rather brief) diagnosis for Trogonophina, simply stating "*Dentes cum maxillis concreti*", but again still no explicit mention of a type genus was made; this is also exactly the case for his subsequent works (Bonaparte 1840a: 286, 1840b: 99),

where he applied the name with the same exactly diagnosis but again with no explicit type genus mention. Later on, the same author added the number of species he included in that group (i.e., one) and its geographic distribution as "Africa" (Bonaparte 1850, 1852). Duméril and Bibron (1839) used the name Trogonophides, providing also a thorough description of *Trogonophis wiegmanni*, however, it is evident in their text that this name was simply an informal plural name for the genus *Trogonophis*, for which they were also using the informal singular term "Le Trogonophide". Gray (1840: 42) was the first to explicitly mention a genus ("*Trogonophis*, Kaup") associated with his family group name Trogonophidæ, while Fitzinger (1843) was the first to explicitly mention both a genus ("*Trogonophis*. Kaup") and a species ("*Trogonoph. Wiegmanni*. Kaup") associated with his family group name Trogonophes. Nevertheless, an explicit mention of a type genus is not a formal requirement for family-group names that were established before 1999 but instead it is enough an indirect inference of the genus from the stem of the family-group name (see ICZN 1999: Article 11.7). Accordingly, authorship of Trogonophidae should be attributed to Bonaparte (1838a).

This being said and now that the proper authorship of the family-group name is clarified, a further comment on the proper spelling of the name is also required. Taking into consideration that the proper authorship of the family-group name is Bonaparte (1838a), it follows that this Trogonophidina would be transformed into Trogonophididae, a spelling that has not appeared the literature. It should be noted that some, mostly recent, authors have used the spelling Trogonophiidae (e.g., Pyron *et al.* 2013, Čerňanský *et al.* 2015a, Zheng and Wiens 2016, Burbrink *et al.* 2020). Nevertheless, the spelling that has had the most frequent appearance in the literature is Trogonophidae (e.g., Gray 1840, Cope 1887, Taylor 1951, El-Assy and Al-Nassar 1976, Gans 1978, Estes 1983, Charig and Gans 1990, Bailon 2000, Kearney 2002, 2003, Augé 2005, 2012, Vidal and Hedges 2005, Maisano *et al.* 2006, Gans and Montero 2008, Vidal *et al.* 2008a, Wiens *et al.* 2010, 2012, Longrich *et al.* 2015, Baeckens *et al.* 2017, Hawkins *et al.* 2022, Araújo Salvino *et al.* 2024, Bell *et al.* 2024). Following ICZN (1999: Article 29.5), the spelling of a family-group name that is in prevailing usage should be maintained, even if this spelling is not the original spelling and even if its derivation from the name of the type genus is not grammatically correctly formed. Accordingly, the proper spelling of this family-group name is Trogonophidae.

Terastiodontosaurus marcelosanchezi Georgalis & Smith sp. nov.

Figs 2–17, 22A; Supporting Information, Figs S1–S6

Zoobank registration. urn:lsid:zoobank.org:act:881978AE-4954-4D2C-8D6E-12CD56CB4C20.

Etymology. The species epithet is named after Prof. Marcelo Sánchez-Villagra, director of the Palaeontological Institute of the University of Zurich, as an honour for his major contributions to palaeontology, zoology, and evolutionary biology, as well as the kind friendship and his great support to the first author (G.L.G.) for many years.

Holotype. A right maxilla (ONM CBI-1-645) (Figs 2–3).

Paratype. A left dentary (ONM CBI-1-646) (Figs 4–5, 22A).

Referred specimens. Four premaxillae (ONM CBI-1-658, ONM CBI-1-672, ONM CBI-1-711, and ONM CBI-1-1021), five right maxillae (ONM CBI-1-649, ONM CBI-1-651, ONM CBI-1-654, ONM CBI-1-667, and ONM CBI-1-1017), six left maxillae (ONM CBI-1-648, ONM CBI-1-653, ONM CBI-1-1012, ONM CBI-1-1016, ONM CBI-1-1018, and ONM CBI-1-1022), one right maxilla fragment (ONM CBI-1-650), five right dentaries (ONM CBI-1-656, ONM CBI-1-660, ONM CBI-1-666, ONM CBI-1-1013, and ONM CBI-1-1020), ten left dentaries (ONM CBI-1-647, ONM CBI-1-655, ONM CBI-1-657, ONM CBI-1-659, ONM CBI-1-661, ONM CBI-1-662, ONM CBI-1-668, ONM CBI-1-670, ONM CBI-1-1014, and ONM CBI-1-1015), a fragment of the coronoid process of a left dentary (ONM CBI-1-664), and 17 tooth bearing bone fragments (ONM CBI-1-652 and ONM CBI-1-671 [16 elements]). Tentatively also: numerous presacral vertebrae (ONM CBI-1-673, ONM CBI-1-682, ONM CBI-1-685, ONM CBI-1-687, ONM CBI-1-691 [“lot / batch” with numerous vertebrae], ONM CBI-1-706 [“lot / batch” with numerous vertebrae], ONM CBI-1-820, ONM CBI-1-833, ONM CBI-1-860) and two caudal vertebrae (ONM CBI-1-686 and ONM CBI-1-689).

Diagnosis. *Terastiodontosaurus marcelosanchezi* gen. et sp. nov. can be referred to Amphisbaenia based on the prominent and enlarged median premaxillary tooth, the large anterior premaxillary foramina, the low tooth count on maxilla and dentary, the ventral extension of the mandibular symphysis below Meckel’s groove, the broad insertion fossa for mandibular adductor muscles on the posterolateral surface of the dentary, and the strong and elevated coronoid process of the dentary. *Terastiodontosaurus marcelosanchezi* gen. et sp. nov. can be referred to Trogonophidae based on the presence of acrodont dentition, closely appressed (“fused”) teeth, the interdigitating suture between the frontal and the facial process of the maxilla, and ectopterygoid abutting the posteromedial corner of the maxilla.

Terastiodontosaurus marcelosanchezi gen. et sp. nov. is united with *Trogonophis wiegmanni* by: thick enamel on marginal teeth, and “twinning” of paired premaxillary teeth, with median tooth separated by a diastema from paired teeth. *Terastiodontosaurus marcelosanchezi* is united with *Todrasaurus gheerbranti* by: thick enamel on marginal teeth, extremely enlarged (> 60% longer than adjacent teeth) dentary tooth 3–4 positions from the rear, and small “hills” on posterior dentary teeth. *Terastiodontosaurus marcelosanchezi* gen. et sp. nov. can be differentiated from all other amphisbaenians by the combination of the following features: very

large size (with maximum known maxilla length exceeding 16 mm and maximum dentary length of 17 mm), the flat apical surface of the cheek teeth, the position of the largest tooth on the maxilla, the number of maxillary teeth (usually three maxillary teeth), the ratio of the largest maxillary tooth length to the total maxillary tooth row length (between 0.5 and 0.7), and the position of the largest tooth on the dentary (fourth from posterior).

Type locality and horizon. Chambi 1 (CBI-1), Djebel Chambi, Kassérine region, western part of Central Tunisia, Tunisia; late early to early middle Eocene (late Ypresian to early Lutetian).

Geographical and stratigraphical range. Taxon known exclusively from its type locality.

Nomenclatural remark on the new taxon. The authorship of this new genus and species should be referred to as *Terastiodontosaurus* Georgalis & Smith gen. nov. (for the new genus) and *Terastiodontosaurus marcelosanchezi* Georgalis & Smith gen. et sp. nov. (for the new species), following the Article 50.1 and the "recommendation 50A concerning multiple authors" of the International Code of Zoological Nomenclature (ICZN 1999).

DESCRIPTION

Holotype

Figs 2–3

The holotype right maxilla (ONM CBI-1-645) is almost complete (Figs 2–3). The premaxillary process curves up anterodorsally, forming part of the medial border of the external naris. The sharp rim weakens anteriorly, and the anterior portion of the process as a whole slopes ventrolaterally. The dorsal surface is slightly striated, probably where it was overlapped by the septomaxilla. The ventral surface of the premaxillary process curves upward and is more coarsely striated where it overlaps the premaxilla. The superior alveolar canal opens anteriorly through two foramina: a dorsally directed foramen on the medial side of the facial process, and an anteriorly directed foramen just anterior to the facial process; between them the canal is roofed, but there appears to be a narrow groove, as if two growing folds of perichondral bone met over a channel but did not fully fuse. Anterior to the anterior opening of the superior alveolar canal the dorsal surface of the premaxillary process is coarsely striated; here it was probably overlain by the septomaxilla, into which the neurovascular structure(s) of the superior alveolar nerve continued. It is unclear whether the division of the anterior opening of the superior alveolar canal marks a

separation of the course of the subnarial artery and superior alveolar nerve, as in Iguanidae (Oelrich 1956, Smith 2009).

On the medial side of the premaxillary process is a strong, dorsomedially facing facet for the vomer. Behind this the palatal shelf is restricted and its dorsal surface hollows out, where Jacobson's organ sat; together with the vomer here the maxilla formed the fenestra vomeronasalis externa. Posterior to the cavity for Jacobson's organ the maxilla possesses a distinct medial process that contacts the horizontal wing of the vomer. The process continues laterally across the palatal shelf and extends posterodorsally as a weak ridge on the medial surface of the facial process of the maxilla. In other squamates, Smith and Gauthier (2013) identified this as the "nasolacrimal ridge" after ascertaining a relationship with the lacrimal duct. Behind this process the palatal shelf is medially extensive. A distinct palatine process is absent, but an extensive, striated facet for the palatine articulation is present. The (posterior) superior alveolar foramen opens at the level of the anterior end of the palatine facet. A distinct facet for the ectopterygoid cannot be discerned, but it must have been an abutting one, and it may be confluent with the palatine facet.

The posterior process of the maxilla is broad and flares sharply outwards (or laterad *fide* Gans and Montero 2008). Although striated surfaces of this maxilla commonly show tiny holes, the entire posterior surface of the posterior process is heavily porous as well as coarsely striated. Dorsally, the posterior process is thick and also coarse longitudinal striation; there is no evidence that a distinct element articulated on this suborbital part of the maxilla.

The facial process is thick. A rough facet for the nasal bone is found on the anterior margin of the facial process and turns posterodorsally as it ascends the process. There is a distinct change in angulation below the peak of the facial process, and the facet behind it – now more on the medial than the anterior surface of the facial process – is smoother; probably the change marks the boundary between the nasal and part of the frontal facet. Immediately behind its apex the facial process is deeply notched, almost certainly to receive a tongue-like process of the frontal bone. Additionally, there is a number of rough, anteroventrally trending ridges and grooves posterior to the frontal notch, which possibly indicate a more extensive overlap of the maxilla on the prefrontal (like in lizards) than is observed today in *Trogonophis wiegmanni*.

The lateral surface of the maxilla is porous and weakly rugose in its dorsal part, with some longitudinal grooves and ridges on the posterior process. There are three distinct labial foramina, all of them more or less above the level of the largest tooth. The two anterior ones are more closely spaced, while there is a considerable distance between the middle and posterior one, the latter being also the largest. These foramina communicate internally, as expected, with the superior alveolar canal, which runs longitudinally through the maxilla just above the tooth row. It conveys the

superior alveolar nerve, which passes from the orbit into the maxillary canal through the superior alveolar foramen, as well as the maxillary artery (Oelrich 1956).

The dentition is acrodont. The maxilla possesses only three teeth, of which the second is by far the largest (some 75% longer than the next-largest tooth) and in fact covers much of the ventral portion of the bone; this tooth is followed in size by the anteriormost tooth, while the posteriormost tooth is considerably tiny. The teeth are closely appressed, with no interdental gaps between them. All three teeth are much flattened, particularly the two largest ones: their dorsoventral height is extremely low. Moreover, µCT scan reveals that the enamel is extremely thick (Supporting Information, Fig. S1A). Several nutritive foramina are present at the base of the teeth.

Paratype

Figs 4–5

The paratype left dentary (ONM CBI-1-646) is relatively complete (Figs 4–5). It is referred to the same species on the basis of co-occurrence as well as the following derived morphological features: great enamel thickness, reduced tooth-row length and tooth count, presence of a greatly enlarged tooth, the "hill" on the small, posteriormost teeth, and the apically flat teeth in the middle.

The symphysis is broad and is anterodorsally inclined. As in other amphisbaenians (Longrich *et al.* 2015) it is not restricted to the area above the Meckelian groove but rather curves anteroventrally around it and terminates posteroventrally in a sharp corner. It appears as though the Meckelian groove is closed and fused immediately behind the symphysis and that the Meckelian cartilage itself might be ossified as an anterodorsally-posteroventrally extensive wedge in the centre of the symphysis, but this interpretation is not fully clear.

Meckel's groove is open (Figs 4, 5B–C). Above it is the indistinct supra-Meckelian lip (of Bhullar and Smith 2008), above which is the subdental shelf (Rage and Augé 2010) that extends medial to the tooth row. The subdental shelf commences below the posterior portion of the first tooth. It is narrow anteriorly and becomes gradually wider in the posterior half of the dentary, and behind the tooth row it grades into the coronoid process. The part of the groove in which Meckel's cartilage was situated is relatively narrow throughout most of its length, but it widens a bit posteriorly just in front of the mandibular foramen. That groove is straight for most of its length but turns up strongly near the symphysis, giving it a hockey-stick shape, as in other amphisbaenians (Longrich *et al.* 2015). Posteriorly in the dentary there are two strong, elongate facets below the groove for Meckel's cartilage, for the angular and the splenial. The presence of two distinct facets strongly suggests that those mandibular elements were discrete, not fused, as in *Trogonophis wiegmanni*, where only one facet is present; of course, without the remainder of the mandible this

cannot be taken as certain. The angular facet extends as far anteriorly as the anterior end of the enlarged tooth (fourth from the back), whereas the splenial facet only just passes the posterior end of the enlarged tooth. The ventral margin of the dentary behind the symphysis is straight.

The dentary possesses a posterodorsally ascending coronoid process just behind the posteriormost tooth. The dorsal tip of the process is incomplete but even the preserved portion extends high above the tooth row, as in other amphisbaenians. The process is prominent and thick. There is a strong diagonal ridge on its lateral surface that delineates the adductor fossa dorsally. The ridge is narrower at its base but grows thick and porous as it curves dorsally and then diminishes; it may have served as an attachment site for other jaw adductors, probably via a bodenaponeurosis.

The mandibular canal runs across the length of the dentary, transmitting the inferior alveolar nerve and mandibular artery; it communicates with the labial foramina present in the labial surface of the dentary and also with the nutritive foramina at the bases of the teeth. Its entrance is the mandibular foramen, which is located well behind the tooth-row at the level of the anterior edge of the coronoid process. In labial view (Figs 4A, 5A), four labial foramina are present in the anterior half of the dentary.

The dentary bears eight acrodont teeth, of which the largest is the fourth from posterior. The posteriormost tooth is the smallest one. The first two teeth are bulbous, and the anteriormost tooth is procumbent, extending beyond the anterior margin of the symphysis. Like in the holotype maxilla described above, the teeth are closely appressed, with almost no interdental gaps between them (at maximum only tiny empty spaces between some but not all teeth). All teeth except for the first two are much flattened (particularly the two largest ones), with the exception of the two anteriormost ones, which are bulbous and tall. The posterior teeth have tiny central cusps. Multiple nutritive foramina are situated above the subdental shelf ventrally to the each of the tooth bases.

Referred specimens

Premaxillae (Figs 6–8)

The most complete premaxillae are ONM CBI-1-672 and ONM CBI-1-711, which include a large portion of the nasal process, whereas this structure is mostly broken in ONM CBI-1-658 and ONM CBI-1-1021 (Figs 6–8; Supporting Information, Fig. S2). The nasal process is large, dorsoventrally elongated and moderately wide; it gradually narrows in width apically. Given its preserved extent, it is likely that the nasal process reached the frontals, a condition unique to Trogonophidae among amphisbaenians (Kearney 2003), but more complete specimens are needed to verify this. A pair of large anterior premaxillary foramina is developed at the base of the nasal process.

These are the anterior openings for the ethmoidal nerve that enters the premaxilla through the posterior premaxillary foramina on the posterior side of the nasal process. No rostral process or rostral blade is present. The palatal shelf or alveolar plate is most complete in ONM CBI-1-672 (Figs 7C–D, 8P–R), but it is ONM CBI-1-658 (Figs 6F–G, 8J–L) that most clearly shows it to be bipartite.

The dentition is acrodont. On the alveolar plate, there are five teeth, all of bulbous morphology. The central median tooth is the most robust and prominent (a synapomorphy of amphisbaenians; see Gans 1978, Smith 2009). µCT scans reveal that the median tooth possesses great apical enamel thickness (Supporting Information, Fig. S1C). There is a diastema between the median tooth and the lateral ones that contrasts strongly with the otherwise close appression of the teeth generally and gives the impression of the lateral two teeth being "twinned." In fact, in the two pairs of lateral teeth, the dental gaps between the teeth are almost absent. A slight vertical striation is observable on all teeth, being more distinct in the central tooth.

Maxillae (Figs 9–12)

The available maxillae pertain to different-sized individuals, as it can be attested by the drastic size range between the smallest and the largest specimens (see Supporting Information, Figs S3–S4). The most complete maxillae are the holotype (ONM CBI-1-645), and the specimens ONM CBI-1-649 (Figs 9E–F, 11J–Q) and ONM CBI-1-654 (Fig. 11A–I), which are both significantly smaller. In fact, the holotype ONM CBI-1-645 (Figs 2–3) represents the largest known individual of *Terastiodontosaurus marcelosanchezi* gen. et sp. nov., whereas ONM CBI-1-649 represents one of the smallest among our sample. Nevertheless, the morphology of the maxillae is overall very similar. Here we focus on comparisons.

The anterodorsally trending premaxillary process is best preserved or complete in ONM CBI-1-654 (Fig. 11A–I), ONM CBI-1-649 (Figs 9E–F, 11J–Q), the holotype ONM CBI-1-645 (Figs 2–3), as well as in the fragmentary specimens ONM CBI-1-1012 (Fig. 12G–I), ONM CBI-1-1016 (Fig. 12J–L), ONM CBI-1-1018 (Fig. 12M–O), and ONM CBI-1-1022 (Fig. 12P–R). The outwardly flaring posterior process of the maxilla is most complete in ONM CBI-1-654 (Fig. 11A–I), followed in completeness by the holotype ONM CBI-1-645 (Figs 2–3), ONM CBI-1-649 (Figs 9E–F, 11J–Q), ONM CBI-1-651 (Fig. 10E–J), ONM CBI-1-653 (Fig. 11R–U), ONM CBI-1-667 (Fig. 12A–C), and ONM CBI-1-1017 (Fig. 12D–F). A medial process that contacts the horizontal wing of the vomer is clearest in the holotype (ONM CBI-1-645) and, especially in ONM CBI-1-648 (Figs 9B–C, 10B–C) and ONM CBI-1-649 (Figs 9E–F, 11K–Q). The porosity and ridge like form of the labial surface, observed in the holotype ONM CBI-1-645 (Figs 2A, 3A, 3F), is otherwise only evident in the second largest specimen (ONM CBI-1-651; Fig. 10E), and

is absent in all other smaller specimens, in which this surface is almost completely smooth. This suggests that this feature is subject to size / ontogenetic variation.

Labial foramina are three, placed almost in a row, in the holotype ONM CBI-1-645 (Figs 2A, 3A) and in ONM CBI-1-649 (Figs 9G, 11J); in both these specimens, the two anterior foramina are more closely spaced. ONM CBI-1-648 also has three labial foramina (Fig. 9A), but the posterior two foramina are more closely spaced. In ONM CBI-1-649, there is also a further foramen situated dorsal to the row of the three foramina, situated approximately above the first foramen. Even more, in ONM CBI-1-654, there are two small foramina above the two of three foramina (Fig. 11A). The number of foramina cannot be fully assessed in the remaining incomplete maxillae. The superior alveolar foramen is usually relatively large.

Similar to the holotype (ONM CBI-1-645), maxillae almost always bear three teeth, of which the second is by far the largest and in fact covers much of the ventral portion of the bone; this tooth is followed in size by the anteriormost tooth, while the posteriormost tooth is tiny. However, there are two notable exceptions, denoting some degree of variability: in ONM CBI-1-651, there is a fourth tiny tooth located posteromedially to the third tooth, not in line with it (Fig. 10F), while in ONM CBI-1-649, the tiniest tooth is absent so that specimen bears only two teeth (Figs 9G, 11M–O). A further, interesting variation occurs also in the right maxilla fragment ONM CBI-1-650, where the anterior (smaller) preserved tooth is quite different from the same tooth in other specimens, being extremely narrow (Figs 9D, 10K–M). We tentatively attribute this variation as being intraspecific (or even ontogenetic). This could be indeed the case, taking into consideration that especially if the more anterior teeth are being “de-emphasized” in favour of the huge tooth (which serves as the prey “cracker”), and thus the anterior teeth perhaps become more of a remnant / vestige, then one would expect a greater variation. Moreover, again in the same specimen, there seems to be a considerable gap between the two preserved teeth (Figs 9D, 10K–M); this is unusual, because in most remaining maxillae and dentaries, the teeth are closely appressed, with no interdental gaps between them (but in ONM CBI-1-653 the third tooth is somewhat more widely separated; Fig. 11T).

Notably also, in some cases, there is a distinct “hill” forming onto the smallest tooth or teeth. This is the case with ONM CBI-1-651 (where the “hill” is prominent in both the small third and fourth teeth; Fig. 10E, I–J), as well as in ONM CBI-1-653 (Fig. 11S–U).

Several nutritive foramina are always present at the base of the teeth in all specimens, in the remnants of the subdental gutter, however, their number and size is variable. Usually, these foramina are mostly at the medial side of the maxilla, however, there is also some variation: in ONM CBI-1-650, they are equally present in both labial and medial aspects of the bone (Figs 9D, 10K–L).

In order to facilitate quantitative investigation, we introduce the ratio of largest tooth length on the maxilla to total tooth row length of the maxilla. This was complete only in two specimens:

Holotype, ONM CBI-1-645: largest tooth length, 4.9 mm / total tooth row length, 9.5 mm; ratio, 0.52.

ONM CBI-1-649: largest tooth length, 2.6 / total tooth row length, 3.7 / ratio, 0.70.

ONM CBI-1-651: largest tooth length, 3.7 / total tooth row length, 7.3 / ratio, 0.51.

ONM CBI-1-654: largest tooth length, 2.3 / total tooth row length, 4.1 / ratio, 0.56.

Besides, some information on this ratio can be tentatively also gleaned from some incomplete maxillae:

ONM CBI-1-650: largest tooth length, 4.8 / preserved tooth row length (incomplete), 7.8; estimated ratio, < 0.62.

ONM CBI-1-648: largest tooth length, 3.2 / preserved tooth row length (incomplete), 5.6; estimated ratio, < 0.57.

Dentaries (Figs 13–16)

Apart from the paratype dentary ONM CBI-1-646, all remaining dentaries are rather incomplete. The available sample denotes a range of sizes, but substantially less disparate than the maxillary sample (cf. Supporting Information, Figs S3–S6). The paratype ONM CBI-1-646 represents one of the largest individuals, with the fragmentary dentary ONM CBI-1-659 pertaining to a more or less similar size. All dentaries closely approach in overall morphology the paratype ONM CBI-1-646 described above. Some specimens are nevertheless highly incomplete, sometimes preserving only the anterior portion of the dentary (e.g., ONM CBI-1-1014, ONM CBI-1-1015, ONM CBI-1-1020), while ONM CBI-1-664 is just a fragment of the coronoid process of a left dentary.

The tooth row is complete only in the paratype ONM CBI-1-646, where it comprises eight acrodont teeth, the largest being the fourth one (counting from posteriorly). Otherwise, the tooth row is almost complete in ONM CBI-1-657 (Figs 14A, 15A–C), which preserves all but the seventh tooth (counting from posteriorly). In that specimen, also the fourth tooth is the largest one and the posteriormost tooth is the tiniest one (both counting from posteriorly). One important difference in ONM CBI-1-657 is that there appears to be a dental gap between the anteriormost tooth and the succeeding tooth position (we cannot though be certain that this is not an artefact). Otherwise, in all specimens, all teeth are almost adjoined, with almost no interdental gaps between them (at maximum only tiny empty spaces between some, but not all teeth, do exist). Like in the paratype ONM CBI-1-646, also in ONM CBI-1-

647, ONM CBI-1-655, ONM CBI-1-657, ONM CBI-1-662, ONM CBI-1-666, ONM CBI-1-1014, ONM CBI-1-1015, and ONM CBI-1-1020, the anteriormost tooth is more bulbous and dorsoventrally high and projects beyond the anterior surface of the symphysis. This is also the case for the second anteriormost tooth in the paratype ONM CBI-1-646, as well as in ONM CBI-1-647, ONM CBI-1-655, ONM CBI-1-662, ONM CBI-1-666, ONM CBI-1-1014, ONM CBI-1-1015, and ONM CBI-1-1020, which is also relatively bulbous and dorsoventrally tall. In dentary ONM CBI-1-670, the teeth are not that flattened but apparently represent the anterior teeth (2^{nd}, 3^{rd}, or 4^{th} [counting from anteriorly]), near the symphysis.

Like in the maxillae, there is a distinct "hill" on the tiny teeth (e.g., ONM CBI-1-646, ONM CBI-1-657). Great enamel thickness is also found on the dentary teeth.

Nutritive foramina are opened at the base of various teeth above the subdental shelf in all dentaries; their number is not consistent and it can vary between tooth positions and individuals at the same position. In ONM CBI-1-657, these are poorly developed.

The Meckel's groove is open in all specimens where this can be studied, most notably ONM CBI-1-660. Due to their incompleteness, besides the paratype dentary ONM CBI-1-646, which bears four, the exact number of labial foramina cannot be assessed in the remaining dentaries. Interestingly though, ONM CBI-1-659 is pierced by several (at least nine) tiny foramina in its labial surface, most of which are closely spaced.

As in the case of the maxillae above, in order to facilitate further quantitative investigation, we introduce the ratio of largest dentary tooth length to the total tooth row length of the maxilla. This was complete only in two specimens:

Paratype ONM CBI-1-646: largest tooth length, 2.8 mm / total tooth row length, 11.9 mm; ratio, 0.24.

ONM CBI-1-657: largest tooth length, 1.6 mm / total tooth row length, 6.4 mm; ratio, 0.25.

Besides these specimens for which ratios could be calculated, the following dentaries provide data on the length of the largest tooth in further specimens:

ONM CBI-1-647: largest tooth length, 2.9 mm.

ONM CBI-1-659: largest tooth length, 2.3 mm.

ONM CBI-1-655: largest tooth length, 1.9 mm.

ONM CBI-1-656: largest tooth length, 1.5 mm.

Vertebrae (Fig. 17)

Vertebrae are tentatively referred to the same taxon on the basis of co-occurrence and the fact that large numbers of jaws have only yielded a single species of amphisbaenian thus far from the locality.

Presacral vertebrae range in size between around 1 and 5 mm (Fig. 17A–U). They are procoelous and dorsoventrally compressed. In anterior view, the prezygapophyses are strongly inclined, much exceeding in height the anterodorsal edge of the neural canal. There is no zygosphene. The cotyle is elliptical and strongly depressed. In posterior view, the condyle is also elliptical and strongly depressed. The neural arch is depressed. The lateral walls of the neural arch form moderately robust centropostzygapophyseal laminae (sensu Georgalis *et al.* 2018b). There is no zygantrum. In dorsal view, the prezygapophyses extend anterolaterally. The prezygapophyseal articular facets are large and broad; in some specimens, there are prominent prezygapophyseal accessory processed. There is no neural spine. The interzygapophyseal constriction is deep. There is practically no posterior median notch of the neural arch. In ventral view, the centrum is flattened, with only slightly concave lateral margins. Two usually large, occasionally asymmetrical subcentral foramina are present, one at each lateral side of the ventral surface of the centrum. The synapophyses are robust and more or less rounded. In lateral view, the neural arch rises distinctly, with a gentle curve towards its posterior end. Each prezygapophysis is connected to the related postzygapophysis by a relatively low interzygapophyseal ridge.

Caudal vertebrae have haemapophyses fused to the centrum. A short anterior caudal vertebra has forked lymphapophyses (Fig. 17V–W), whereas more elongate posterior caudal vertebrae have unitary pleurapophyses (Fig. 17X–Y). If the number of caudal to presacral vertebrae can be determined, the methodology of Smith (2013) might be used to estimate the proportion of caudal vertebrae and so to constrain the relative length of the tail.

RESULTS OF THE PHYLOGENETIC ANALYSIS

Our main analysis used only two topological constraints: Afrobaenia and South American Amphisbaenidae. Fully consistent with all recent phylogenetic analyses (e.g., Kearney 2003, Müller *et al.* 2011, Gauthier *et al.* 2012, Jones *et al.* 2013, Čerňanský *et al.* 2015a, Longrich *et al.* 2015, Zheng and Wiens 2016, Streicher and Wiens 2017, Simões *et al.* 2018, Burbrink *et al.* 2020, Singhal *et al.* 2021, Tałanda *et al.* 2022, Brownstein *et al.* 2023, Čerňanský and Vasilyan 2024), our analysis finds strong support for amphisbaenian monophyly (Fig. 18). The position of *Cryptolacerta*

hassiaca Müller, Hipsley, Head, Kardjilov, Hilger, Wuttke & Reisz, 2011, from the early to middle Eocene of Messel, Germany, originally described as a link between lacertids and amphisbaenians by Müller *et al.* (2011), is unresolved (but see also Longrich *et al.* 2015, Brownstein *et al.* 2022, Čerňanský and Vasilyan 2024). In general, higher-level relationships within Amphisbaenia are poorly supported, but our analysis shares the basal position of Rhineuridae with Gauthier *et al.* (2012), which was the first purely morphological analysis to recover this topology. A surprise was the close relationship between the unnamed amphisbaenian from Adrar-Mgorn 1 of Augé and Rage (2006) to Blanidae, although with poor support (BS < 0.50); furthermore, if all higher-level relationships within Afrobaenia (e.g., Graboski *et al.* 2022) are enforced, its position becomes unresolved. This unnamed pleurodont form represents the second amphisbaenian from the locality of Adrar-Mgorn 1 in Morocco (the other being *Todrasaurus gheerbranti*), and was originally described by Augé and Rage (2006) as bearing some resemblance to both blanids and amphisbaenids, while the phylogenetic analysis of Longrich *et al.* (2015) recovered it as an Amphisbaenia incertae sedis. The cadeid *Cadea palirostrata* Dickerson, 1916, was assessed with relatively strong support as the sister-taxon of Afrobaenia, i.e., the group encompassing Cadeidae, Trogonophidae, and Amphisbaenidae (BS = 0.80). *Terastiodontosaurus marcelosanchezi* gen. et sp. nov. was inferred with moderate support (BS = 0.65, 1 unambiguous character state change, Bremer support 1; Table 1) to be the sister-taxon of *Todrasaurus gheerbranti*, and the two together were inferred with strong support to be the sister-taxon of *Trogonophis wiegmanni* (BS = 0.95, 5 unambiguous character state changes, Bremer support 3), a novel result. The herein novel topology of *Todrasaurus* differs from that of Longrich *et al.* (2015), who had tentatively recovered this Moroccan taxon on the stem of Afrobaenia (Longrich *et al.* 2015). Moreover, Trogonophidae (comprising *Trogonophis* and its stem plus *Diplometopon zarudnyi* Nikolskyi, 1907) was inferred to be monophyletic with strong support (BS = 0.96, 26 unambiguous character state changes, Bremer support 5). Enforcing all major topological constraints within Afrobaenia (*fide* Graboski *et al.* 2022) did not affect the relationships within Trogonophidae (including fossil taxa) or its basal position in Afrobaenia.

DISCUSSION

Taxonomic identification and comparisons

The new fossil cranial material from the late early – early middle Eocene of Chambi is characterized by an array of anatomical features (i.e., a heavy premaxilla with prominent facial processes and a median azygous tooth that is most robust and prominent, the presence of large anterior premaxillary foramina, the low tooth count

on maxilla and dentary, the interdigitating maxilla-frontal suture, the broad insertion area for mandibular adductors on the posterolateral surface of the dentary, the strong coronoid process of the dentary, the elongated nasal process of the premaxilla, and the acrodont dentition) that allow referral to Amphisbaenia, and more specifically suggest an affinity with Trogonophidae (Gans 1960, Charig and Gans 1990, Kearney 2003, Augé and Rage 2006, Gans and Montero 2008). All preserved cranial material from Chambi corresponds to the so called "snout segment" of the amphisbaenian skull (*sensu* Gans and Montero 2008) and the mandibles, although the abundance of the material suggests that other elements might be discovered – in any case, such "snout segment" elements, together with frontals, generally appear to be the most common cranial remains in the amphisbaenian fossil record (Estes 1983, Augé 2012).

Terastiodontosaurus marcelosanchezi gen. et sp. nov. bears some certain degree of resemblance with extinct and extant trogonophids, but on the other hand, possesses also some highly distinctive features that can readily differentiate it from all other amphisbaenians.

More specifically, *Terastiodontosaurus marcelosanchezi* gen. et sp. nov. is very distinct from the older *Todrasaurus gheerbranti*, known exclusively from its holotype left dentary (UM THR 407) from the late Paleocene (Thanetian) of Adrar-Mgorn 1, Morocco. We here provide, for the first time, photographs and µCT 3D images of the holotype of *Todrasaurus* (Figs 19–21), in order to further investigate its anatomy and demonstrate with clarity these differences from *Terastiodontosaurus* gen. nov. These substantial differences among the Moroccan and the new Tunisian taxon include the shape of teeth in the two taxa (all teeth much taller and amblyodont in *Todrasaurus*), the type of tooth implantation (fully acrodont in *Terastiodontosaurus* vs. more pleurodont in *Todrasaurus*), the number of dentary teeth (8 in *Terastiodontosaurus* vs. probably fewer in *Todrasaurus* [4 preserved in its holotype but there might have been more in life]), shape of subdental shelf (highly concave in *Todrasaurus*), the position of the enlarged tooth on the dentary (the 4th position counting from posteriorly in *Terastiodontosaurus* vs. the 3rd position counting from posteriorly in *Todrasaurus*), and the overall size (with *Terastiodontosaurus* being much larger).

It is further worth noting that in the original establishment and description of *Todrasaurus gheerbranti*, Augé and Rage (2006) claimed that this taxon possessed also a splenial, a feature that they considered as distinctive, stating that this structure is otherwise present in amphisbaenians solely in the North American Rhineuridae (Kearney *et al.* 2005; but see Gans and Montero 2008, who claim that a splenial is absent also in Rhineuridae); in any case, a splenial has been described also in other amphisbaenians, such as the extinct *Cuvieribaena* Čerňanský, Augé & Rage, 2015a from the Eocene of France (Čerňanský *et al.* 2015a) and occasionally in the extant *Blanus* Wagler, 1830 (e.g., Blain *et al.* 2007, Villa *et al.* 2019, Čerňanský 2023). However, the splenial is not clearly discernible in the original drawing of the holotype

of *Todrasaurus gheerbranti* in Augé and Rage (2006: fig. 2) and the element was not labeled there by the authors. Based on our newest investigation of the holotype of *Todrasaurus* using µCT, we were further unable to detect the presence of a splenial in that specimen (Fig. 20). As such, we see no reason to claim that a splenial was indeed present in *Todrasaurus*. Furthermore, Maisano *et al.* (2006) showed that in *Diplometopon*, the compound bone and splenial appear to be co-ossified. This seems to be also the case, and in fact is even more prominent, in *Trogonophis* (Fig. 22; Supporting Information, Fig. S7). Finally, in *Terastiodontosaurus* gen. nov., the splenial seems to be present, as there are two distinct facets medially on the dentary of the Chambi taxon, although it is unclear whether the splenial was fused to the angular.

Terastiodontosaurus marcelosanchezi gen. et sp. nov. shows great similarity to the type genus of Trogonophidae, *Trogonophis*. *Terastiodontosaurus marcelosanchezi* resembles the extant *Trogonophis wiegmanni* (the sole valid extant species of *Trogonophis*) in terms of: the shape of the frontal notches of the facial process of the maxilla; the premaxilla with one enlarged central azygous tooth separated from two "twinned" lateral teeth by a diastema greater than the interdental spaces of the remainder of the marginal dentition; the presence of 8 teeth on the dentary (primitive feature); one highly enlarged tooth in the maxilla; the presence of 3 maxillary labial foramina, with the two ones close to each other (variable); strongly flared posterior process of the maxilla (Gans and Montero 2008). On the other hand though, there are important differences between *Terastiodontosaurus marcelosanchezi* and *Trogonophis wiegmanni*, including: the shape of the teeth; the position of the enlarged dentary tooth; the number of maxillary teeth (almost always three in *Terastiodontosaurus* gen. nov., with the exception of ONM CBI-1-651 [= three plus a tiny one] and ONM CBI-1-649 [= two]) vs. usually four in *Trogonophis wiegmanni*, but can rarely be three [e.g., YPM HERR 6903; Supporting Information, Fig. S7]); the ratio of the largest maxilla tooth length to the maxillary total tooth row length (always > 0.5 in *Terastiodontosaurus*, vs. almost always < 0.5 in *Trogonophis* [the only known exception being 0.51 in YPM HERR 6903, where notably there are only three teeth, as if the largest tooth "took over space" for one of the smaller teeth]; see Table 2); the ratio of the largest dentary tooth length to the dentary total tooth row length; the premaxilla in *Terastiodontosaurus* is taller.

It is worth noting that beyond the extant species, there is also an extinct species assigned to *Trogonophis*, i.e., *Trogonophis darelbeidae* Bailon, 2000, from the Late Pliocene–Early Pleistocene of Ahl al Oughlam, Morocco (Bailon 2000). This Plio-Pleistocene taxon bears much resemblance with the extant *Trogonophis wiegmanni*, from which it was differentiated by certain features in the dentary, premaxilla, and quadrate (Bailon 2000). *Trogonophis darelbeidae* possesses three teeth in its maxilla, but still nevertheless, *Terastiodontosaurus marcelosanchezi* gen. et sp. nov. is much different from the former taxon in terms of: the shape of the dentary teeth; the

position of the enlarged dentary tooth; the ratio of the length of the largest dentary tooth to tooth row length; the number of labial foramina on the maxilla (only two in *Trogonophis darelbeidae*); the premaxilla in *Terastiodontosaurus* gen. nov. is taller; and the central azygous tooth of the premaxilla is more robust in *Terastiodontosaurus* (see text and figures in Bailon 2000).

Terastiodontosaurus gen. nov. differs greatly from the remaining three extant trogonophid genera (*Agamodon*, *Diplometopon*, and *Pachycalamus*). Indeed, it can be differentiated from them by: much different shape of teeth (in all extant taxa); number of maxillary teeth (two in *Agamodon*); degree of flaring of the posterior process of the maxilla (weaker in the remaining three genera); position of the largest tooth on the maxilla (in all extant taxa); ratio of the length of the largest maxillary tooth to the total tooth row length; number of dentary teeth (eight in *Terastiodontosaurus* vs. six in *Diplometopon* and *Pachycalamus*, and five in *Agamodon*); position of the largest tooth on the dentary; ratio of the length of the largest dentary tooth to the total tooth row length; the shape and size of the premaxillary teeth (see descriptions and figures in Gans 1960, El-Assy and Al-Nassar 1976, Maisano *et al.* 2006, Hawkins *et al.* 2022).

One remarkable feature observed in the µCT scans of *Terastiodontosaurus* gen. nov. and *Todrasaurus* is the great apical enamel thickness on their teeth. The enamel appears to be considerably thicker on all tooth tips (Fig. 23; Supporting Information, Fig. S1). This feature is present in *Trogonophis wiegmanni* as well but is lacking in *Diplometopon zarudnyi*. Based on our observations on µCT scans of various amphisbaenian taxa, such enamel thickness appears to be absent from rhineurids, bipedids, and amphisbaenids. If indeed unique to *Trogonophis* and its stem, then this feature could represent a synapomorphy to that group, as is presently inferred from our phylogenetic results. Interestingly, in the maxilla ONM CBI-1-649 of *Terastiodontosaurus*, there are areas of both the largest and the second largest teeth, in which enamel is very thin or almost absent layer (Supporting Information, Fig. S1B), seemingly the result of apical wear caused by abrasion (i.e., resulting from tooth-food particle contact) or attrition (i.e., resulting from tooth-tooth contact).

The cranial anatomy of trogonophids shows intraspecific variation, with differences concerning the number and position of labial foramina, the interdigitation between the frontals and parietal, and the extent of co-ossification among the occipital complex, fused basioccipital and parabasisphenoid, as it has been recently exemplified for *Diplometopon* (Hawkins *et al.* 2022). The shape of the premaxilla and maxilla is also variable, particularly regarding the presence or absence of a rostral blade cleft in the premaxillae and the number, size, and placement of the labial foramina and the point of the frontal processes in the maxillae (Hawkins *et al.* 2022). Moreover, there is significant degree of sexual dimorphism observed in the extant *Trogonophis wiegmanni*: even though males and females have the same total lengths,

the former have considerably larger heads and tails than the latter (Martín *et al.* 2012).

The abundance of the preserved material of *Terastiodontosaurus marcelosanchezi* gen. et sp. nov., consisting of several maxillae, dentaries, and premaxillae, pertaining to a variety of different individuals of different sizes (Minimum Number of Individuals [MNI] for premaxillae, maxillae and dentaries equal to four, six and eleven, respectively), allows some assessment of the intraspecific variation of the new taxon and more precise comparisons with other trogonophid taxa. In any case, as it is exemplified in the descriptions above, the observed variation in the premaxillae, maxillae, and dentaries of *Terastiodontosaurus marcelosanchezi* seems to be relatively low. Indeed, the most important variation is the deviation of the typical formula of three maxillary teeth that is observed in ONM CBI-1-651 (three teeth plus a tiny one) and ONM CBI-1-649 (two teeth). Notably, ONM CBI-1-649 that has only two teeth represents the smallest available individual. On the other hand, in ONM CBI-1-651, the unique maxilla with four teeth (three plus a tiny one), the extra fourth tiny tooth is situated posteriorly from the posteriormost small tooth; although it is situated not exactly in a row with the other teeth (but rather a bit more medially), this does not represent a replacement tooth, because the teeth are not replaced. The tooth ratios we introduced above also show variation, although together they point to population means that distinguish *Terastiodontosaurus* from other trogonophids (see also Table 2). As for the characteristic "hill" that is present in some small teeth of maxillae and dentaries, these could be present because these teeth had not been much abraded, like the large ones. Finally, the number, spacing, and positions of labial foramina and nutritive foramina in both maxillae and dentaries, show also some degree of variation.

Regarding the vertebrae from Chambi, these pertain to Amphisbaenia based on the dorsoventrally compressed centrum with a nearly flat ventral surface and roughly parallel lateral margins, the massive and hemisphaerical synapophyses, the absence of zygosphene, and a dorsally weakly convex neural arch lacking a neural spine (Estes 1983, Georgalis *et al.* 2018b). Among Amphisbaenia, vertebrae appear to be rather homogeneous and similar among different taxa, usually not allowing distinction at the genus or even family level (Georgalis *et al.* 2018b). A notable exception is Rhineuridae, the vertebrae of which are characterized by longitudinal striae on the vertebrae and a denticulate neural arch (Berman 1973, Estes 1983, Folie *et al.* 2013). Vertebrae of Trogonophidae do not seem to possess adequate diagnostic features, but admittedly only a few studies have dealt with these bones in this group. It seems that only the monumental work of Gans (1960) provided some observations and figures for vertebrae of all trogonophid genera, however, even in this work figuring was confined solely to the anterior vertebrae. Apparently, his focus on anterior vertebrae was attributable to the fact that this author had highlighted the fusion of

the cervical vertebrae as characteristic of Trogonophidae, being most prominent in *Agamodon* (Gans 1960). Earlier, Zangerl (1945) had noticed that in *Trogonophis*, all transverse processes in caudal vertebrae point forward, however, this feature should be more widely evaluated before it is used taxonomically. Augé (2012: fig. 4c) also provided a figure of the dorsal view of a presacral vertebra of *Agamodon*. Recently, Araújo Salvino *et al.* (2024) investigated, through µCT scanning, the atlanto-axial complex of various trogonophid species, revealing a feature unique among amphisbaenians and so a synapomorphy of Trogonophidae, i.e., the pointed (instead of spade-shaped) odontoid process of the axis. It is worth noting that Čerňanský *et al.* (2015a, 2020) mentioned that, similarly to the condition observed in rhineurids, vertebrae of trogonophids too possess a denticulate vertebral posterior margin, further stating that this feature was also variably present in some amphisbaenids. There are few published observations that would confirm or refute this assumption. In the African amphisbaenid *Geocalamus acutus* (collection of A.H. uncat.) we find denticulation to be well developed in the anterior one-half of the presacral vertebral column (Supporting Information, Fig. S8), but in multiple specimens of *Trogonophis wiegmanni* (e.g., SMF-PH 566, SMF PH-567) it is essentially absent throughout. The figured presacral vertebra of *Agamodon* in Augé (2012: fig. 4c) shows some ridges, but still not the prominent denticulation that is otherwise observed in rhineurids. At present the development of fluting or denticulations of the neural arch in extant Trogonophidae is uncertain.

Vertebrae of fossil (or subfossil) *Trogonophis* have been documented only in Stoetzel *et al.* (2008). Given that *Terastiodontosaurus marcelosanchezi* gen. et sp. nov. is the only recognized amphisbaenian taxon among the abundant cranial fossil material from Chambi, it seems reasonable to assume at present that most of the fossil vertebrae from Chambi pertain to the said taxon. However, taking into consideration the overall high diversity of Eocene amphisbaenians in Europe and North America, coupled with the fact that the late Paleocene of Adrar-Mgorn 1 in Morocco yielded two amphisbaenian forms, we cannot exclude the possibility that a second amphisbaenian taxon was also present in Chambi and for which there is currently no available cranial material. Moreover, there is considerable size disparity among the available amphisbaenian vertebrae from Chambi and some of them are very small, with centrum lengths only around 1 mm. Accordingly, while the referral of most of the vertebral material from Chambi to *Terastiodontosaurus marcelosanchezi* is probable, we consider the referral in any particular case as tentative.

Diet and bite force

Amblyodonty is characterized by the presence of large and blunt teeth. Blunt teeth can be observed among an array of distantly related squamates and are considered to represent adaptations for crushing hard-shelled prey items (Edmund 1969, Böhme *et*

al. 2022). Indeed, these have been described in various lizard taxa that are known to feed on molluscs, including scincids (Edmund 1969), teiids (Peyer 1929, Presch 1974, Dalrymple 1979, Leite *et al.* 2021), extinct lacertids (Roček 1984, Augé 2005, Čerňanský *et al.* 2016b, 2017, Georgalis *et al.* 2021), a few amphisbaenians (see below), anguids (Klembara *et al.* 2010, 2014, 2017, Smith and Gauthier 2013, Loréal *et al.* 2023, 2024), varanids (Mertens 1942, Rieppel and Labhardt 1979, D'Amore 2015), iguanians (Estes and Williams 1984, Herrel and Holanova 2008), and some Cretaceous mosasaurs (Bardet *et al.* 2005), as well as snakes feeding on hard-bodied arthropods (Rajabizadeh *et al.* 2021, Böhme *et al.* 2022).

Amblyodont dentition is rare among amphisbaenians. Besides the herein documented *Terastiodontosaurus* gen. nov., amblyodonty is otherwise observed solely in, the late Paleocene African *Todrasaurus*, the late Paleocene North American *Oligodontosaurus* Gilmore, 1942, the Eocene European *Cuvieribaena*, the extant trogonophid *Trogonophis*, and a single species of the extant *Amphisbaena*, the insular endemic *Amphisbaena ridleyi* Boulenger, 1890 (Gilmore 1942, Gans 1960, Pregill 1984, Augé and Rage 2006, Čerňanský *et al.* 2015a, this paper). Dietary study of one insular population of *Trogonophis wiegmanni* during the springtime showed that it is at least partly durophagous, selecting and feeding on snails, which it crushes and swallows with the shell (Martín *et al.* 2013). It should be noted that this species had previously been considered – based on mainland populations – to feed on ants and termites (e.g., Schleich *et al.* 1996). Martín *et al.* (2013) suggested on the basis of its dentition, its documented diet, and the flaring of the jugal process of the maxilla (which would provide more space for the jaw adductor musculature) that *T. wiegmanni* could be a snail specialist. Baeckens *et al.* (2017) further suggested that there are modifications to the musculature of *T. wiegmanni* that allows it to bite harder than its head size would normally allow.

Based on the dissection of the specimen of *Trogonophis wiegmanni* (MNHN-RA-1987.1895), we attempted to make a bite force estimation for *Terastiodontosaurus marcelosanchezi* gen. et sp. nov. The muscle data for the specimen (MNHN-RA-1987.1895) of *Trogonophis wiegmanni* are provided in Table 3. Our calculations estimated a bite force for the *Trogonophis* MNHN specimen of 9.6 N at the tip of the jaw and 14.2 N at the largest tooth. These results are similar to in vivo measurements of two *Trogonophis* specimens of slightly smaller size (lower jaw length: 7.99 ± 0.62 mm vs. 11.74 mm for MNHN-RA-1987.1895), which produced 8.31 ± 1.42 N at the middle of the tooth row. Based on these results we estimated the bite force of the paratype (ONM CBI-1-646) of *Terastiodontosaurus marcelosanchezi* to be 16.71 N at the tip of the jaw and 24.83 N at the largest tooth. This would allow *Terastiodontosaurus* to crush a wide variety of snails (Fig. 24).

Size estimation and locomotion of *Terastiodontosaurus marcelosanchezi* gen. et sp. nov.

The holotype maxilla of *Terastiodontosaurus marcelosanchezi* gen. et sp. nov. has a length of 16.3 mm. Based on the linear dimensions of the maxilla and skull in *Trogonophis wiegmanni* (Table 2), and assuming isometry of growth and identical skull proportions in the adult, we estimate that the individual from which the holotype of *Terastiodontosaurus marcelosanchezi* derives had a skull length of 53.8 mm. This renders it the largest known amphisbaenian to have ever lived, as judged by skull size.

Indeed, all other known amphisbaenians, either extinct or extant, appear to be smaller than the new taxon from Chambi. *Listromycter leakeyi* Charig & Gans, 1990, from the Early Miocene of Kenya, is known only by its holotype (NHMUK PV R 8292), an almost complete skull missing only the lower jaw. Its premaxilla (characterized as "enormous" by Charig and Gans 1990) is 12.7 mm in length and these authors estimated a total skull length of 36 mm ("estimated length of whole skull, measured in a straight line from tip of premaxillary rostral process to occipital condyle: about 36 mm."), leading them to suggest this taxon to represent the largest known amphisbaenian (Charig and Gans 1990). Only slightly smaller is *Spathorhynchus fossorium* Berman, 1973, from the Eocene of the USA, with a skull length of 35.4 mm (Berman 1973, Müller *et al.* 2016). Other large species are *Spathorhynchus natronicus* Berman, 1977, from the early Oligocene of the USA (skull length estimated at 28 mm, according to Berman 1977), *Ototriton solidus* Loomis, 1919, from the Eocene of the USA (32 mm according to Estes 1983), and *Macrorhineura skinneri* MacDonald, 1970, from the Early Miocene of the USA (also 32 mm according to Estes 1983).

Extrapolation of skull length for *Terastiodontosaurus marcelosanchezi* gen. et sp. nov. is probably fairly accurate, given its strong overall similarity to extant *Trogonophis wiegmanni*, but extrapolation of total length is much less certain. Maximal presacral vertebral count in *Trogonophis wiegmanni* is c. 77 (Table 2; Hoffstetter and Gasc 1969), and in *Agamodon* spp. it is no higher, but in *Diplometopon zarudyi* and *Pachycalamus brevis* it nearly reaches 90. The count in *Trogonophis wiegmanni* is lower than in almost other extant Amphisbaenia except *Agamodon* (Hoffstetter and Gasc 1969). Assuming this value is applicable to *Terastiodontosaurus marcelosanchezi*, then we extrapolate for the individual from which the holotype maxilla derives a total length of 781 mm (Table 2). Supposing that this number may have been higher (e.g., 90 presacral vertebrae), then a value > 900 mm is likely for the new extinct amphisbaenian taxon.

Amongst extant amphisbaenians, *Amphisbaena alba* is the largest species, reaching a maximum total length of 810 mm (Colli and Zamboni 1999, Feldman *et al.*

2016, Jared *et al.* 2024) and a skull length of more than 31 mm (31.8 mm in Montero and Gans 1999; 36.59 mm in specimen FMNH 195924 [Digimorph]; but less than 30 mm in several other published specimens [e.g., Clark and Rene Hernandez 1994, Montero and Gans 1999]), followed by *Dalophia gigantea* (Peracca, 1903), and a few species of *Monopeltis* Smith, 1848, *Leposternon* Wagler, 1824, and *Amphisbaena* Linnaeus, 1758, which also achieve large (but not very large) sizes (Gans and Montero 2008, see Feldman *et al.* 2016).

Practically all extant amphisbaenians represent burrowing animals, which only rarely appear on the surface, outside their subterranean environments (Gans 1969, 1978, Gans and Montero 2008, Vidal *et al.* 2008). Nevertheless, certain features in *Terastiodontosaurus* gen. nov. (e.g., the very large size; the tall premaxilla) seem to contradict this natural history pattern and suggest instead that the new Tunisian taxon was likely a surface dweller (Fig. 24). This is further supported by the extreme size of the new taxon, which would render subterranean habits as less likely; as a matter of fact, the largest extant amphisbaenian, *Amphisbaena alba*, only rarely makes burrows in captivity (Jared *et al.* 2024). The preferred habitat of Amphisbaenia is also related to their coloration, with deeply burrowing species like *Rhineura floridana* (Baird, 1858) and *Agamodon* spp. almost devoid of pigmentation, hence appearing pinkish, whereas species that spend considerable time much closer to the surface like *Amphisbaena alba* and *Trogonophis wiegmanni* show distinct pigmentation patterns (Gans 1978). Given our inferences concerning its preferred habitat, we can safely assume that *Terastiodontosaurus* had pigmented skin.

Altogether our study points to remarkable new insights into the biology of Amphisbaenia. With a skull size > 5 cm in length, *Terastiodontosaurus* gen. nov. was larger than any previously known amphisbaenian, living or extinct, and accordingly it was probably more of a surface-dweller than a strictly fossorial animal. This broadens our understanding of amphisbaenian evolutionary ecology and the limits of the amphisbaenian body-plan. That this animal probably lived during around the Early Eocene Climatic Optimum (Zachos *et al.* 2001) is noteworthy in view of the relationship between ambient temperature and maximum body size within a higher taxonomic group (Makarieva *et al.* 2005, Head *et al.* 2009). Furthermore, the documentation of characteristics associated with molluscivory, such as flared jugal processes of the maxilla and thick tooth enamel, in stem representatives of *Trogonophis* suggest that this lineage has conserved this unusual aspect of its niche for tens of millions of years down to the present-day.

Trogonophidae origins and biogeography

Terastiodontosaurus marcelosanchezi gen. et sp. nov. represents a substantial contribution to the so far poorly known African fossil record of Amphisbaenia,

representing only the fifth named extinct species from the continent, adding to *Lophocranion rusingense* Charig & Gans, 1990, and *Listromycter leakeyi* Charig & Gans, 1990, both from the Early Miocene of Rusinga Island, Kenya, and the aforementioned trogonophids *Todrasaurus gheerbranti* from the late Paleocene of Morocco, and *Trogonophis darelbeidae* from the Plio-Pleistocene of Morocco. Moreover, the abundant Chambi material adds to the extremely scarce Paleogene Afro-Arabian record of Amphisbaenia, which were so far exclusively known from the holotype of *Todrasaurus gheerbranti* from the late Paleocene (Thanetian) of Adrar-Mgorn 1, Morocco (Augé and Rage 2006, this paper) and indeterminate remains from the late Paleocene (Thanetian) of Adrar-Mgorn 1, Morocco (Augé and Rage 2006), the early Eocene (middle Ypresian) of N'Tagourt 2, Morocco (Augé and Rage 2006), the early–middle Eocene (late Ypresian–early Lutetian) of Glib Zegdou HGL50, Algeria (Rage *et al.* 2021), the middle Eocene of Black Crow, Namibia (Rage *et al.* 2013), and the late Eocene (earliest Priabonian) of Birket Qarun 2, Fayum, Egypt (El-Hares *et al.* 2022) (see also Fig. 1 above). Note that amphisbaenian vertebrae described by Rage *et al.* (2013) from the locality of Silica North in Sperrgebiet, Namibia, were originally considered to be middle Eocene in age, but recent studies have reappraised that site to be much younger, pertaining to the late Oligocene or even the Early Miocene (Coster *et al.* 2012, Marivaux *et al.* 2014, Sallam and Seiffert 2016, 2020, Rage *et al.* 2021, El-Hares *et al.* 2022, Smith and Georgalis 2022). Accordingly, it is evident that the Paleogene record of Amphisbaenia in the (then isolated) Afro-Arabia seems so far to be almost exclusively known from the northern margins of the continent. This pattern contrasts the relatively high extant diversity of the group in sub-Saharan Africa, where amphisbaenians represent a principal component of the squamate faunas (e.g., Broadley *et al.* 1976, Broadley and Broadley 1997, Gans 2005). This Paleogene distribution is apparently collection-biased, as Paleogene northern African fossil localities have been more intensively investigated and sampled.

Moreover, the new material from Chambi further adds to the extremely poor fossil record of Trogonophidae, which was so far confined solely to the holotype of *Todrasaurus gheerbranti* from the late Paleocene (Thanetian) of Adrar-Mgorn 1, Morocco (Augé and Rage 2006, this paper), the material of *Trogonophis darelbeidae* from the Plio-Pleistocene of Ahl al Oughlam, Morocco (Bailon 2000), and material of the extant species *Trogonophis wiegmanni* from the Holocene (Neolithic) of El Harhoura 2, Morocco (Stoetzel *et al.* 2008) and the Holocene (Neolithic) of Gueldaman Cave, Algeria (Saidani *et al.* 2016), plus a mentioned (but not described) record from the Late Pleistocene of Ifri n'Ammar, Morocco (Mouhsine *et al.* 2022).

Interestingly, most molecular studies have suggested that the split of Trogonophidae from the remaining amphisbaenians took place only at around the Eocene. Graboski *et al.* (2022) placed this divergence date estimate of Trogonophidae at around 44 Ma (i.e., middle Eocene). A similar result is also the case in other recent

studies, including Vidal and Hedges (2005), who placed this divergence at approximately 43–23 Ma, Vidal *et al.* (2008) at around 51 Ma, and Pyron (2017) and Burbrink *et al.* (2020), at around the mid-Paleogene. In the combined analysis of Longrich *et al.* (2015), Trogonophidae was found to diverge from other Afrobaenia in the early Eocene, and the basal divergence in Trogonophidae (between *Trogonophis* and *Diplometopon* + *Agamodon*) in the late Eocene. An even younger (early Oligocene; 31.5 Ma) age for the divergence of *Trogonophis* from *Amphisbaena* was estimated in the combined phylogeny of Brownstein *et al.* (2023), while the same divergence was estimated as even younger (approximately 20 Ma) in Jones *et al.* (2013). Only the molecular analysis of Zheng and Wiens (2016) placed the split of Trogonophidae from its sister group, Amphisbaenidae, at a much older time, around 80 Ma, with *Trogonophis* splitting from *Diplometopon* at around 41 Ma.

The close relationship between *Todrasaurus gheerbranti* recovered in this study (see above Fig. 23) indicates that the basal divergence of Trogonophidae took place before the end of the Thanetian, i.e., late Paleocene. Our study therefore pushes back the known origin of the group substantially. *Todrasaurus gheerbranti* can serve as a critical new fossil calibration for molecular studies of Amphisbaenia.

Amphisbaenia witnessed an astonishing history of long ocean dispersals, as it has been implied by both the fossil record (Longrich *et al.* 2015) and molecular data (Vidal *et al.* 2008a, Graboski *et al.* 2022). It has to be noted though that Tałanda (2016) suggested instead that amphisbaenian dispersals occurred mainly through existing land bridges or at least across not-so-distant marine barriers. Nevertheless, transatlantic rafting during the Eocene has been suggested for various amphisbaenian groups (Vidal *et al.* 2008, Longrich *et al.* 2015, Graboski *et al.* 2022). Although amphisbaenians are almost strictly burrowing reptiles, swimming capabilities have even been observed in certain extant taxa, either in order to escape extreme situations or even to find new food resources (Quinteros-Muñoz *et al.* 2023); of course, such swimming capabilities fall far short of performance expectations for crossing a long sea barrier. As a matter of fact, such long distance, overseas dispersals of amphisbaenians would only be possible by using “floating islands of vegetation” (“floatons”, “flotsams”), aided by some marine currents and wind (Houle 1998, Vidal *et al.* 2008, Bandoni de Oliveira *et al.* 2009, Longrich *et al.* 2015, Marivaux *et al.* 2023). This may explain the long dispersal routes over large marine barriers in their geologic past, their current geographic distribution, and their current presence in remote islands (Vidal *et al.* 2008, Longrich *et al.* 2015, Graboski *et al.* 2022). Dispersals are a major key to the evolution of reptile assemblages over time (Longrich *et al.* 2015); this is particularly true for Afro-Arabia, a landmass that was isolated for practically the whole Paleogene and shows an astonishing diversity of dispersals of non-marine vertebrates from and to other continents, particularly during the Eocene (see Georgalis 2021). Longrich *et al.* (2015) suggested that stem afrobaenians (i.e., in

their analysis, the total group encompassing Cadeidae, Trogonophidae, and Amphisbaenidae) dispersed directly from North America to Africa, via marine dispersal, during the Paleocene or early Eocene; this opinion was criticized by Tałanda (2016), who further noticed that this scenario was incompatible with marine palaeocurrent reconstructions and that no other vertebrate group is known to have dispersed from North America directly to Africa during the Paleogene. Longrich *et al.* (2015) further suggested that the ancestor of Trogonophidae originated in Africa. The identification of the new trogonophid *Terastiodontosaurus marcelosanchezi* gen. et sp. nov. from the late early – early middle Eocene of Tunisia gives some strength to this latter assumption. Nevertheless, more fossil remains are necessary in order to fully comprehend the early evolutionary and biogeographic patterns of Amphisbaenia. We anticipate that rich and diverse African fossil assemblages, such as Chambi, will decipher further valuable clues about the origins and fossil record of these charismatic squamates.

ACKNOWLEDGEMENTS

We are grateful to Mehdi Mouana (ISE-M) and Anne-Lise Charruault (ISE-M) for facilitating access of the fossil material, as well as µCT scanning and 3D imaging of specimens. None of the fossil material from Chambi would have been extracted and prepared without the patience and tenacity of Anne-Lise Charruault. L.M. and R.T. are very grateful to Anne-Lise Charruault, Suzanne Jiquel, Bernard Marandat, Anusha Ramdarshan, Anthony Ravel, and Monique Vianey-Liaud (ISE-M), Gilles Merzeraud† (Géosciences Montpellier), and Faouzi M'Nasri (ONM, Tunis) for their assistance during the field seasons in the Kasserine region. We would like to thank Nicolas Vidal (MNHN) for allowing us to dissect a specimen of *Trogonophis* from the collections of MNHN. Stevie Kennedy-Gold (MCZ), Carol Spencer (MVZ), Jessie Maisano (UT Austin), and staff at the California Academy of Sciences and the Field Museum of Natural History are thanked for access to digital imagery. Anika Vogel (SMF) assisted with specimen curation. Special thanks go to Hermann Schleich (*Anfibios y Reptiles en Conservación, Instituto y Nucleo Zoológico*, Spain). For help with 3D imaging we thank Kacper Węgrzyn (ISEZ). We also thank Simon Baeckens (University of Antwerp) for sharing information on the feeding habits of extant *Trogonophis* and Ben Creisler on comments on the spelling of Trogonophidae. We finally thank Jaime Chirinos for preparing the life reconstruction of the new taxon presented in Fig. 24. The quality of the manuscript was enhanced by the useful comments provided by the Editor in Chief Jeffrey Streicher, the Associate Editor Marc Young, and five reviewers: Andrej Čerňanský, Mateusz Tałanda, and three anonymous ones. Tis is ISE-M publication n° 2024-247 SUD.

FUNDING

G.L.G. acknowledges funding from the research project no. 2023/49/B/ST10/02631 financed by the National Science Center of Poland (Narodowe Centrum Nauki). G.L.G. also acknowledges travel support from Marcelo Sánchez-Villagra (Palaeontological Institute of the University of Zurich), the Georges and Antoine Claraz-Donation, and Lionel Hautier (ISE-M) for enabling him to travel and study the fossil material from Chambi. Fieldwork and fossil extraction were performed in the framework of the ANR-ERC PALASIAFRICA (ANR-08-JCJC-0017). K.T.S. acknowledges the Senckenberg Research Institute for collection expansion support.

CONFLICT OF INTEREST

The authors confirm that have no conflicts of interests.

DATA AVAILABILITY

All fossil specimens of *Terastiodontosaurus marcelosanchezi* gen. et sp. nov. from Chambi described herein are permanently curated at the collections of ONM. The holotype (UM THR 407) of *Todrasaurus gheerbranti* from the late Paleocene of Adrar-Mgorn 1, Morocco, is permanently curated at the collections of UM.

3D model files of several premaxillae, maxillae, and dentaries of *Terastiodontosaurus marcelosanchezi* (including the holotype and paratype specimens) plus the holotype dentary of *Todrasaurus gheerbranti* are deposited in MorphoMuseuM (Georgalis *et al.* 2024). https://doi.org/10.18563/journal.m3.245

REFERENCES

Alexander AA, Gans C. The pattern of dermal-vertebral correlation in snakes and amphisbaenians. *Zoologische Mededelingen* 1966; **31**:171–190.

Araújo Salvino C, Hernandéz-Morales C, Daza JD, Nunes PMS. Comparative anatomy and evolution of the atlantoaxial complex in the fossorial lineage Amphisbaenia (Squamata: Lacertoidea). *The Anatomical Record* 2024; 1–26.

Augé M. Evolution des lézards du Paléogène en Europe. *Mémoires du Muséum national d'Histoire naturelle, Paris* 2005; **192**:1–369.

Augé M. Amphisbaenians from the European Eocene: a biogeographical review. *Palaeobiodiversity and Palaeoenvironments* 2012; **92**:425–443.

Augé ML, Rage J-C. Le Garouillas et les sites contemporains (Oligocene, MP 25) des Phosphorites du Quercy (Lot, Tarn-et-Garonne, France) et leurs faunes de vertebres. 2. Amphibiens et squamates. *Palaeontographica Abteilung A* 1995; **236**:11–32.

Augé ML, Rage J-C. Herpetofaunas from the upper Paleocene and lower Eocene of Morocco. *Annales de Paléontologie* 2006; **92**:235–253.

Baeckens S, García-Roa R, Martín J, Ortega J, Huyghe K, Van Damme R. Fossorial and durophagous: implications of molluscivory for head size and bite capacity in a burrowing worm lizard. *Journal of Zoology* 2017; **301**:193–205.

Bailon S. Amphibiens et reptiles du Pliocène terminal d'Ahl al Oughlam (Casablanca, Maroc). *Geodiversitas* 2000; **22**:539–558.

Baird SF. 1858. Description of new genera and species of North American lizards in the Museum of the Smithsonian Institution. *Proceedings of the Academy of Natural Sciences of Philadelphia* 1858; **1858**: 253–256.

Bandoni de Oliveira F, Molina EC, Marroig G. Chapter 3. Paleogeography of the South Atlantic: a route for primates and rodents into the New World? In: Garber PA, Estrada A, Bicca-Marques JCB, Heymann EW, Strier KB, (eds). *South American Primates: Comparative Perspectives in the Study of Behavior, Ecology, and Conservation*. Chicago: Springer 2009; pp. 55–68.

Bardet N, Suberbiola XP, Iarochène M, Amalik M, Bouya B. Durophagous Mosasauridae (Squamata) from the Upper Cretaceous phosphates of Morocco, with description of a new species of *Globidens*. *Netherlands Journal of Geosciences* 2005; **84**:167–175.

Bedriaga J. *Amphisbaena cinerea* Vand. und *A. strauchi* v. Bedr. Erster Beitrag zur Kenntniss der Doppelschleichen. *Archiv für Naturgeschichte* 1884; **50**:23–77.

Bell CJ, Cadena C, Meza A, Rudie L, Lewis PJ. Cranial anatomy of the "round-headed" Amphisbaenian *Zygaspis quadrifrons* (Squamata, Amphisbaenia) based on high-resolution x-ray computed tomography. *The Anatomical Record* 2024; **307**:495–532.

Benoit J, Adnet A, Essid EM, Ben Haj Ali M, Marivaux L, Merzeraud G, Merigeaud S, Vianey-Liaud M, Tabuce R. Cranial remain from Tunisia provides new clues for the origin and evolution of Sirenia (Mammalia, Afrotheria) in Africa. *PLoS ONE* 2013a; **8**:1–9.

Benoit J, Essid EM, Marzougui W, Khayati Ammar H, Lebrun R, Tabuce R, Marivaux L. New insights into the ear region anatomy and cranial blood supply of advanced stem Strepsirhini: evidence from primate petrosals from the Eocene of Chambi, Tunisia. *Journal of Human Evolution* 2013b; **65**:551–572.

Benoit J, Orliac MJ, Tabuce R. The petrosal of *Chambius* (Macroscelidea, Afrotheria) from the Eocene of Djebel Chambi (Tunisia) and the evolution of the ear region in elephant-shrews. *Journal of Systematic Palaeontology* 2013c; **11**:907–923.

Berman DS. *Spathorhynchus fossorium*, a middle Eocene amphisbaenian (Reptilia) from Wyoming. *Copeia* 1973; **4**:704–721.

Berman DS. *Spathorhynchus natronicus*, a new species of rhineurid amphisbaenian (Reptilia) from the Early Oligocene of Wyoming. *Journal of Paleontology* 1977; **51**:986–991.

Bhullar B-AS, Smith KT. Helodermatid lizard for the Miocene of Florida, the evolution of the dentary in Helodermatidae, and comments on dentary morphology in Varanoidea. *Journal of Herpetology* 2008; **42**:286–302.

Blain H-A. Contribution de la paléoherpétofaune (Amphibia y Squamata) à la connaissance de l'évolution du climat et du paysage du Pliocène supérieur au Pléistocène moyen d'Espagne. *Treballs del Museu de Geologia de Barcelona* 2009; **16**:39–170.

Blain H-A, Bailon S, Agustí J. Anurans and squamate reptiles from the latest early Pleistocene of Almenara- Casablanca-3 (Castellon, East of Spain). Systematic, climatic and environmental considerations. *Geodiversitas* 2007; **29**:269–295.

Böhme W, Schleich H, Wipfler B, Koppetsch T. On the dentition of the Cape Verdean endemic lizard genus *Chioninia* Gray, 1845, with a discussion of ecological implications in the giant species *C. coctei* (Duméril & Bibron, 1839) (Squamata, Scincidae). *Spixiana* 2022; **45**:131–144.

Bolet A, Delfino M, Fortuny J, Almécija S, Robles JM, Alba DM. An amphisbaenian skull from the European Miocene and the evolution of Mediterranean worm lizards. *PLoS ONE* 2014; **9**:e98082.

Bonaparte CL. Amphibiorum tabula analytica. *Nuovi annali delle scienze naturali* 1838a; **1**:391–397.

Bonaparte CL. Synopsis Vertebratorum Systematis. *Nuovi annali delle scienze naturali* 1838b; **2**:105–133.

Bonaparte CL. *Amphibia Europaea. Ad systema nostrum vertebratorum ordinata*. *Memorie della Reale Accademia delle Scienze di Torino, Serie II* 1839; **2**:385–456.

Bonaparte CL. A new systematic arrangement of vertebrated animals. *Transactions of the Linnean Society of London* 1840a; **18**:247–304.

Bonaparte CL. Prodromus systematis herpetologiae. *Nuovi Annali delle Scienze naturali, Bologna* 1840b; **4**:90–101.

Bonaparte CL. *Conspectus systematum herpetologiae et amphibiologiae. Editio altera reformata*. Lugduni Batavorum: E. J. Brill 1850; 1 pl.

Bonaparte CL. Conspectus systematum herpetologiae et amphibiologiae. Editio altera reformata. (Continuazione). *Nuovi Annali delle Scienze naturali, Bologna, Serie III* 1852; **5**:89–96 and 477–480.

Boulenger GA. Reptilia. In Ridley HN., (ed), Notes on the zoology of Fernando Noronha. *Journal of the Linnean Society London, Zoology* 1890; **20**:481–482.

Brizuela S, Albino AM. Los reptiles escamosos del Plioceno de la costa Atlántica entre Mar del Plata y Miramar, Provincia de Buenos Aires, Argentina. *Revista Del Museo Argentino de Ciencias Naturales, Nueva Serie* 2012; **14**:47–56.

Broadley DG, Broadley S. A revision of the African genus *Zygaspis* Cope (Reptilia: Amphisbaenia). *Syntarsus* 1997; **4**:1–24.

Broadley DG, Gans C, Visser J. Studies on amphisbaenians (Amphisbaenia, Reptilia) 6. The genera *Monopeltis* and *Dalophia* in southern Africa. *Bulletin of the American Museum of Natural History* 1976; **157**:311–486.

Brownstein CD, Simões TR, Caldwell MW, Lee MSY, Meyer DL, Scarpetta SG. The affinities of the Late Triassic *Cryptovaranoides* and the age of crown squamates. *Royal Society Open Science* 2023; **10**:230968.

Burbrink FT, Grazziotin GF, Pyron RA, Cundall D, Donnellan S, Irish F, Keogh JS, Kraus F, Murphy RW, Noonan B, Raxworthy CJ, Ruane S, Lemmon AR, Lemmon EM, Zaher H. Interrogating genomic-scale data for Squamata (lizards, snakes, and amphisbaenians) shows no support for key traditional morphological relationships. *Systematic Biology* 2020; **69**:502–520.

Camolez T, Zaher H. Levantamento, identificação e descrição da fauna de Squamata do Quaternário brasileiro (Lepidosauria). *Arquivos de Zoologia, Museu de Zoologia Da Universidade de São Paulo* 2010; **41**:1–96.

Čerňanský A. New lizard material from two Early Miocene localities in France: Montaigu-le-Blin (MN 2) and Crémat (MN 3). *Geobios* 2023; **80**:15–28.

Čerňanský A, Augé M, Rage J-C. A complete mandible of a new amphisbaenian reptile (Squamata, Amphisbaenia) from the late Middle Eocene (Bartonian, MP 16) of France. *Journal of Vertebrate Paleontology* 2015a; **35**:e902379.

Čerňanský A, Bolet A, Müller J, Rage J-C, Augé M, Herrel A. A new exceptionally preserved specimen of *Dracaenosaurus* (Squamata, Lacertidae) from the Oligocene of France as revealed by micro-computed tomography. *Journal of Vertebrate Paleontology* 2017; **37**:e1384738.

Čerňanský A, Klembara J, Müller J. The new rare record of the late Oligocene lizards and amphisbaenians from Germany and its impact on our knowledge of the European terminal Palaeogene. *Palaeobiodiversity and Palaeoenvironments* 2016a; **96**:559–587.

Čerňanský A, Klembara J, Smith KT. Fossil lizard from central Europe resolves the origin of large body size and herbivory in giant Canary Island lacertids. *Zoological Journal of the Linnean Society* 2016b; **176**:861–877.

Čerňanský A, Rage J-C, Klembara J. The Early Miocene squamates of Amöneburg (Germany): the first stages of modern squamates in Europe. *Journal of Systematic Palaeontology* 2015b; **13**:97–128.

Čerňanský A, Syromyatnikova EV, Jablonski D. The first record of amphisbaenian and anguimorph lizards (Reptilia, Squamata) from the upper Miocene Solnechnodolsk locality in Russia. *Historical Biology* 2020; **32**:869–879.

Čerňanský A, Vasilyan D. Roots of the European Cenozoic ecosystems: lizards from the Paleocene (~MP 5) of Walbeck in Germany. *Fossil Record* 2024; **27**:159–186.

Charig A, Gans C. Two new amphisbaenians from the Lower Miocene of Kenya. *Bulletin of the British Museum (Natural History) (Geology)* 1990; **46**:387–400.

Clark JM, Rene Hernandez R. A new burrowing diapsid from the Jurassic La Boca Formation of Tamaulipas, Mexico. *Journal of Vertebrate Paleontology* 1994; **14**:180–195.

Colli GR, Zamboni DS. Ecology of the worm lizard *Amphisbaena alba* in the Cerrado of Central Brazil. *Copeia* 1999; **1999**:733–742.

Cope ED. Catalogue of batrachians and reptiles of Central America and Mexico. *Bulletin of the United States National Museum* 1887; **32**:7–98.

Coster P, Benammi M, Mahboubi M, Tabuce R, Adaci M, Marivaux L, Bensalah M, Mahboubi S, Mahboubi A, Maameri C, Jaeger J-J. Chronology of the early-middle continental Eocene deposits of Africa: magnetic stratigraphy and biostratigraphy of the El Kohol and Glib Zegdou formations, Algeria. *Geological Society of America Bulletin* 2012; **124**:1590–1606.

Court N, Hartenberger JL. An enigmatic new mammal from the Eocene of North Africa. *Journal of Vertebrate Paleontology* 1992; **13**:267–269.

Court N, Hartenberger JL. 1993. A new species of hyracoid mammal *Titanohyrax* from the Eocene of Tunisia. *Palaeontology* 1993; **35**:309–317.

Crochet J-Y. *Kasserinotherium tunisiense* nov. gen. sp., troisième marsupial découvert en Afrique (Eocène inférieur de Tunisie). *Comptes rendus de l'Académie des Sciences, Paris* 1986; **302**:923–926.

D'Amore DC. Illustrating ontogenetic change in the dentition of the Nile monitor lizard, *Varanus niloticus*: a case study in the application of geometric morphometric methods for the quantification of shape–size heterodonty. *Journal of Anatomy* 2015; **226**:403–419.

Dalrymple G. On the jaw mechanism of the snail-crushing lizards: *Dracaena* Daudin 1802 (Reptilia, Lacertilia, Teiidae). *Journal of Herpetology* 1979; **13**:303–311.

Delfino M. A Pleistocene amphisbaenian from Sicily. *Amphibia-Reptilia* 2003; **24**:407–414.

Delfino M, Bailon S, Pitruzzella G. The late Pliocene amphibians and reptiles from ''Capo Mannu D1 Local Fauna'' (Mandriola, Sardinia, Italy). *Geodiversitas* 2011; **33**:357–382.

Dickerson MC. Description of a new amphisbaenian collected by the late Dr. Charles S. Mead in 1911 on the Isle of Pines, Cuba. *Bulletin of the American Museum of Natural History* 1916; **35**:659–662.

Digimorph.org. *Digital morphology: a National Science Foundation digital library at the University of Texas at Austin*. Austin: The High Resolution X-ray Computed Tomography Facility at the University of Texas at Austin, 2002–2024. Retrieved from http://www.digimorph.org/.

Duméril AMC, Bibron G. *Erpétologie générale ou histoire naturelle complète des reptiles. Tome cinquième. Contenant l'histoire de quatre-vingt-trois genres et de deux cent sept especes des trois dernieres familles de l'ordre des sauriens, savoir : les lacertiens, les chalcidiens et les scincoïdiens*. Paris: Librairie Encyclopédique de Roret 1839; 854 pp.

Edmund AG. Dentition. In: Gans C, Bellairs Ad'A, Parsons TS, (eds). *Biology of the Reptilia, Vol. 1 (Morphology A)*. London and New York: Academic Press 1969; pp. 117–200.

El-Assy YS, Al-Nassar NA. 1976. Morphological study of the cranial osteology of the amphisbaenian *Diplometopon zarudnyi*. *Journal of the University of Kuwait (Science)* 1976; **3**:113–141.

El-Hares MA, Zaher H, El-Mekkawy D, El-Sayed S, Seiffert ER, Sallam HM. New records of legless squamates from the lowest upper Eocene deposits of the Fayum Depression, Egypt. *Journal of Vertebrate Paleontology* 2022; **41**:e1992770.

Estes R. Sauria Terrestria, Amphisbaenia. In Wellnhofer P, (ed). *Encyclopedia of Paleoherpetology, part 10a*. Stuttgart and New York: Gustav Fischer Verlag 1983; 249 pp.

Estes R, Williams EE. Ontogenetic variation in the molariform teeth of lizards. *Journal of Vertebrate Paleontology* 1984; **4**:96–107.

Fedorov A, Beichel R, Kalpathy-Cramer J, Finet J, Fillion-Robin J-C, Pujol S, Bauer C, Jennings D, Fennessy F, Sonka M, Buatti J, Aylward SR, Miller JV, Pieper S, Kikinis R. 3D Slicer as an image computing platform for the quantitative imaging network. *Magnetic Resonance Imaging* 2012; **30**:1323–1341.

Feldman A, Sabath N, Pyron RA, Mayrose I, Meiri S. Body sizes and diversification rates of lizards, snakes, amphisbaenians and the tuatara. *Global Ecology and Biogeography* 2016; **25**:187–197.

Fitzinger LJFJ. *Systema reptilium. Fasciculus primus. Amblyglossae*. Vindobonae (= Vienna): Braumüller et Seidel Bibliopolas 1843; vi + 106 pp.

Folie A, Smith R, Smith T. New amphisbaenian lizards from the Early Paleogene of Europe and their implications for the early evolution of modern amphisbaenians. *Geologica Belgica* 2013; **16**:227–235.

Gans C. Studies on amphisbaenids (Amphisbaenia, Reptilia). 1. A taxonomic revision of the Trogonophinae, and a functional interpretation of the amphisbaenid adaptive pattern. *Bulletin of the American Museum of Natural History* 1960; **119**:129–204.

Gans C. Amphisbaenians – reptiles specialized for a burrowing existence. *Endeavour* 1969; **28**:146–151.

Gans C. The characteristics and affinities of the Amphisbaenia. *Transactions of the Zoological Society of London* 1978; **34**:347–416.

Gans C. Checklist and bibliography of the Amphisbaenia of the world. *Bulletin of the American Museum of Natural History* 2005; **289**:1–130.

Gans C, Montero R. Two new fossil amphisbaenids (Reptilia: Squamata) from the Pleistocene of Lagoa Santa (Minas Gerais, Brazil). *Steenstrupia* 1998; **24**:9–22.

Gans C, Montero R. An atlas of amphisbaenian skull anatomy. In: Gans C, Gaunt A, Adler K, (eds). *Biology of the Reptilia. Volume 21. Morphology I. The skull and appendicular locomotor apparatus of Lepidosauria*. Ithaca: Society for the Study of Amphibians and Reptiles 2008; pp. 621–738.

Gardner JD, Rage J-C. The fossil record of lissamphibians from Africa, Madagascar, and the Arabian Plate. In: Gardner JD, Přikryl T, (eds). Contributions in Honour of Zbyněk Roček. *Palaeobiodiversity and Palaeoenvironments* 2016; **96**:169–220.

Gauthier JA, Kearney M, Maisano JA, Rieppel O, Behike ADB. Assembling the squamate tree of life: perspectives from the phenotype and the fossil record. *Bulletin of the Peabody Museum of Natural History* 2012; **53**:3–308.

Georgalis GL. First pan-trionychid turtle (Testudines, Pan-Trionychidae) from the Palaeogene of Africa. *Papers in Palaeontology* 2021; **7**:1919–1926.

Georgalis GL, Čerňanský A, Göktaş F, Alpagut B, Şarbak A, Mayda S. The antiquity of Asian chameleons – first potential Chamaeleonidae and associated squamate fauna from the Lower and Middle Miocene of Anatolia. *Journal of Vertebrate Paleontology* 2023; **42**:e2160644.

Georgalis GL, Čerňanský A, Klembara J. Osteological atlas of new lizards from the Phosphorites du Quercy (France), based on historical, forgotten, fossil material. *Geodiversitas* 2021; **43**:219–293.

Georgalis GL, Halaçlar K, Mayda S, Kaya T, Ayaz D. First fossil find of the *Blanus strauchi* complex (Amphisbaenia, Blanidae) from the Miocene of Anatolia. *Journal of Vertebrate Paleontology* 2018a; **38**:e1437044.

Georgalis GL, Smith KT, Marivaux L, Herrel A, Essid EM, Khayati Ammar H, Marzougui W, Temani R, Tabuce R. 3D models related to the publication: The world's largest Worm Lizard - a new giant trogonophid (Squamata, Amphisbaenia) with extreme dental adaptations from the Eocene of Chambi, Tunisia. *MorphoMuseuM* 2024. https://doi.org/10.18563/journal.m3.245

Georgalis GL, Villa A, Delfino M. The last amphisbaenian (Squamata) from continental Eastern Europe. *Annales de Paléontologie* 2018b; **104**:155–159.

Georgalis GL, Villa A, Ivanov M, Delfino M. New diverse amphibian and reptile assemblages from the late Neogene of northern Greece provide novel insights into the emergence of extant herpetofaunas of the southern Balkans. *Swiss Journal of Palaeontology* 2024; **143**. https://doi.org/10.1186/s13358-024-00332-7

Georgalis GL, Villa A, Vlachos E, Delfino M. Fossil amphibians and reptiles from Plakias, Crete: a glimpse into the earliest late Miocene herpetofaunas of southeastern Europe. *Geobios* 2016; **49**:433–444.

Gervais P. Recherches sur l'ostéologie de plusieurs espèces d'Amphisbènes, et remarques sur la classification de ces reptiles. *Annales des Sciences Naturelles* 1853; **20**:293–312.

Gheerbrant E, Hartenberger JL. Nouveau mammifère insectivore (?Lipotyphla ?Erinaceomorpha) de l'Eocène inférieur de Chambi (Tunisia). *Paläontologische Zeitschrift* 1999; **73**:143–156.

Gilmore CW. Fossil Lizards of North America. *National Academy of Sciences, Memoir* 1928; **22**:201 pp.

Gilmore, C. Paleocene faunas of the Polecat Bench Formation, Park County, Wyoming, Part II. Lizards. *Proceedings of the American Philosophical Society* 1942; **85**:159–167.

Goloboff P, Catalano S. TNT, version 1.5, with a full implementation of phylogenetic morphometrics. *Cladistics* 2016; **32**:221–238.

Goloboff P, Farris, Nixon K. *TNT. Tree Analysis Using New Technology. Program and documentation*. 2003; available at http://www.lillo.org.ar/phylogeny/tnt/

Goloboff P, Farris, Nixon K. TNT, a free program for phylogenetic analysis. *Cladistics* 2008; **24**:774–786.

Graboski R, Grazziotin FG, Mott T, Rodrigues MT. The phylogenetic position of Ridley's Worm Lizard reveals the complex biogeographic history of New World insular amphisbaenids. *Molecular Phylogenetics and Evolution* 2022; **173**:107518.

Gray JE. Zoological Collection. In: *Synopsis of the contents of the British Museum*. London: G. Woodfall and Son, Angel Court, Skinner Street 1840; pp. 18–152.

Gray JE. *Catalogue of the Tortoises, Crocodiles, and Amphisbaenians in the Collection of the British Museum*. London: British Museum of Natural History 1844; 80 pp.

Gray JE. A revision of the genera and species of Amphisbænians, with the descriptions of some new species now in the collection of the British Museum. *Proceedings of the Scientific Meetings of the Zoological Society of London* 1865; **1865**:442–455.

Günther ACLG. Description of new species of reptiles from eastern Africa. Annals and Magazine of Natural History, series 5 1880; **6(33)**:234–238.

Günther ACLG. Description of the amphisbaenians and ophidians collected by Prof. I. Bayley Balfour in the island of Socotra. *Proceedings of the Zoological Society of London* 1881; **1881**:461–462.

Hartenberger JL. Hypothèse paléontologique sur l'origine des Macroscelidea. *Comptes rendus de l'Académie des Sciences, Paris* 1986; **302**:247–249.

Hartenberger J-L, Crochet J-Y, Martinez C, Feist M, Godinot M, Mannai Tayech B, Marandat B, Sigé B. Le gisement de mammifères de Chambi (Éocène, Tunisie centrale) dans son contexte géologique. Apport à la connaissance de l'évolution des mammifères en Afrique. In: Aguilar J-P, Legendre S, Michaux J, (eds). *Actes du Congrès Biochrom'97, Montpellier, 14-17 Avril. Biochronologie mammalienne du Cénozoïque en Europe et domaines reliés*. Montpellier: Ecole pratique des hautes études, Institut de Montpellier, Mémoires et travaux de l'Institut de Montpellier 1997; **21**:233–244.

Hartenberger J-L, Crochet J-Y, Martinez C, Marandat B, Sigé B. The Eocene mammalian fauna of Chambi (Tunisia) in its geological context. In: Gunnell GF, (ed), *Eocene Biodiversity: Unusual Occurrences and Rarely Sampled Habitats*. New York: Kluwer Academic/Plenum 2001; pp. 237–250.

Hartenberger J-L, Marandat B. A new genus and species of an early Eocene Primate from North Africa. *Human Evolution* 1992; **7**:9–16.

Hawkins RK, Bell CJ, Olori JC, Stocker MR. Intraspecific variation in the cranial osteology of *Diplometopon zarudnyi* (Squamata: Amphisbaenia: Trogonophidae). *Journal of Morphology* 2022; **283**:1359–1375.

Head JJ, Bloch JI, Hastings AK, Bourque JR, Cadena EA, Herrera FA, Polly PD, Jaramillo CA. Giant boid snake from the Palaeocene neotropics reveals hotter past equatorial temperatures. *Nature* 2009; **457**:715–717.

Head JJ, Müller J. Chapter 8 - Amphibians and Squamates from the Baynunah Formation. In: Bibi F, Kraatz B, Beech MJ, Hill A, (eds.). *Sands of Time: Ancient Life in the Late Miocene of Abu Dhabi, United Arab Emirates*. Cham: Springer Nature Switzerland, Vertebrate Paleobiology and Paleoanthropology 2022; pp. 111–123.

Hembree DI. Phylogenetic revision of Rhineuridae (Reptilia: Squamata: Amphisbaenia) from the Eocene to Miocene of North America. *The University of Kansas Paleontological Contributions* 2007; **15**:1–20.

Herrel A, Aerts P, De Vree F. Static biting in lizards: functional morphology of the temporal ligaments. *Journal of Zoology, London* 1998; **244**:135–143.

Herrel A, Holanova V. Cranial morphology and bite force in *Chamaeleolis* lizards – adaptations to molluscivory? *Zoology* 2008; **111**:467–475.

Herrel A, Spithoven L, Van Damme R, De Vree F. Sexual dimorphism of head size in *Gallotia galloti*; testing the niche divergence hypothesis by functional analyses. *Functional Ecology* 1999; **13**:289–297.

Hipsley CA, Müller J. Relict endemism of extant Rhineuridae (Amphisbaenia): testing for phylogenetic niche conservatism in the fossil record. *The Anatomical Record* 2014; **297**:473–481.

Hoffstetter R. Squamates de type moderne. In: Piveteau J, (ed). *Traité de Paléontologie, vol. 5*. Paris: Masson 1955; pp. 606–662.

Hoffstetter R. Revue des récentes acquisitions concernant l'histoire et la systématique des Squamates. Problèmes actuels de paléontologie-Évolution des Vertébrés. *Colloques internationaux du Centre National de la Recherche Scientifique* 1962; **104**:243–279.

Hoffstetter R, Gasc J. Vertebrae and ribs of modern reptiles. In: Gans C, Bellairs Ad'A, Parsons TS, (eds). *Biology of the Reptilia, Vol. 1 (Morphology A)*. London and New York: Academic Press 1969; pp. 201–310.

Houle A. Floating islands: a mode of long-distance dispersal for small and medium-sized terrestrial vertebrates. *Diversity and Distributions* 1998; **4**:201–216.

International Commission of Zoological Nomenclature (ICZN). *International Code of Zoological Nomenclature, 4th Edition*. London: The International Trust for Zoological Nomenclature 1999.

Ivanov M, Čerňanský A, Bonilla-Salomón I, Luján ÀH. Early Miocene squamate assemblage from the Mokrá-Western Quarry (Czech Republic) and its palaeobiogeographical and palaeoenvironmental implications. *Geodiversitas* 2020; **42**:343–376.

Jared C, de Barros Filho JD, Jared SGS, Alexandre C, Mailho-Fontana PL, Almeida-Santos SM, Antoniazzi MM. Peering into the unknown world of amphisbaenians (Squamata, Amphisbaenia): A summary of the life history of *Amphisbaena alba*. *Acta Zoologica* 2024.

Jiménez-Hidalgo E, Smith KT, Guerrero-Arenas R, Alvarado-Ortega J. The first late Eocene continental faunal assemblage from tropical North America. *Journal of South American Earth Sciences* 2015; **57**:39–48.

Jones MEH, Anderson CJ, Hipsley CA, Müller J, Evans SE, Schoch R. Integration of molecules and new fossils supports a Triassic origin for Lepidosauria (lizards, snakes, and tuatara). *BMC Evolutionary Biology* 2013; **13**:208.

Kaup JJ. *Trogonophis*, Eine neue Amphibiengattung, den Amphisbaenen zunächst verwandt. *Isis von Oken* 1830; **23**:880–881.

Kearney M. Appendicular skeleton in amphisbaenians (Reptilia: Squamata). *Copeia* 2002; **2002**:719–738.

Kearney M. Systematics of the Amphisbaenia (Lepidosauria: Squamata) based on morphological evidence from recent and fossil forms. *Herpetological Monographs* 2003; **17**:1–74.

Kearney M, Maisano JA, Rowe T. Cranial anatomy of the extinct amphisbaenian *Rhineura hatcherii* (Squamata, Amphisbaenia) based on high-resolution X-ray computed tomography. *Journal of Morphology* 2005; **264**:1–33.

Klembara J, Böhme M, Rummel M. 2010. Revision of the anguine lizard *Pseudopus laurillardi* (Squamata, Anguidae) from the Miocene of Europe, with comments on paleoecology. *Journal of Paleontology* 2010; **84**:159–196.

Klembara J, Dobiašová K, Hain M, Yaryhin O. Skull anatomy and ontogeny of legless lizard *Pseudopus apodus* (Pallas, 1775): heterochronic influences on form. *The Anatomical Record* 2017; **300**:460–502.

Klembara J, Hain M, Dobiašová K. 2014. Comparative anatomy of the lower jaw and dentition of *Pseudopus apodus* and the interrelationships of species of subfamily Anguinae (Anguimorpha, Anguidae). *The Anatomical Record* 2014; **297**:516–544.

Kuhn O. Die Familien der fossilen Amphibien und Reptilien. *Bericht der naturforschenden Gesellschaft Bamberg* 1960; **37**:20–52.

Kuhn O. *Die Reptilien, System und Stammesgeschichte*. Krailing bei München: Verlag Oeben 1966; 154 pp.

Kuhn O. *Amphibien und Reptilien. Katalog der Subfamilien und höheren Taxa mit Nachweis des ersten Auftretens*. Stuttgart: G. Fischer 1967; 124 pp.

Lebrun R. MorphoDig, an open-source 3d freeware dedicated to biology. In: *IPC5 The 5th International Palaeontological Congress*, Paris 2012.

Lee MSY. Convergent evolution and character correlation in burrowing reptiles: towards a resolution of squamate relationships. *Biological Journal of the Linnean Society* 1998; **65**:369–453.

Leite AT de S, Poscai AN, da Silva Casas AL. Revisiting the feeding anatomy of the semi-aquatic lizard *Dracaena guianensis* Daudin, 1801 (Reptilia, Sauria) from the Western Brazilian Amazon. *Journal of Morphological Sciences, Brazilian Society of Anatomy* 2021; **38**:44–50.

Leonard KC, Worden N, Boettcher M, Dickinson E, Omstead KM, Burrows AM, Hartstone-Rose A. Anatomical and ontogenetic influences on muscle density. *Scientific Reports* 2021; **11**:2114.

Longrich NR, Vinther J, Pyron RA, Pisani D, Gauthier JA. Biogeography of worm lizards (Amphisbaenia) driven by end-Cretaceous mass extinction. *Proceedings of the Royal Society B* 2015; **282**:20143034.

Loomis FB. An amphibian from the Eocene. *The American Journal of Science* 1919; **197**:217–219.

Loréal E, Georgalis GL, Čerňanský A. *Pseudopus pannonicus* (Squamata), the largest known anguid lizard — redescription of the type material and new specimens from the Neogene and Quaternary of Hungary and Poland. *The Anatomical Record* 2024.

Loréal E, Syromyatnikova E, Danilov IG, Čerňanský A. The easternmost record of the largest anguine lizard that has ever lived – *Pseudopus pannonicus* (Squamata, Anguidae): new fossils from the late Neogene of Eastern Europe. *Fossil Record* 2023; **26**:51–84.

MacDonald J. Review of the Miocene Wounded Knee faunas of southwestern South Dakota. *Bulletin of the Los Angeles County Museum of Natural History Science* 1970; **8**:1–82.

Maisano JA, Kearney M, Rowe T. Cranial anatomy of the spade-headed amphisbaenian *Diplometopon zarudnyi* (Squamata, Amphisbaenia) based on high-resolution X-ray computed tomography. *Journal of Morphology* 2006; **267**:70–102.

Makarieva AM, Gorshkov VG, Li B-L. Temperature-associated upper limits to body size in terrestrial poikilotherms. *Proceedings of the Royal Society of London, Series B* 2005; **272**:2325–2328.

Marivaux L, Essid EM, Marzougui W, Khayati Ammar H, Adnet S, Marandat B, Merzeraud G, Tabuce R, Vianey-Liaud M. A new and primitive species of *Protophiomys* (Rodentia, Hystricognathi) from the late middle Eocene of Djebel el Kébar, Central Tunisia. *Palaeovertebrata* 2014; **38**:e2.

Marivaux L, Essid EM, Marzougui W, Khayati Ammar H, Merzeraud G, Tabuce R, Vianey-Liaud M. The early evolutionary history of anomaluroid rodents in Africa: new dental remains of a zegdoumyid (Zegdoumyidae, Anomaluroidea) from the Eocene of Tunisia. *Zoologica Scripta* 2015; **44**:117–134.

Marivaux L, Negri FR, Antoine P-O, Stutz NS, Condamine FL, Kerber L, Pujos F, Ventura Santos R, Alvim AMV, Hsiou AS, Bissaro Júnior MC, Adami-Rodrigues K, Ribeiro AM. An eosimiid primate of South Asian affinities in the Paleogene of Western Amazonia and the origin of New World monkeys. *Proceedings of the National Academy of Sciences, USA* 2023; **120**:e2301338120.

Marivaux L, Ramdarshan A, Essid EM, Marzougui W, Khayati Ammar H, Lebrun R, Marandat B, Merzeraud G, Tabuce R, Vianey-Liaud M. *Djebelemur*, a tiny pre-tooth-combed primate from the Eocene of Tunisia: a glimpse into the origin of crown Strepsirhines. *PLoS ONE* 2013; **8**:e80778.

Martín J, Ortega J, López P, Pérez-Cembranos A, Pérez-Mellado V. Fossorial life does not constrain diet selection in the amphisbaenian *Trogonophis wiegmanni*. *Journal of Zoology* 2013; **291**:226–233.

Martín J, Polo-Cavia N, Gonzalo A, López P, Civantos E. Sexual dimorphism in the North African amphisbaenian *Trogonophis wiegmanni*. *Journal of Herpetology* 2012; **46**:338–341.

Mendez J, Keys A. Density and composition of mammalian muscle. *Metabolism* 1960; **9**:184–188.

Mertens R. Die Familie der Warane (Varanidae). Zweiter Teil: Der Schädel. *Abhandlungen der Senckenbergischen Naturforschen den Gesellschaft* 1942; **465**:117–234.

Montero R, Gans C. The head skeleton of *Amphisbaena alba* Linnaeus. *Annals of the Carnegie Museum* 1999; **68**:15–80.

Mouhsine T, Amani F, Mikdad A. *Agama bibronii* (Sauria : Agamidae) et *Chamaeleo chamaeleon* (Sauria : Chamaeleonidae) d'Ifri n'Ammar (Rif Oriental, Maroc). *Quaternaire* 2022; **33**:151–168.

Mourer-Chauviré C, Essid EM, Khayati Ammar H, Marivaux L, Marzougui W, Temani R, Vianey-Liaud M, Tabuce R. New remains of the very small cuckoo, *Chambicuculus pusillus* (Aves, Cuculiformes, Cuculidae) from the late Early or early Middle Eocene of Djebel Chambi, Tunisia. *Palaeovertebrata* 2016; **40**:1–4.

Mourer-Chauviré C, Tabuce R, Marivaux L, Vianey-Liaud M, Ben Haj Ali M. 2013. A small galliform and a small cuculiform from the Eocene of Tunisia. In: Göhlich UB, Kroh A. (eds.), Paleornithological Research 2013 - Proceedings of the 8th International Meeting of the Society of Avian Paleontology and Evolution. *Verlag Naturhistorisches Museum Wien, Vienna* 2013; pp. 1–15.

Müller AH. *Lehrbuch der Paläozoologie. Band III. Vertebraten. Teil 2. Reptilien und Vögel*. Jena: Gustav Fischer Verlag 1968; 657 pp.

Müller J. Beiträge zur Anatomie und Naturgeschichte der Amphibien. *Zeitschrift für Physiologie* 1831; **4**:190–275.

Müller J, Hipsley CA, Head JJ, Kardjilov N, Hilger A, Wuttke M, Reisz R. Eocene lizard from Germany reveals amphisbaenian origins. *Nature* 2011; **473**:364–367.

Müller J, Hipsley CA, Maisano JA. Skull osteology of the Eocene amphisbaenian *Spathorhynchus fossorium* (Reptilia, Squamata) suggests convergent evolution and reversals of fossorial adaptations in worm lizards. *Journal of Anatomy* 2016; **229**:615–630.

Nikolski AM. Reptiles et amphibiens, reçueillis par Mr. N.A. Zaroudny en Perse en 1903–1904. *Annales de le Museum de Zoologie, Académie impériale des Sciences de St. Pétérsbourg* 1907; **10**:260–301.

Oelrich TM. The anatomy of the head of *Ctenosaura pectinata* (Iguanidae). *Miscellaneous Publications of the Museum of Zoology of the University of Michigan* 1956; **94**:1–122.

Peracca MG. Descrizione di una nuova specie del genre *Monopeltis* Smith, del Congo. *Boletim do Museo do Zoologie y Anatomia Comparada, Universidad de Torino* 1903; **18(448)**:1–3.

Peters WCH. Übersicht einiger von dem, durch seine afrikanischen Sprachforschungen rühmlichst bekannten, Herr Missionär C. H. Hahn bei Neu-Barmen, im Hererolande, an der Westküste von Afrika, im 218 südl. Br. gesammelten Amphibien, nebst Beschreibungen der neuen Arten. *Monatsberichte der Berliner Akademie der Wissenschaften* 1862; **1862**:15–26.

Peters WCH. Über eine neue Art und Gattung der Amphisbaenoiden, *Agamodon anguliceps*, mit eingewachsenen Zähnen, aus Barava (Ostafrica) und über die zu den Trogonophides gehörigen Gattungen. *Mathematik und Naturwissenschaftlichen Mitteilung und Sitzungsberichte Kaiserlichen Preussischen Akademie der Wissenschaften zu Berlin* 1882; **1882(3)**:321–326.

Peyer B. Das Gebiss von *Varanus niloticus* L. und von *Dracaena guianensis* Daud. – Ein Beitrag zur Kenntnis des Reptiliengebisses, nebst einem Anhang über die Entstehung der Zahnformen im Allgemeinen. *Revue Suisse de Zoologie* 1929; **36**:71–102.

Presch W. A survey of the dentition of the macroteiid lizards (Teiidae: Lacertilia). *Herpetologica* 1974; **30**:344–349.

Pyron RA. Novel approaches for phylogenetic inference from morphological data and total-evidence dating in squamate reptiles (lizards, snakes, and amphisbaenians). *Systematic Biology* 2017; **66**:38–56.

Pyron RA, Burbrink FT, Wiens JJ. A phylogeny and revised classification of Squamata, including 4161 species of lizards and snakes. *BMC Evolutionary Biology* 2013; **13**:93.

Quinteros-Muñoz O, Gómez-Murillo P, Marca B. Swimming behavior of *Amphisbaena bassleri* (Squamata: Amphisbaenidae) from Bolivia. *Reptiles & Amphibians* 2023; **30**:e19419.

Pregill G. Durophagous feeding adaptations in an amphisbaenid. *Journal of Herpetology* 1984; **18**:186–191.

Rage J-C. Les squamates du Miocène de Béni Mellal, Maroc. *Géologie Méditerranéene* 1976; **2**:57–70.

Rage J-C. Amphibia and Squamata. In: Thomas H, Sen S, Khan M, Battail B, & Ligabue G, (eds.). The Lower Miocene fauna of Al-Sarrar (Eastern province, Saudi Arabia). *Atlal, Journal of Saudi Arabian Archaeology* 1982; **5**:117.

Rage J-C, Adaci M, Bensalah M, Mahboubi M, Marivaux L, Mebrouk F, Tabuce R. Latest Early-early Middle Eocene deposits of Algeria (Glib Zegdou, HGL50), yield the richest and most diverse fauna of amphibians and squamate reptiles from the Palaeogene of Africa. *Palaeovertebrata* 2021; **44**:32 pp.

Rage J-C, Pickford M, Senut B. Amphibians and squamates from the middle Eocene of Namibia, with comments on pre-Miocene anurans from Africa. *Annales de Paléontologie* 2013; **99**:217–242.

Rajabizadeh M, Van Wassenbergh S, Mallet C, Rücklin M, Herrel A. Tooth-shape adaptations in aglyphous colubrid snakes inferred from three dimensional geometric morphometrics and finite element analysis. *Zoological Journal of the Linnean Society* 2021; **191**:454–467.

Ravel A, Adaci M, Bensalah M, Charruault A-L, Essid EM, Khayati Ammar H, Marzougui W, Mahboubi M, Mebrouk F, Merzeraud G, Vianney-Liaud M, Tabuce R, Marivaux L. Origine et radiation initiale des chauves-souris modernes : nouvelles découvertes dans l'Éocène d'Afrique du Nord. *Geodiversitas* 2016; **38**:355–434.

Ravel A, Adaci M, Bensalah M, Mahboubi M, Mebrouk F, Essid EM, Marzougui W, Khayati Ammar H, Charruault A-L, Lebrun R, Tabuce R, Vianey-Liaud M, Marivaux L. New philisids (Mammalia, Chiroptera) from the Early-Middle Eocene of Algeria and Tunisia: new insight into the phylogeny, paleobiogeography and paleoecology of the Philisidae. *Journal of Systematic Palaeontology* 2015; **13**:691–709.

Ravel A, Marivaux L, Tabuce R, Adaci M, Mahboubi M, Mebrouk F, Bensalah M, Ali BH, Essid EM, Vianey-Liaud M. Eocene Chiroptera from Tunisia and Algeria: new insight into the early evolution of bats in North Africa. In: Lehmann T, Schaal SFK, (eds), The World at the Time of Messel: Puzzles in Palaeobiology, Palaeoenvironment and the History of Early Primates. *22nd International Senckenberg Gesellschaft für Naturforschung Frankfurt* 2011; pp. 139–140.

Ravel A, Marivaux L, Tabuce R, Ben Haj Ali M, Essid EM, Vianey-Liaud M. A new large philisid (Mammalia, Chiroptera, Vespertilionoidea) from the late Early Eocene of Chambi, Tunisia. *Palaeontology* 2012; **55**:1035–1041.

Rieppel O, Labhardt L. Mandibular mechanics in *Varanus niloticus* (Reptilia: Lacertilia). *Herpetologica* 1979; **35**:158–163.

Roček Z. Lizards (Reptilia, Sauria) from the lower Miocene locality Dolnice (Bohemia, Czechoslovakia). *Rozpravy Ceskoslovenské Akademie Ved, Rada Matematickych a prírodních Ved* 1984; **94**:3–69.

Saidani N, Merzoug S, Kherbouche F, Stoetzel E. Nouvelles données sur le contexte taphonomique et environnemental des occupations néolithiques de la grotte de Gueldaman GLD1 (Algérie) d'après l'étude des microvertébrés. Journal of Materials and Environmental Science. *Journal of Materials and Environmental Science* 2016; **7**:3800–3817.

Sallam HM, Seiffert ER. 2016. New phiomorph rodents from the latest Eocene of Egypt, and the impact of Bayesian "clock"-based phylogenetic methods on estimates of basal hystricognath relationships and biochronology. *PeerJ* 2016; **4**:e1717.

Sallam HM, Seiffert ER. Revision of Oligocene '*Paraphiomys*' and an origin for crown Thryonomyoidea (Rodentia: Hystricognathi: Phiomorpha) near the Oligocene–Miocene boundary in Africa. *Zoological Journal of the Linnean Society* 2020; **190**:352–371.

Scanferla CA, Montero R, Agnolín FL. The first fossil record of *Amphisbaena heterozonata* from the late Pleistocene of Buenos Aires Province, Argentina. *South American Journal of Herpetology* 2006; **1**:138–142.

Schleich H-H. Neue Reptilienfunde aus dem Tertiär Deutschlands. 8. *Palaeoblanus tobieni* n. gen., n. sp. - neue Doppelschleichen aus dem Tertiär Deutschlands. *Paläontologische Zeitschrift* 1988; **62**:95–105.

Schleich H-H, Kästle W, Kabisch K. *Amphibians and Reptiles of North Africa*. Koenigstein: Koeltz Scientific Publishers 1996; 630 pp.

Schneider CA, Rasband WS, Eliceiri KW. NIH Image to ImageJ: 25 years of image analysis. *Nature Methods* 2012; **9**:671–675.

Sigé B. Rhinolophoidea et Vespertilionoidea (Chiroptera) du Chambi (Eocène inférieur de Tunisie). Aspects biostratigraphique, biogéographique et paléoécologique de l'origine des chiroptères modernes. *Neues Jahrbuch für Geologie und Paläontologie - Abhandlungen* 1991; **182**:355–376.

Simões T, Caldwell MW, Tałanda M, Bernardi M, Palci A, Vernygora O, Bernardini F, Mancini L, Nydam RL. The origin of squamates revealed by a Middle Triassic lizard from the Italian Alps. *Nature* 2018; **557**:706–709.

Singhal S, Colston TJ, Grundler MR, Smith SA, Costa GC, Colli GR, Moritz C, Pyron RA, Rabosky DL. Congruence and conflict in the higher-level phylogenetics of squamate reptiles: an expanded phylogenomic perspective. *Systematic Biology* 2021; **70**:542–557.

Smith A. *Illustrations of the zoology of South Africa : consisting chiefly of figures and descriptions of the objects of natural history collected during an expedition into the interior of South Africa, in the years 1834, 1835, and 1836, fitted out by "The Cape of Good Hope Association for Exploring Central Africa" : together with a summary of African zoology, and an inquiry into the geographical ranges of species in that quarter of the globe. Volume 3, Reptilia*. London: Smith, Elder and Co 1848.

Smith KT. A diverse new assemblage of late Eocene squamates (Reptilia) from the Chadron formation of North Dakota, USA. *Palaeontologia Electronica* 2006; **9**:1–44.

Smith KT. A new lizard assemblage from the earliest Eocene (zone Wa0) of the Bighorn Basin, Wyoming, USA: biogeography during the warmest interval of the Cenozoic. *Journal of Systematic Palaeontology* 2009; **7**:299–358.

Smith KT. New constraints on the evolution of the snake clades Ungaliophiinae, Loxocemidae and Colubridae (Serpentes), with comments on the fossil history of erycine boids in North America. *Zoologischer Anzeiger* 2013; **252**:157–182.

Smith KT. *Pan-Acrodonta* Krister T. Smith, nomen cladi novum. In: de Queiroz K, Cantino PD, & Gauthier JA, (eds). *Phylonyms: A Companion to the PhyloCode*. Boca Raton, Florida: CRC Press 2020; pp. 1165–1168.

Smith KT, Gauthier JA. Early Eocene lizards of the Wasatch Formation near Bitter Creek, Wyoming: diversity and paleoenvironment during an interval of global warming. *Bulletin of the Peabody Museum of Natural History* 2013; **54**:135–230.

Smith KT, Georgalis GL. The diversity and distribution of Palaeogene snakes: a review with comments on vertebral sufficiency. In: Gower D, Zaher H, (eds.), *The Origin and Early Evolution of Snakes*. Cambridge: Cambridge University Press 2022; pp. 55–84.

Smith KT, Schaal S, Sun W, Li CT. Acrodont iguanians (Squamata) from the middle Eocene of the Huadian Basin of Jilin Province, China, with a critique of the taxon "*Tinosaurus*". *Vertebrata PalAsiatica* 2011; **49**:67–84.

Solé F, Essid EM, Marzougui W, Khayati Ammar H, Mahboubi M, Marivaux L, Vianey-Liaud M, Tabuce R. New fossils of Hyaenodonta (Mammalia) from the Eocene localities of Chambi (Tunisia) and Bir el Ater (Algeria), and the evolution of the earliest African hyaenodonts. *Palaeontologia Electronica* 2016; **19**:1–23.

Sternfeld R. *Reptilia. In Wissenschaftliche Ergebnisse der Deutschen Zentral-Afrika Expedition 1907–1908, vol. 4, sect. II, part 9*. Leipzig: Klinkhardt & Biermann 1912; pp. 209–210, pls. vi–ix.

Stocker MR, Kirk EC. The first amphisbaenians from Texas, with notes on other squamates from the middle Eocene Purple Bench locality. *Journal of Vertebrate Paleontology* 2016; **36**:e1094081.

Stoetzel E, Bailon S, El Hajraoui MA, Nespoulet R. Apport sur les connaissances des paléoenvironnements néolithiques du Maroc à partir des Amphibiens-Reptiles de la couche 1 d'El Harhoura 2, Rabat-Temara. *L'Anthropologie* 2008; **112**:731–756.

Streicher JW, Wiens JJ. Phylogenomic analyses of more than 4000 nuclear loci resolve the origin of snakes among lizard families. *Biology Letters* 2017; **13**:20170393.

Sullivan RM. A new Middle Paleocene (Torrejonian) rhineurid amphisbaenian, *Plesiorhineura tsentasi* new genus, new species, from the San Juan Basin, New Mexico. *Journal of Paleontology* 1985; **59**:1481–1485.

Syromyatnikova EV, Kovalenko ES, Kaloyan AA. A fossil record of the Eastern clade of *Blanus* (Amphisbaenia: Blanidae) from the late Miocene of Ukraine. *Geobios* 2021; **69**:69–75.

Syromyatnikova E, Tesakov A, Mayda S, Kaya T, Saraç G. Plio-Pleistocene amphibians and reptiles from Central Turkey: new faunas and faunal records with comments on their biochronological position based on small mammals. *Fossil Imprint* 2019; **75**:343–358.

Tabuce R, Charruault A-L, Adaci M, Bensalah M, Ben Haj Ali M, Essid EM, Marivaux L, Vianey-Liaud M, Mahboubi M. The early Eocene radiation of Hyracoidea (Mammalia, Afrotheria): new fieldwork evidence from northwestern Africa. In: Lehmann T, Schaal SFK, (eds.), The World at the Time of Messel: Puzzles in Palaeobiology, Palaeoenvironment and the History of Early Primates, 22nd International Senckenberg. *Senckenberg Gesellschaft für Naturforschung, Frankfurt* 2011; pp. 161–162.

Tabuce R, Marivaux L, Adaci M, Bensalah M, Hartenberger J-L, Mahboubi M, Mebrouk F, Tafforeau P, Jaeger J-J. Early Tertiary mammals from North Africa reinforce the molecular Afrotheria clade. *Proceedings of the Royal Society of London, B* 2007; **274**:1159–1166.

Tałanda M. Cretaceous roots of amphisbaenian lizards. *Zoologica Scripta* 2016; **45**:1–8.

Tałanda M. Evolution of postcranial skeleton in worm lizards inferred from its status in the Cretaceous stem-amphisbaenian *Slavoia darevskii*. *Acta Palaeontologica Polonica* 2017; **62**:9–23.

Tałanda M, Fernandez V, Panciroli E, Evans SE, Benson RJ. Synchrotron tomography of a stem lizard elucidates early squamate anatomy. *Nature* 2022; **611**:99–104.

Taylor EH. Concerning Oligocene amphisbaenid reptiles. *The University of Kansas Science Bulletin* 1951; **34**:521–558.

Townsend TM, Larson A, Louis E, Macey JR. Molecular phylogenetics of Squamata: the position of snakes, amphisbaenians, and dibamids, and the root of the squamate tree. *Systematic Biology* 2004; **53**:735–757.

Vanzolini PE. A systematic arrangement of the Family Amphisbaenidae (Sauria). *Herpetologica* 1951; **7**:113–123.

Vianey-Liaud M, Comte B, Marandat B, Peigné S, Rage J-C, Sudre J. A new early Late Oligocene (MP 26) continental vertebrate fauna from Saint-Privat-des-Vieux (Alès Basin, Gard, Southern France). *Geodiversitas* 2014; **36**:565–622.

Vianey-Liaud M, Jaeger J-J, Hartenberger J-L, Mahboubi M. Les rongeurs de l'Eocène d'Afrique Nord-Occidentale (Glib Zegdou (Algérie) et Chambi (Tunisie)) et l'origine des Anomaluridae. *Palaeovertebrata* 1994; **23**:93–118.

Vidal N, Azvolinsky A, Cruaud C, Hedges SB. Origin of tropical American burrowing reptiles by transatlantic rafting. *Biology Letters* 2008; **4**:115–118.

Vidal N, Hedges SB. The phylogeny of squamate reptiles (lizards, snakes, and amphisbaenians) inferred from nine nuclear protein-coding genes. *Comptes Rendus Biologies* 2005; **328**:1000–1008.

Vidal N, Hedges SB. The molecular evolutionary tree of lizards, snakes, and amphisbaenians. *Comptes Rendus Biologies* 2009; **332**:129–139.

Villa A, Kirchner M, Alba DM, Bernardini F, Bolet A, Luján ÀH, Fortuny J, Hipsley CA, Müller J, Sindaco R, Tuniz C, Delfino M. Comparative cranial osteology of *Blanus* (Squamata: Amphisbaenia). *Zoological Journal of the Linnean Society* 2019; **185**:693–716.

Wagler JG. *Serpentum brasiliensium species novae ou histoire naturelle des espèces nouvelles de serpens, recueillies et observées pendant le voyage dans l'intérieur du Brésil dans les années 1817, 1818, 1819, 1820, exécuté par ordre de sa majesté le Roi de Bavière*. Monachii (= Munich): Typis F. S. Hübschmanni 1824; 75 pp., 26 pls.

Wagler JG. *Natürliches System der Amphibien, mit vorangehender Classification der Säugthiere und Vögel. Ein Beitrag zur vergleichenden Zoologie*. Munchen, Stuttgart und Tubingen: J.G. Cotta schen Buchhandlung 1830; vi + 354 pp.

Wagner R. *Icones zootomicae. Handatlas zur vergleichenden Anatomie nach fremden und eigenen Untersuchungen*. Leipzig: L. Voss 1841; 44 pp.

Werner F. Reptilia et Amphibia. In Schultze L, (ed), Zoologische und anthropologische Ergebnisse einer Forschungsreise im westlichen und zentralen Südafrika. 4(2, Vertebrata B). *Denkschrift der Medicinisch Naturwissenschaftliche Gesellschaft zu Jena* 1910; **16**:279–370.

Wiens JJ, Hutter CR, Mulcahy DG, Noonan BP, Townsend TM, Sites JW, Reeder TW. Resolving the phylogeny of lizards and snakes (Squamata) with extensive sampling of genes and species. *Biology Letters* 2012; **8**:1043.

Wiens JJ, Kuczynski CA, Townsend T, Reeder TW, Mulcahy DG, Sites JW Jr. Combining phylogenomics and fossils in higher-level squamate reptile phylogeny: molecular data change the placement of fossil taxa. *Systematic Biology* 2010; **59**:674–688.

Zachos JC, Pagani M, Sloan L, Thomas E, Billups K. Trends, rhythms, and aberrations in global climate 65 Ma to present. *Science* 2001; **292**:686–693.

Zangerl R. Contributions to the osteology of the skull of the Amphisbaenidae. *The American Midland Naturalist* 1944; **31**:417–454.

Zangerl R. Contributions to the osteology of the postcranial skeleton of the Amphisbaenidae. *American Midland Naturalist* 1945; **33**:764–780.

Zheng Y, Wiens JJ. Combining phylogenomic and supermatrix approaches, and a time-calibrated phylogeny for squamate reptiles (lizards and snakes) based on 52 genes and 4162 species. *Molecular Phylogenetics and Evolution* 2016; **94**:537–547.

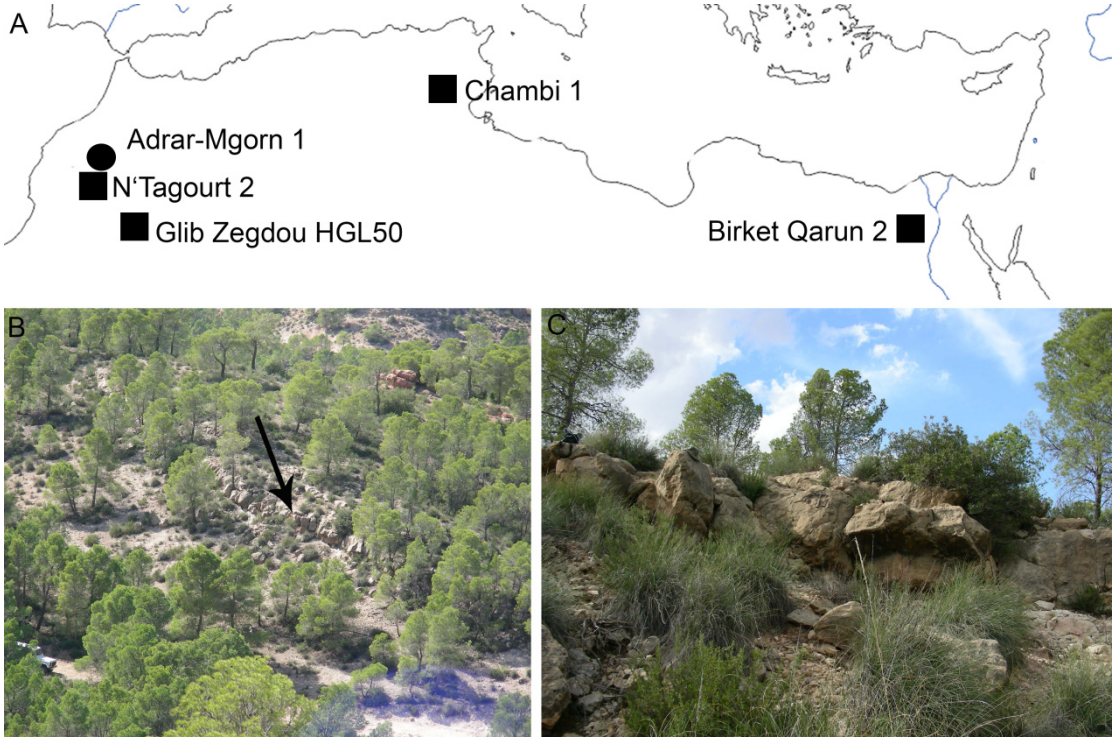

Figure 1. (A) Map of northern Africa, indicating the position of the late early – early middle Eocene locality of Chambi-1 (CBI-1). Also shown are the sole other few Paleogene African localities that have yielded fossil amphisbaenians (with the exception of the record from the middle Eocene of Black Crow, Namibia). Circle for Paleocene, square for Eocene. Map adapted from d-maps (d-maps.com). (B) Photograph of the CBI-1 fossil-bearing locality – arrow indicates the position of the fossiliferous limestone; (C) close-up photograph of the fossiliferous limestone.

Figure 2. Holotype right maxilla (ONM CBI-1-645) of ***Terastiodontosaurus marcelosanchezi*** **gen. et sp. nov.** Photographs of the specimen in labial (A), medial (B), dorsal (C), and ventral (D) views.

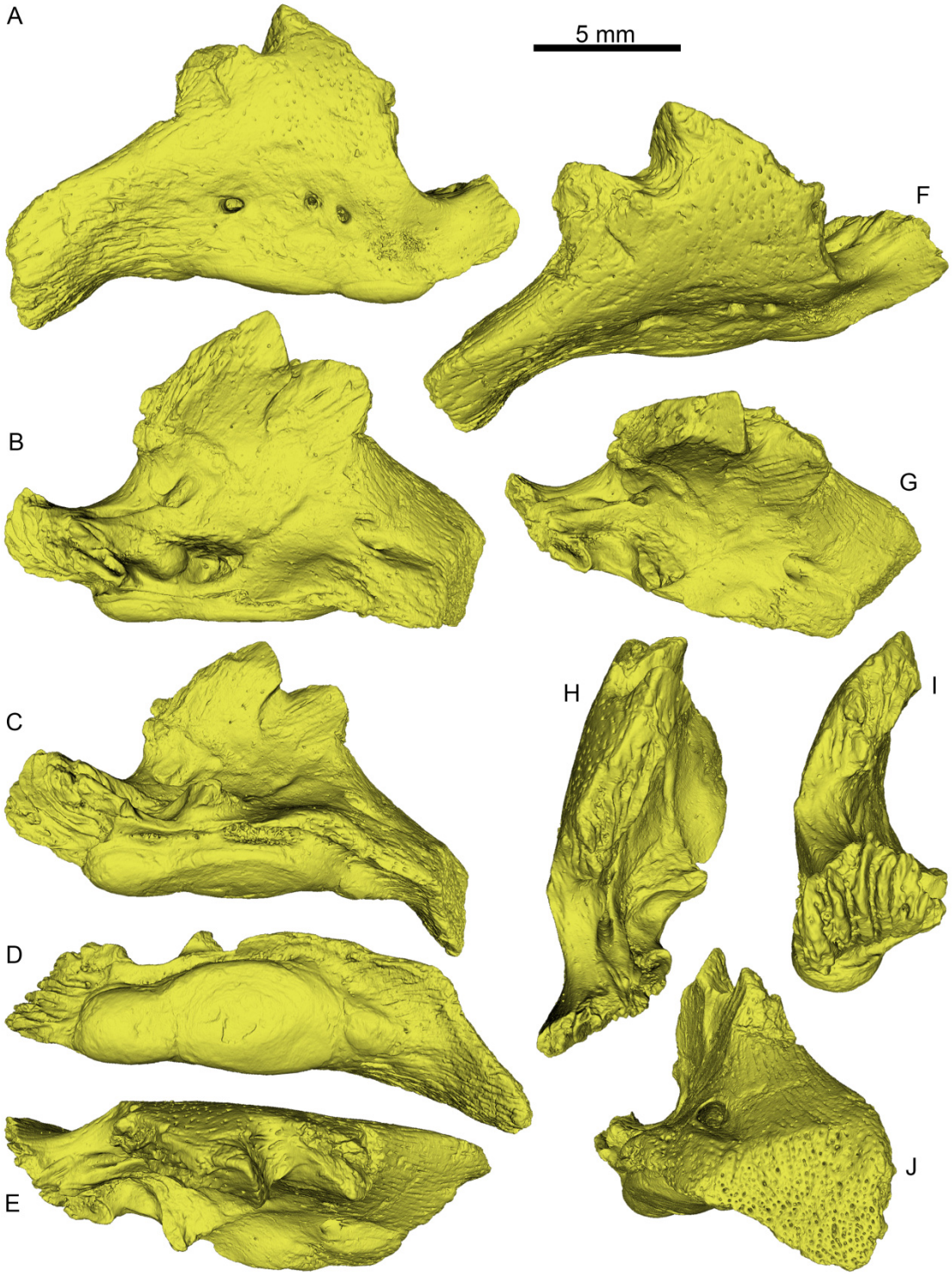

Figure 3. Holotype right maxilla (ONM CBI-1-645) of ***Terastiodontosaurus marcelosanchezi*** **gen. et sp. nov.** µCT 3D images of the specimen in labial (A), medial (B), ventromedial (C), ventral (D), dorsal (E), dorsolateral (F), dorsomedial (G), anterodorsal (H), anterior (I), and posterior (J) views.

Figure 4. Paratype left dentary (ONM CBI-1-646) of ***Terastiodontosaurus marcelosanchezi*** **gen. et sp. nov.** Photographs of the specimen in labial (A), medial (B), and dorsal (C) views.

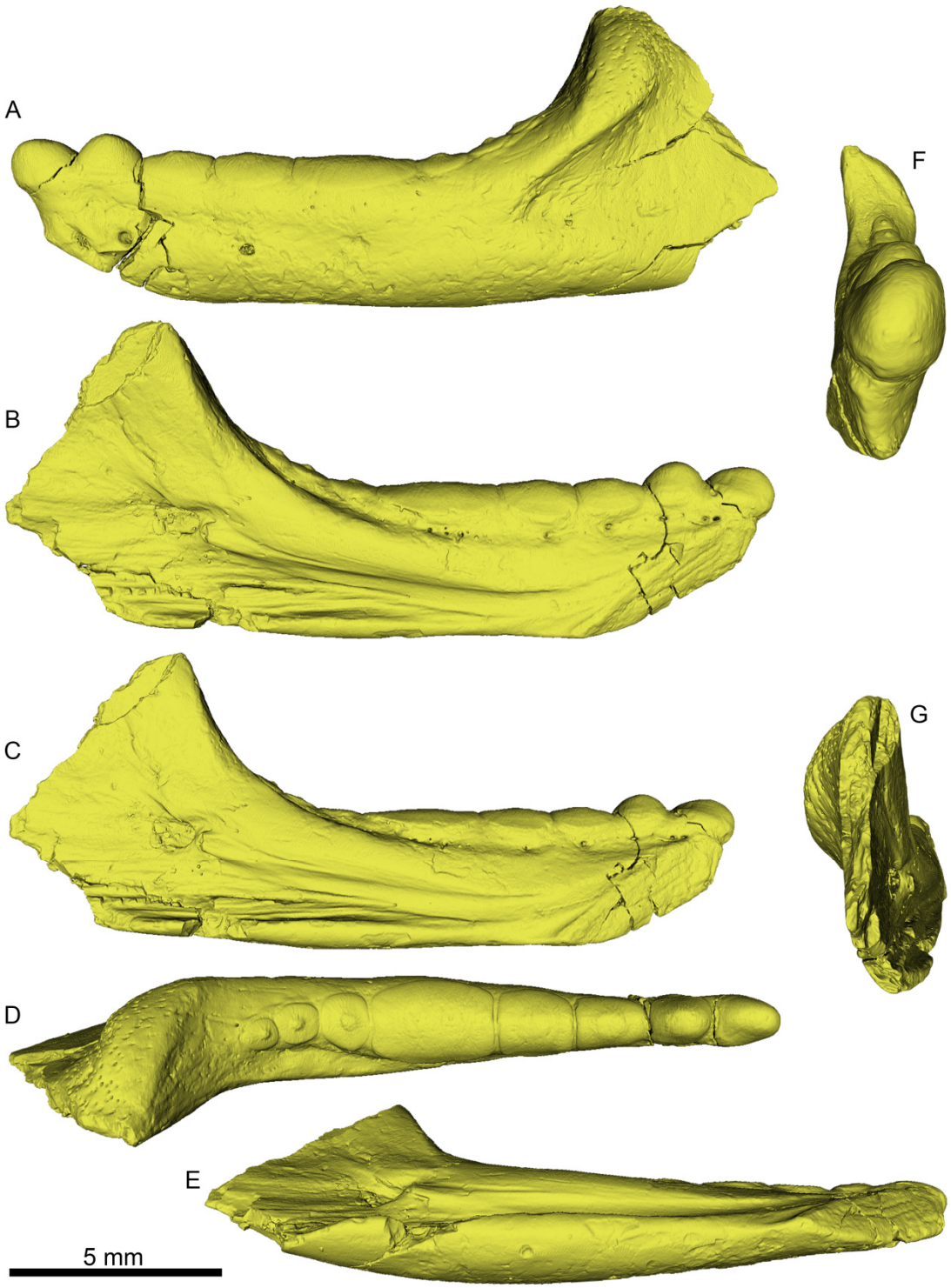

Figure 5. Paratype left dentary (ONM CBI-1-646) of ***Terastiodontosaurus marcelosanchezi*** **gen. et sp. nov.** µCT 3D images of the specimen in labial (A), medial (B), ventromedial (C), dorsal (D), ventral (E), anterodorsal (F), and posterior (G) views. Note that the specimen was slightly damaged during µCT scanning, hence the difference from the photographs in Figure 3.

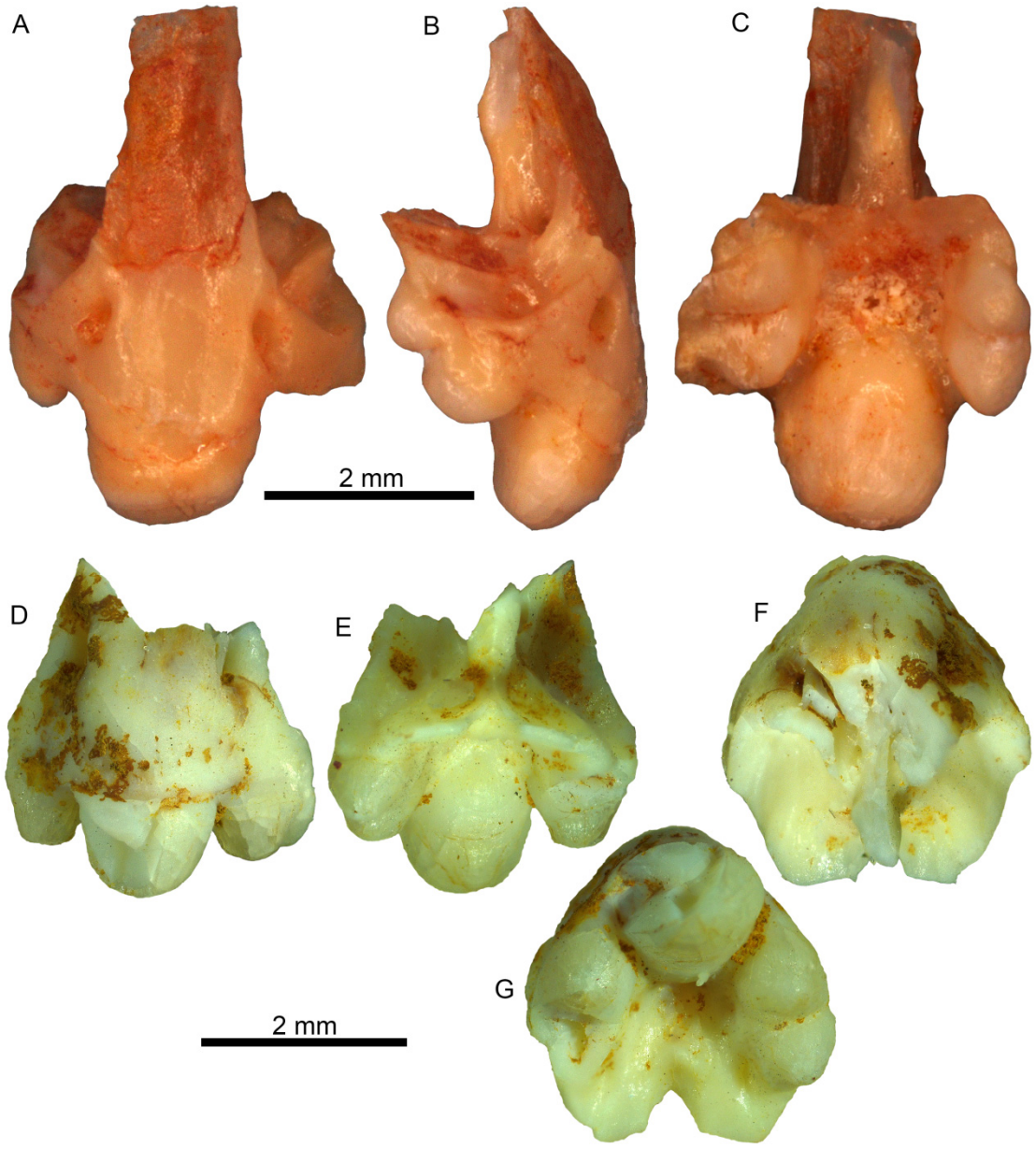

Figure 6. Premaxillae of ***Terastiodontosaurus marcelosanchezi*** **gen. et sp. nov.** Photographs of the larger specimens: (A–C) ONM CBI-1-711 in anterior (A), right lateral (B), and posterior (C) views; (D–G) ONM CBI-1-658 in anterior (D), posterior (E), ventral (F), and dorsal (G) views.

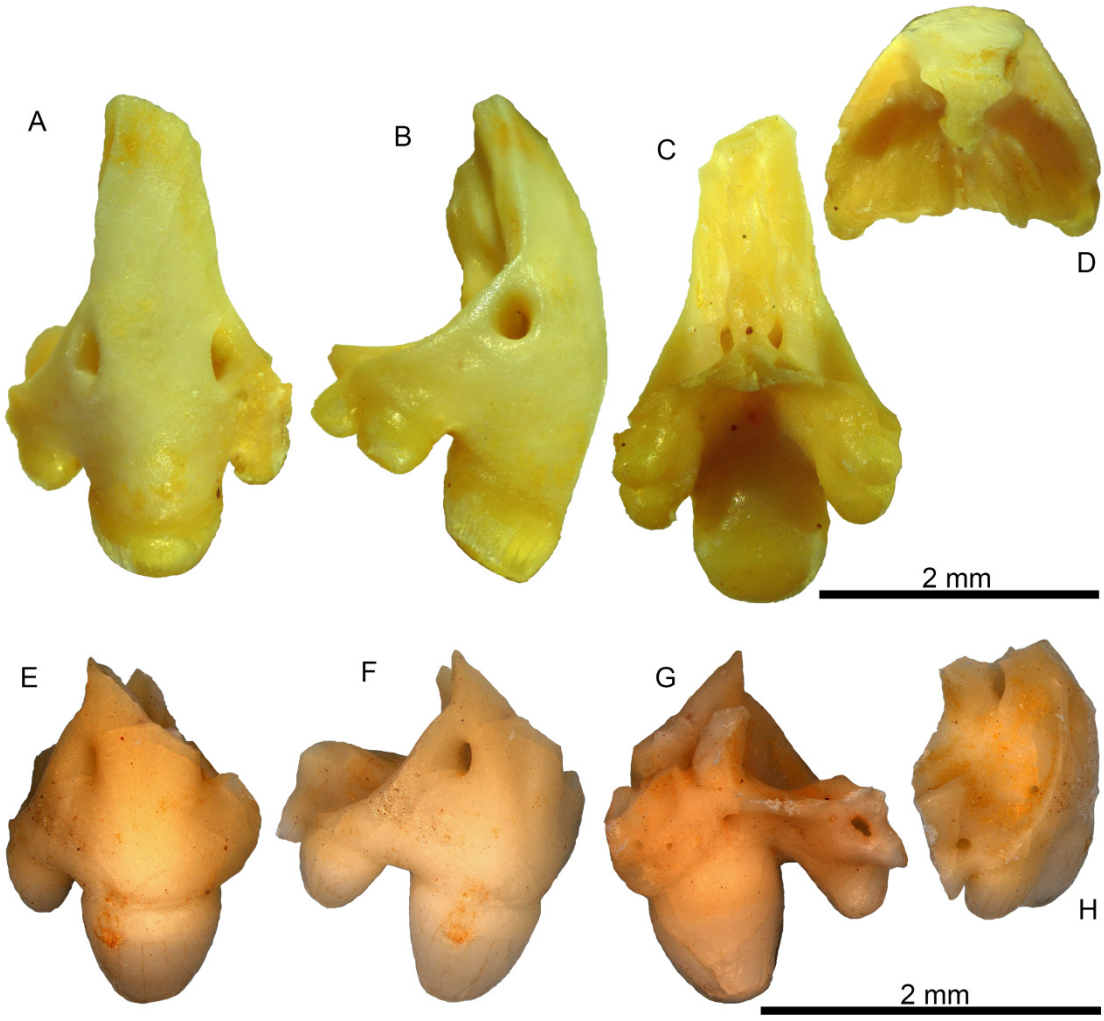

Figure 7. Premaxillae of ***Terastiodontosaurus marcelosanchezi*** **gen. et sp. nov.** Photographs of the smaller specimens: (A–D) ONM CBI-1-672 in anterior (A), right lateral (B), posterior (C), and dorsal (D) views; (E–H) ONM CBI-1-1021 in anterior (E), right anterolateral (F), posterior (G), right dorsolateral (H) views.

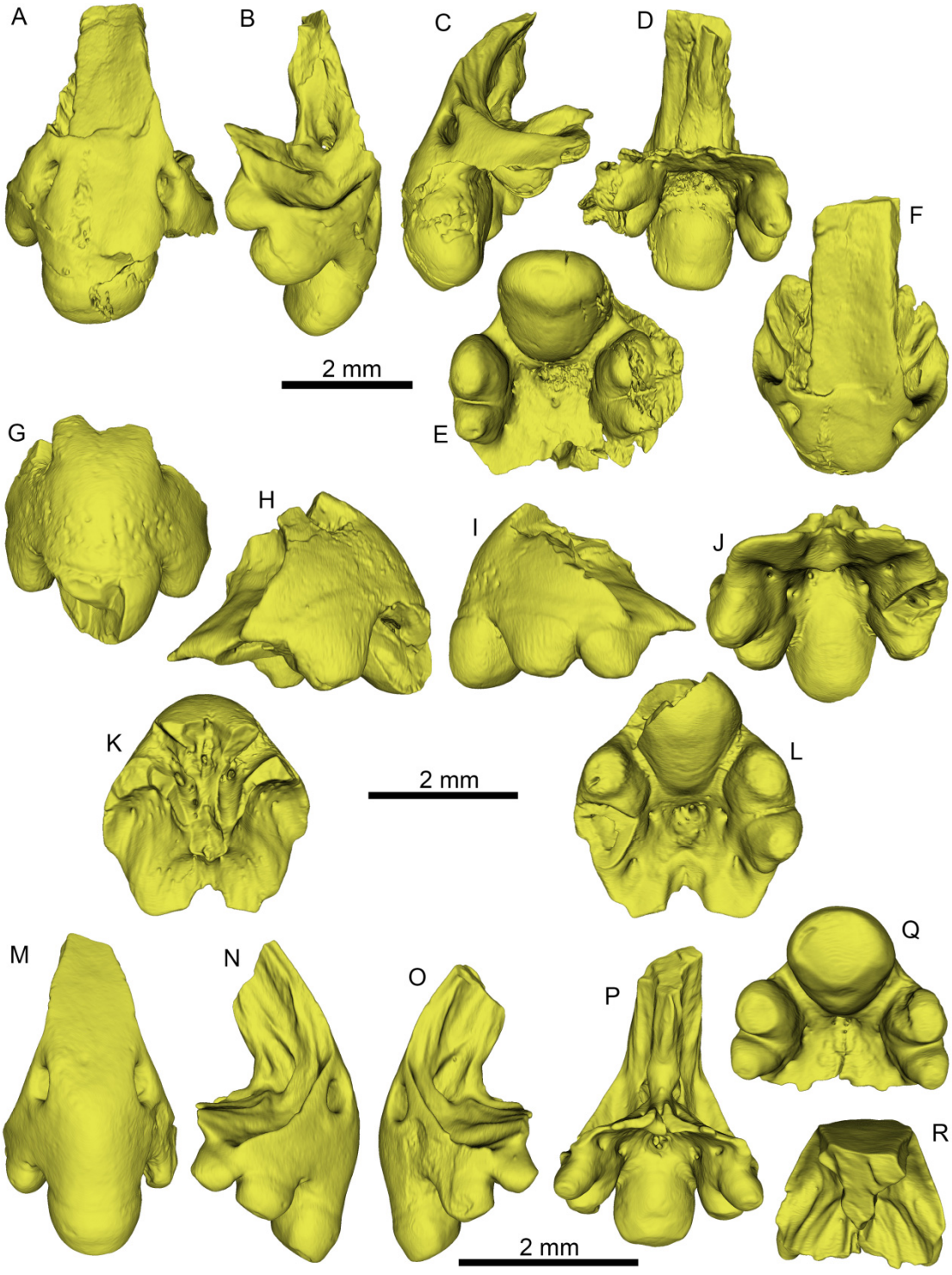

Figure 8. Premaxillae of ***Terastiodontosaurus marcelosanchezi*** **gen. et sp. nov.** 3D images of: (A–F) ONM CBI-1-711 in anterior (A), right lateral (B), left ventrolateral (C), posterior (D), ventral (E), and dorsal (F) views; (G–L) ONM CBI-1-658 in anterior (G), right lateral (H), left lateral (I), posterior (J), dorsal (K), and ventral (L) views; (M–R) ONM CBI-1-672 in anterior (M), right lateral (N), left lateral (O), posterior (P), ventral (Q), and dorsal (R) views.

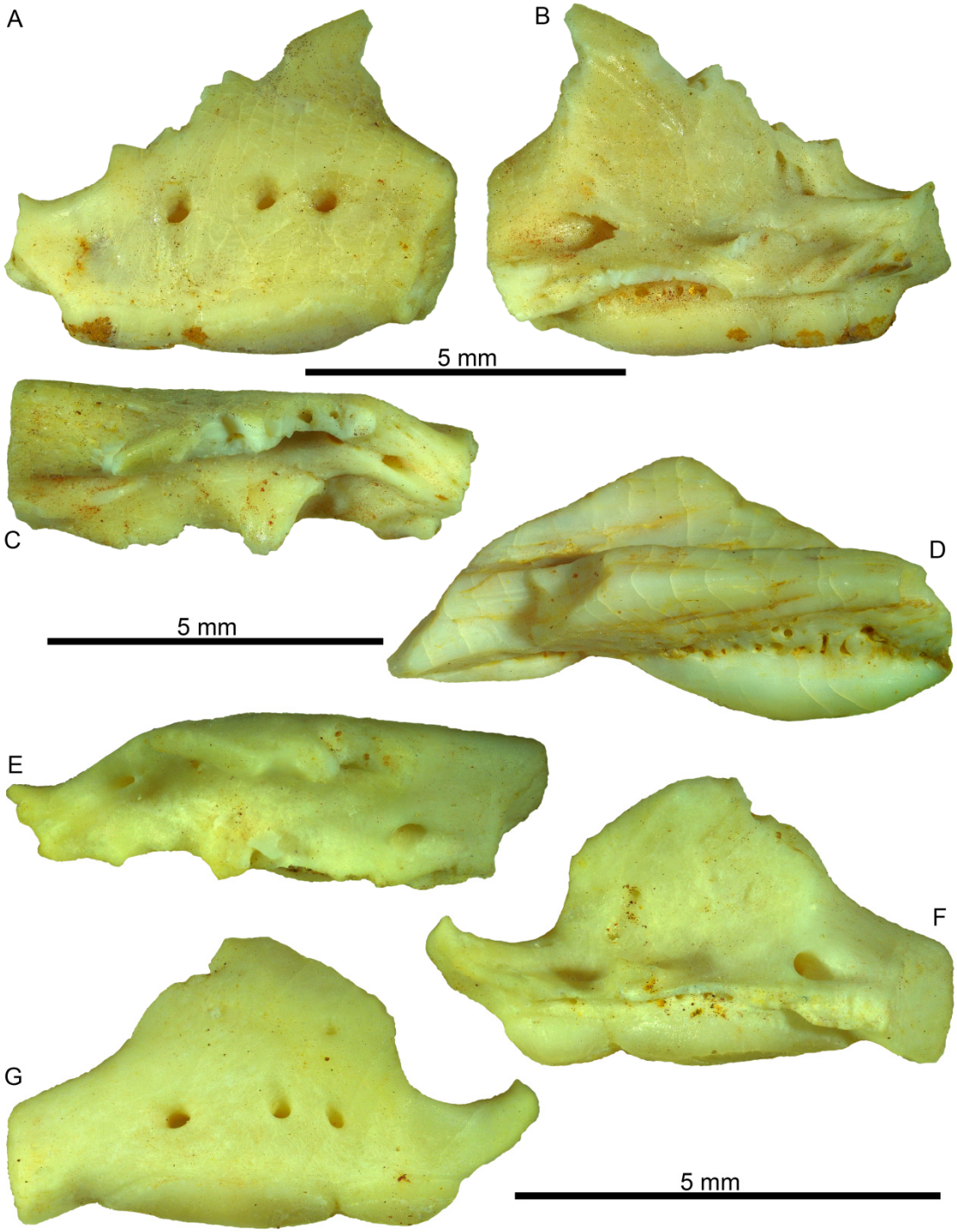

Figure 9. Maxillae of ***Terastiodontosaurus marcelosanchezi*** **gen. et sp. nov.** Photographs of: (A–C) left maxilla ONM CBI-1-648 in labial (A), medial (B), and dorsal (C) views; (D) fragment of right maxilla ONM CBI-1-650 in medial view; (E–G) right maxilla ONM CBI-1-649 of a small-sized individual in dorsal (E), medial (F), and labial (G) views.

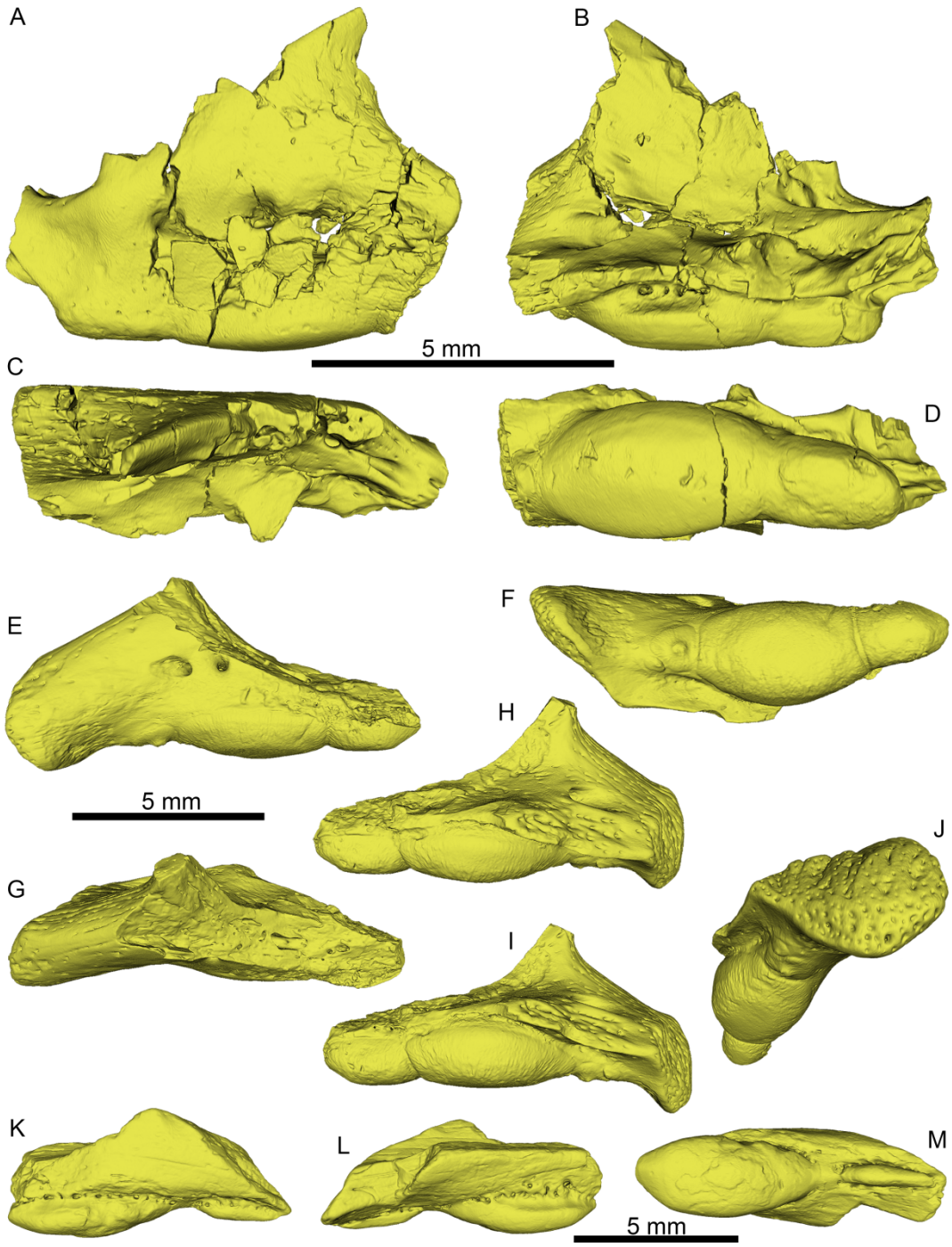

Figure 10. Maxillae of ***Terastiodontosaurus marcelosanchezi*** **gen. et sp. nov.** µCT 3D images of: (A–D) left maxilla ONM CBI-1-648 in labial (A), medial (B), dorsal (C), and ventral (D) views; (E–J) right maxilla ONM CBI-1-651 in labial (E), ventral (F), dorsal (G), medial (H), ventromedial (I), and posteroventral (J) views; (K–M) fragment of right maxilla ONM CBI-1-650 in labial (K), medial (L), and ventral (M) views. Note that specimen ONM CBI-1-648 was slightly damaged during µCT scanning, hence the difference from the photographs in Figure 7.

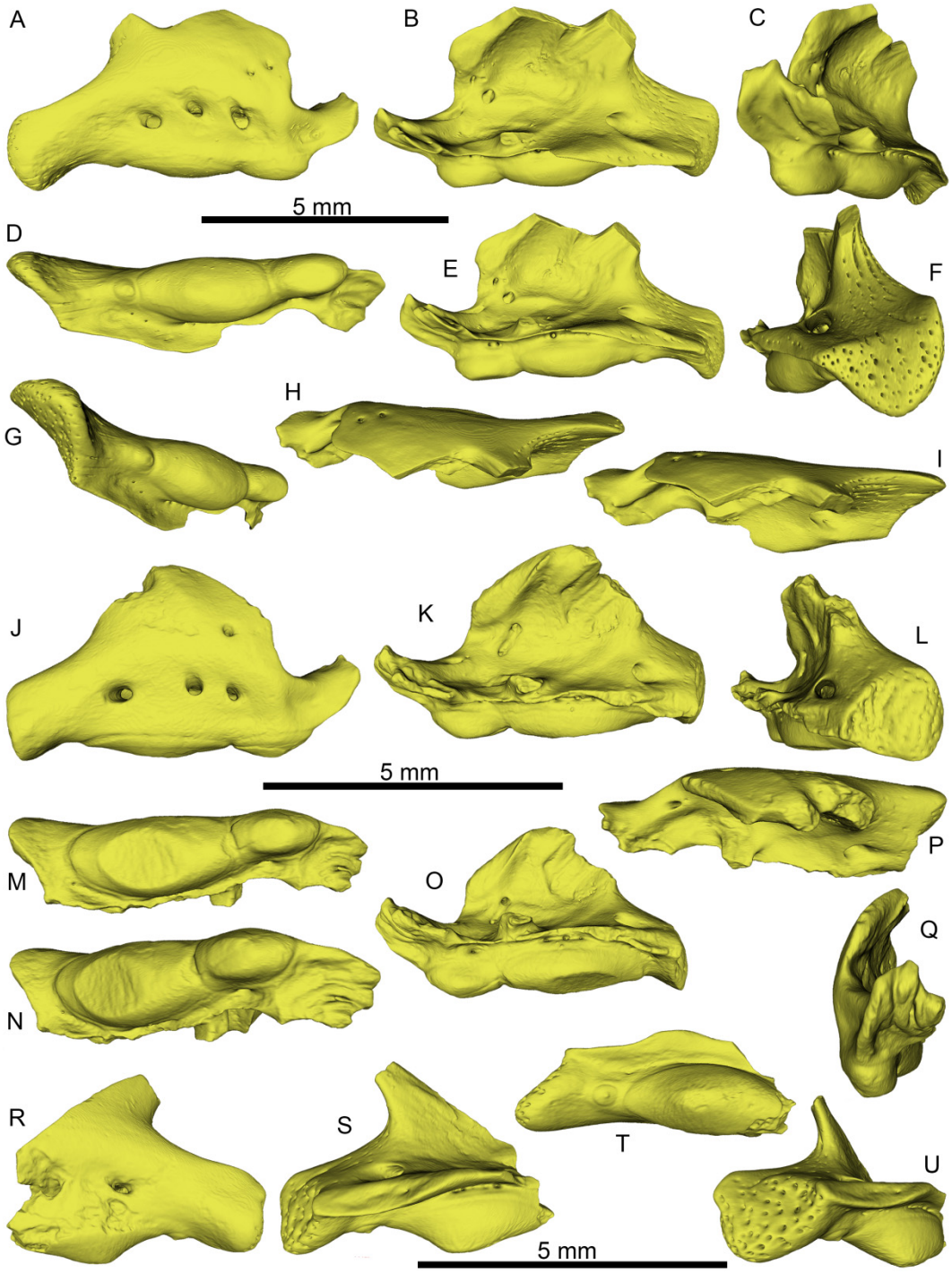

Figure 11. Maxillae of *Terastiodontosaurus marcelosanchezi* gen. et sp. nov., small-sized individuals. µCT 3D images of: (A–I) right maxilla ONM CBI-1-654 in labial (A), medial (B), anteromedial (C), ventral (D), ventromedial (E), posteromedial (F), posteroventral (G), dorsal (H), and dorsomedial (I) views; (J–Q) right maxilla ONM CBI-1-649 in labial (J), medial (K), posteromedial (L), ventral (M), anteroventral (N), ventromedial (O), dorsal (P), and anterior (Q) views; (R–U) posterior portion of left maxilla ONM CBI-1-653 in labial (R), medial (S), ventral (T), and posteromedial (U) views.

Figure 12. Maxillae of ***Terastiodontosaurus marcelosanchezi*** **gen. et sp. nov.** Photographs of: (A–C) posterior fragment of right maxilla ONM CBI-1-667 in labial (A), medial (B), and ventral (C) views; (D–F) posterior fragment of right maxilla ONM CBI-1-1017 in labial (D), ventromedial (E), and ventral (E) views; (G–I) anterior fragment of left maxilla ONM CBI-1-1012 in labial (G), medial (H), and ventral (I) views; (J–L) anterior fragment of left maxilla ONM CBI-1-1016 in labial (J), medial (K), and ventral (L) views; (M–O) anterior fragment of left maxilla ONM CBI-1-1018 in labial (M), medial (N), and ventral (O) views; (P–R) anterior fragment of left maxilla ONM CBI-1-1022 in labial (P), medial (Q), and ventral (R) views.

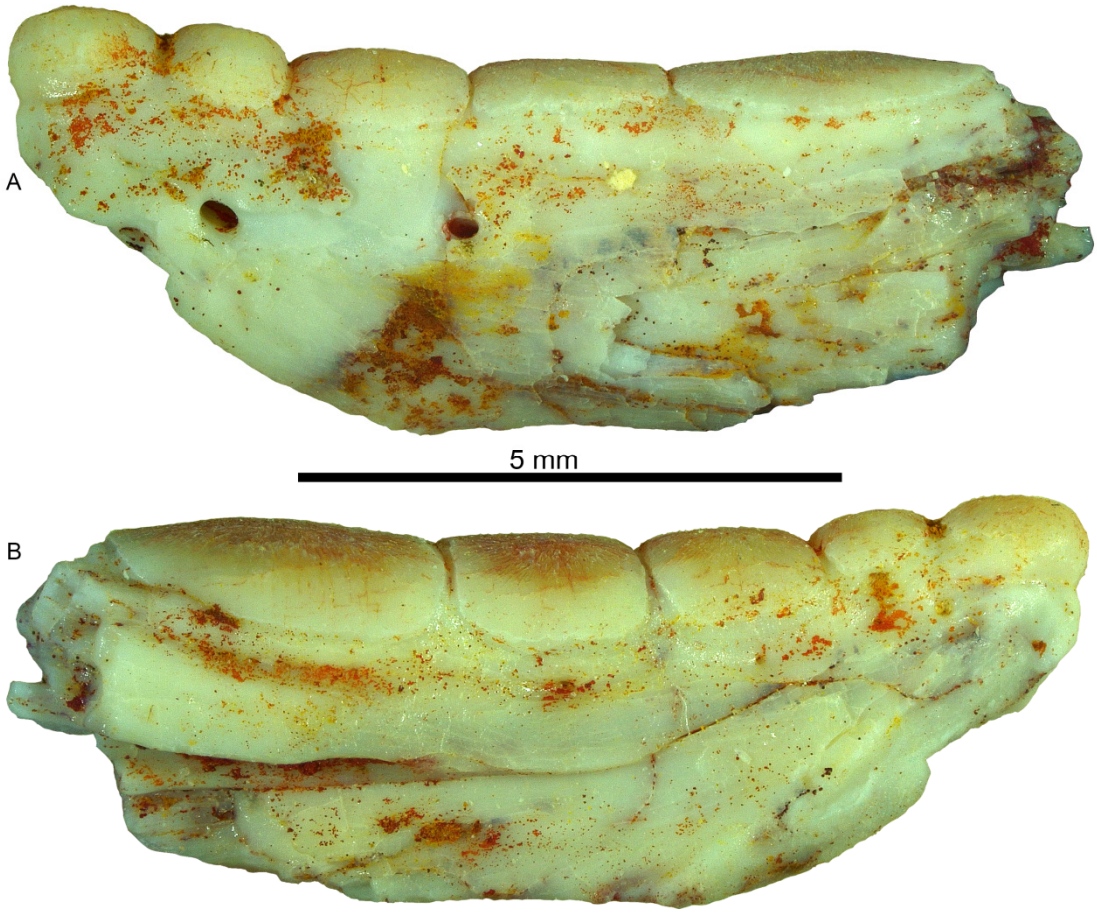

Figure 13. Dentary of ***Terastiodontosaurus marcelosanchezi*** **gen. et sp. nov.** Photographs of left dentary ONM CBI-1-647 in labial (A) and medial (B) views.

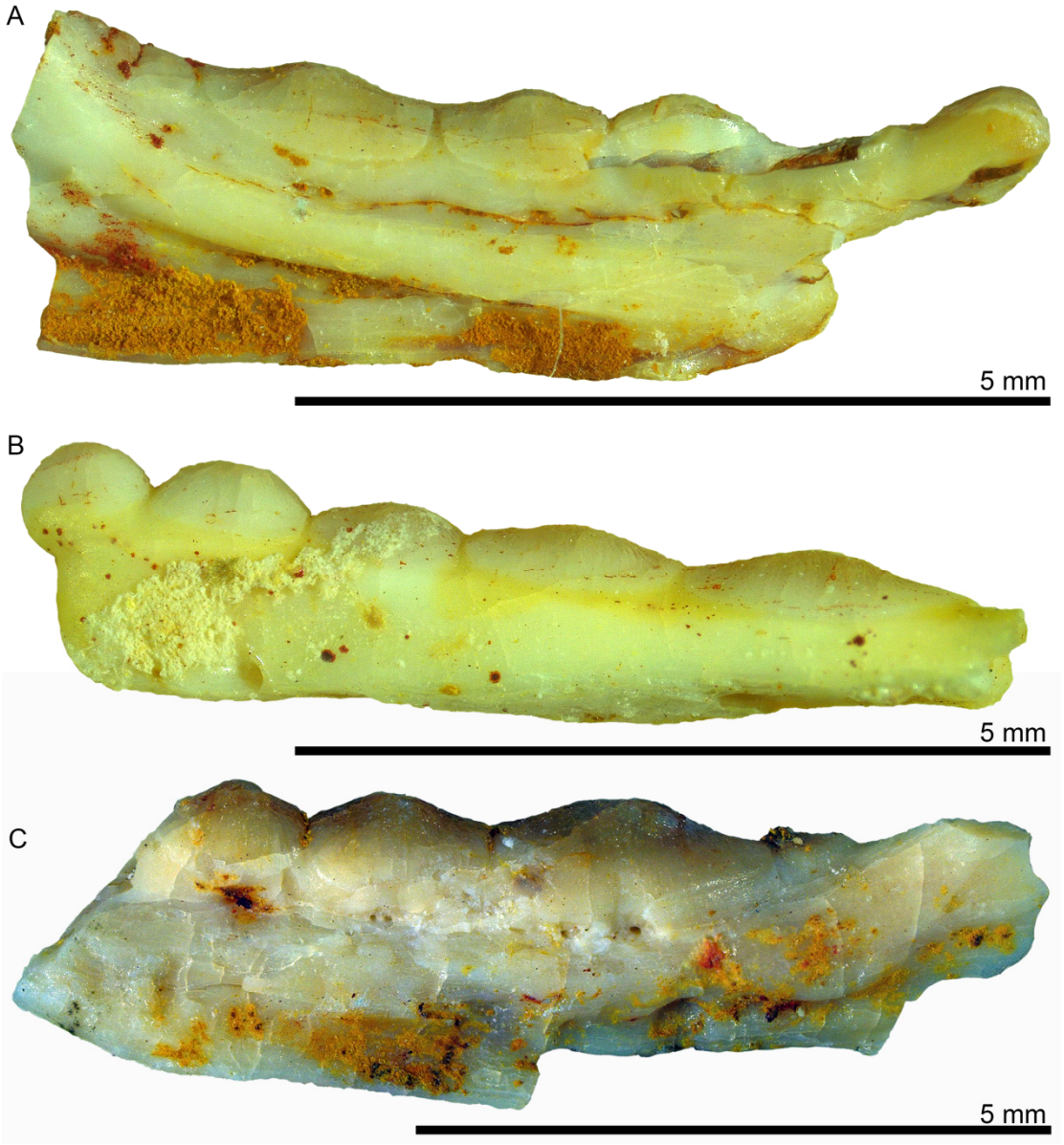

Figure 14. Dentaries of ***Terastiodontosaurus marcelosanchezi*** **gen. et sp. nov.** Photographs of: (A) left dentary ONM CBI-1-657 in medial view; (B) left dentary ONM CBI-1-655 in labial view; (C) right dentary ONM CBI-1-656 in medial view.

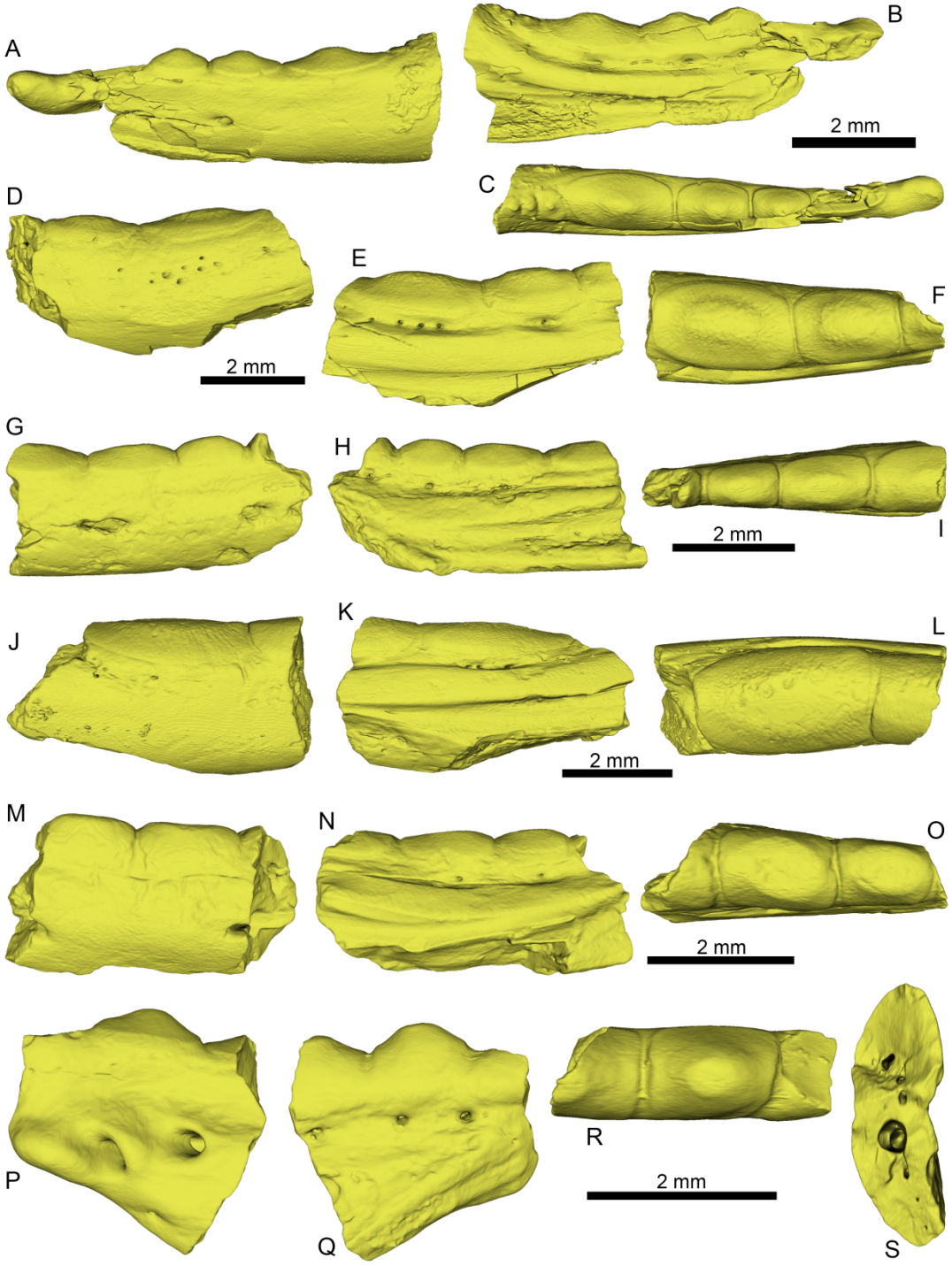

Figure 15. Dentaries of ***Terastiodontosaurus marcelosanchezi*** **gen. et sp. nov.** µCT 3D images of: (A–C) left dentary ONM CBI-1-657 in labial (A), medial (B), and dorsal (C) views; (D–F) left dentary ONM CBI-1-659 in labial (D), medial (E), and dorsal (F) views; (G–I) right dentary ONM CBI-1-660 in labial (G), medial (H), and dorsal (I) views; (J–L) left dentary ONM CBI-1-661 in labial (J), medial (K), and dorsal (L) views; (M–O) left dentary ONM CBI-1-668 in labial (M), medial (N), and dorsal (O) views; (P–S) left dentary ONM CBI-1-670 in labial (P), medial (Q), dorsal (R), and posterior (S) views.

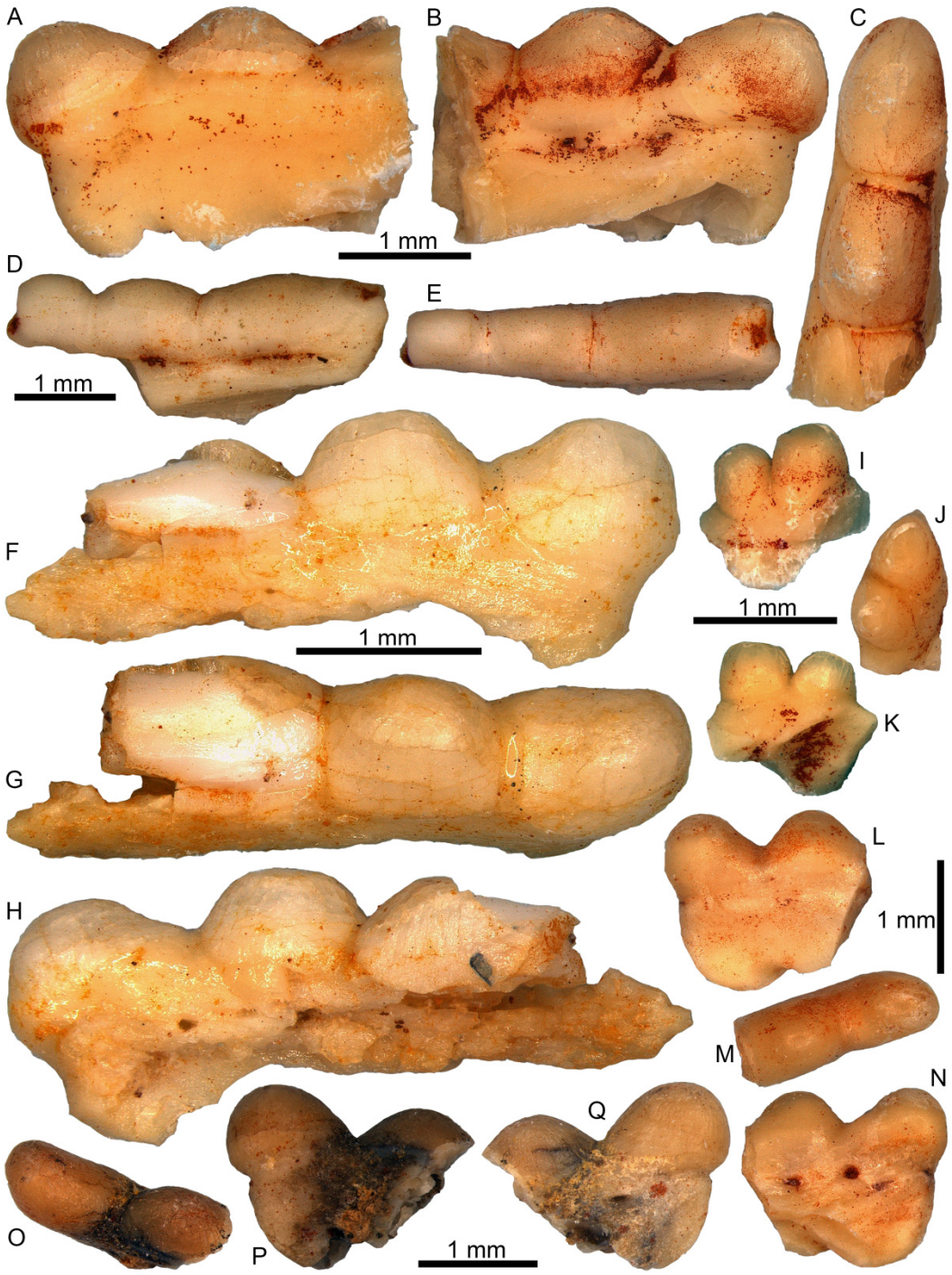

Figure 16. Dentaries of ***Terastiodontosaurus marcelosanchezi*** **gen. et sp. nov.** Photographs of: (A–C) left dentary ONM CBI-1-662 in labial (A), medial (B), and dorsal (C) views; (D–E) right dentary ONM CBI-1-1013 in labial (D) and dorsal (E) views; (F–H) right dentary ONM CBI-1-666 in labial (F), dorsolabial (G), medial (H) views; (I–K) anterior fragment of right dentary ONM CBI-1-1020 in labial (I), dorsal (J), and medial (K) views; (L–N) anterior fragment of left dentary ONM CBI-1-1015 in labial (L), dorsal (M), and medial (N) views; (O–Q) anterior fragment of left dentary ONM CBI-1-1014 in dorsal (O), labial (P), and medial (Q) views.

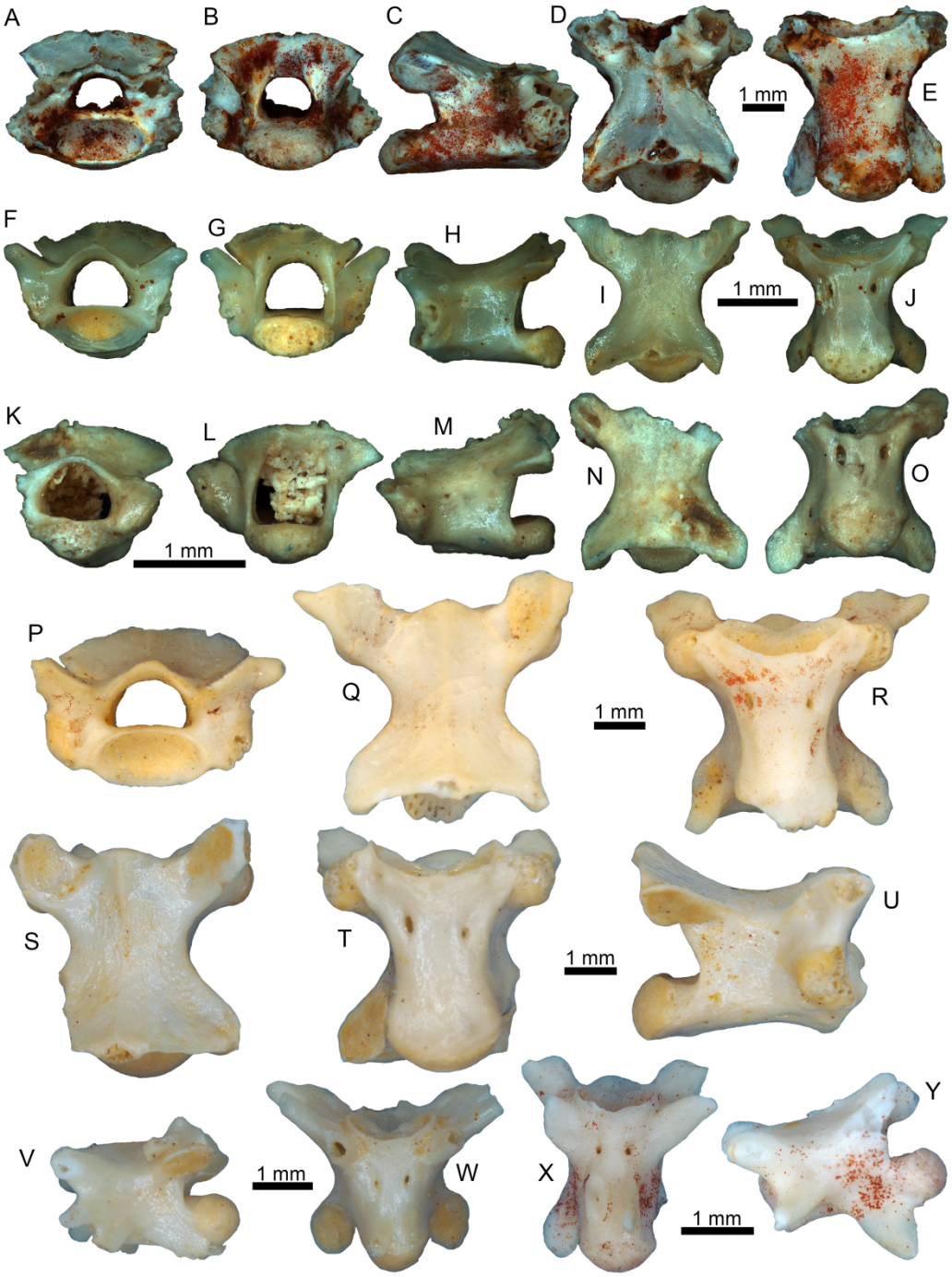

Figure 17. Vertebrae tentatively attributed to ***Terastiodontosaurus marcelosanchezi* gen. et sp. nov.** (A–E) Presacral vertebra ONM CBI-1-833 in anterior (A), posterior (B), right lateral (C), dorsal (D), and ventral (E) views; (F–J) presacral vertebra ONM CBI-1-860 in anterior (F), posterior (G), left lateral (H), dorsal (I), and ventral (J) views; (K–O) presacral vertebra ONM CBI-1-820 in anterior (K), posterior (L), left lateral (M), dorsal (N), and ventral (O) views; (P–R) presacral vertebra ONM CBI-1-682 in anterior (P), dorsal (Q), and ventral (R) views; (S–U) presacral vertebra ONM CBI-1-687 in dorsal (S), ventral (T), and right lateral (U) views; (V–W) anterior caudal vertebra ONM CBI-1-689 in left lateral (V) and ventral (W) views; (X–Y) posterior caudal vertebra ONM CBI-1-686 in ventral (X) and left lateral (Y) views.

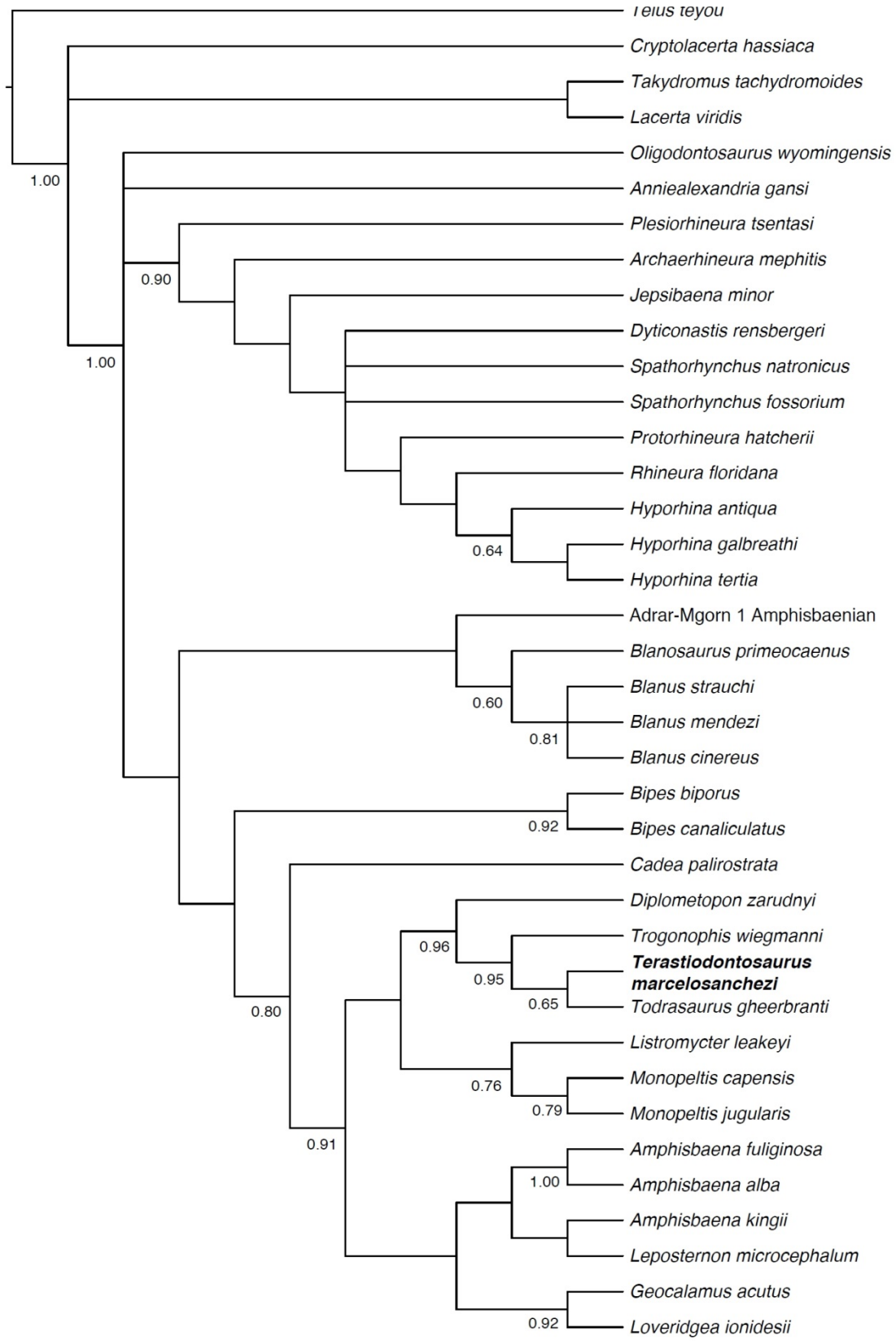

Figure 18. Phylogenetic analysis of Amphisbaenia, strict consensus of MP trees, indicating the position of *Terastiodontosaurus marcelosanchezi* gen. et sp. nov.

Figure 19. *Todrasaurus gheerbranti*, holotype left dentary UM THR 407. Photographs of the specimen in labial (A), medial (B), and dorsal (C) views.

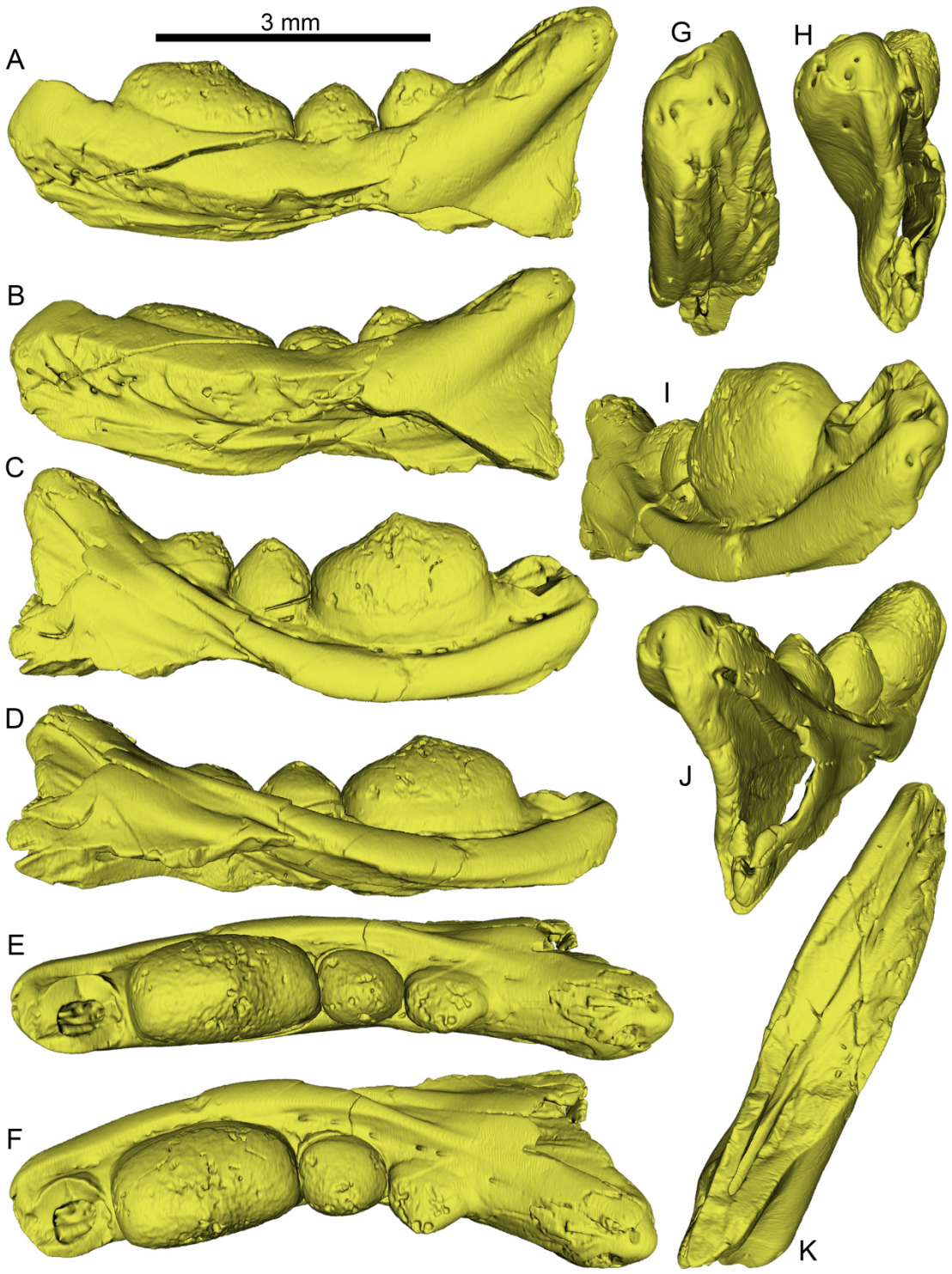

Figure 20. *Todrasaurus gheerbranti*, holotype left dentary UM THR 407. µCT 3D images of the specimen in labial (A), ventrolabial (B), medial (C), ventromedial (D), dorsal (E), dorsomedial (F), anteroventral (G), posterior (H), anteromedial (I), posteromedial (J), and ventral (K) views.

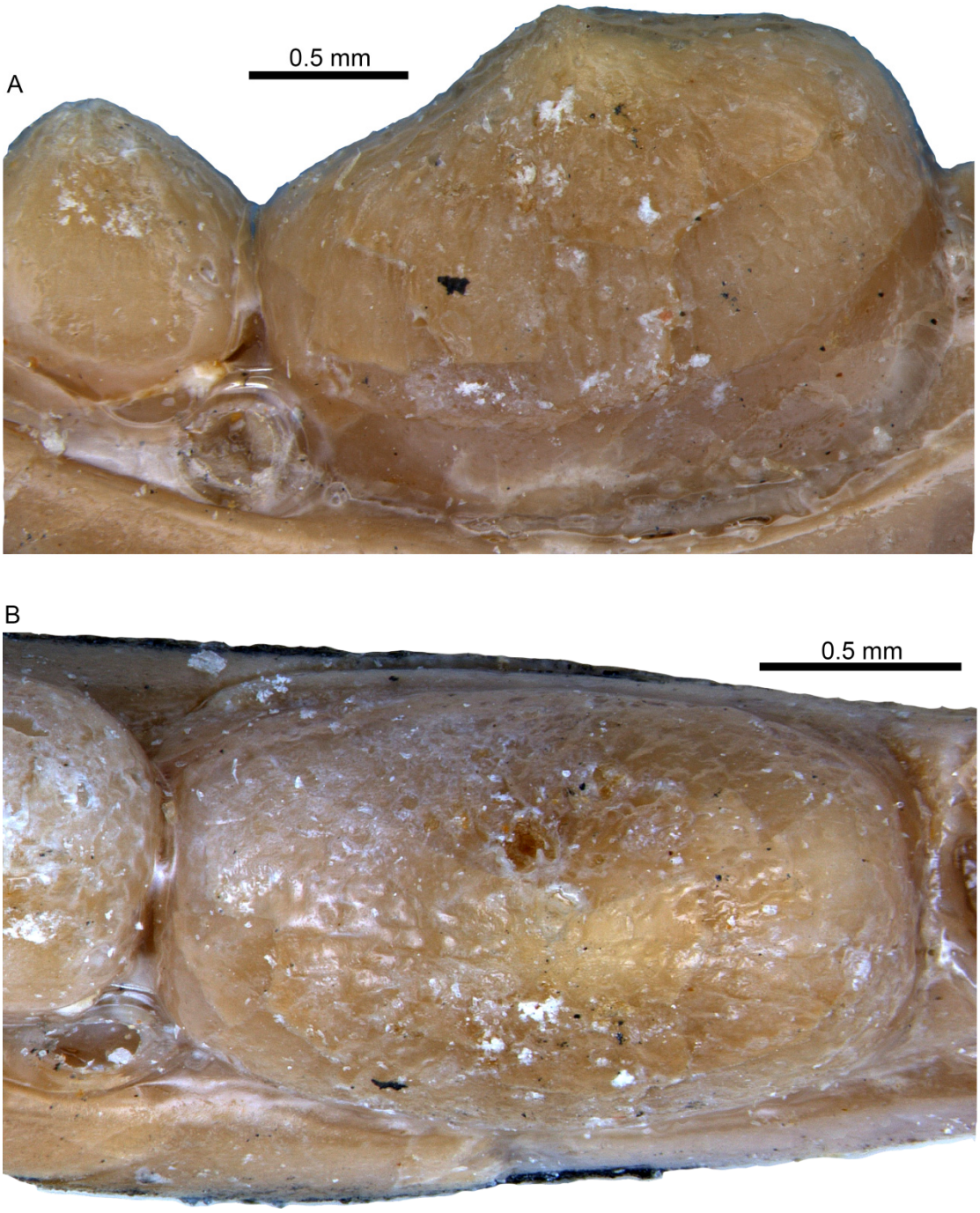

Figure 21. *Todrasaurus gheerbranti*, holotype left dentary UM THR 407. Close up the largest tooth in medial (A) and dorsal (B) views.

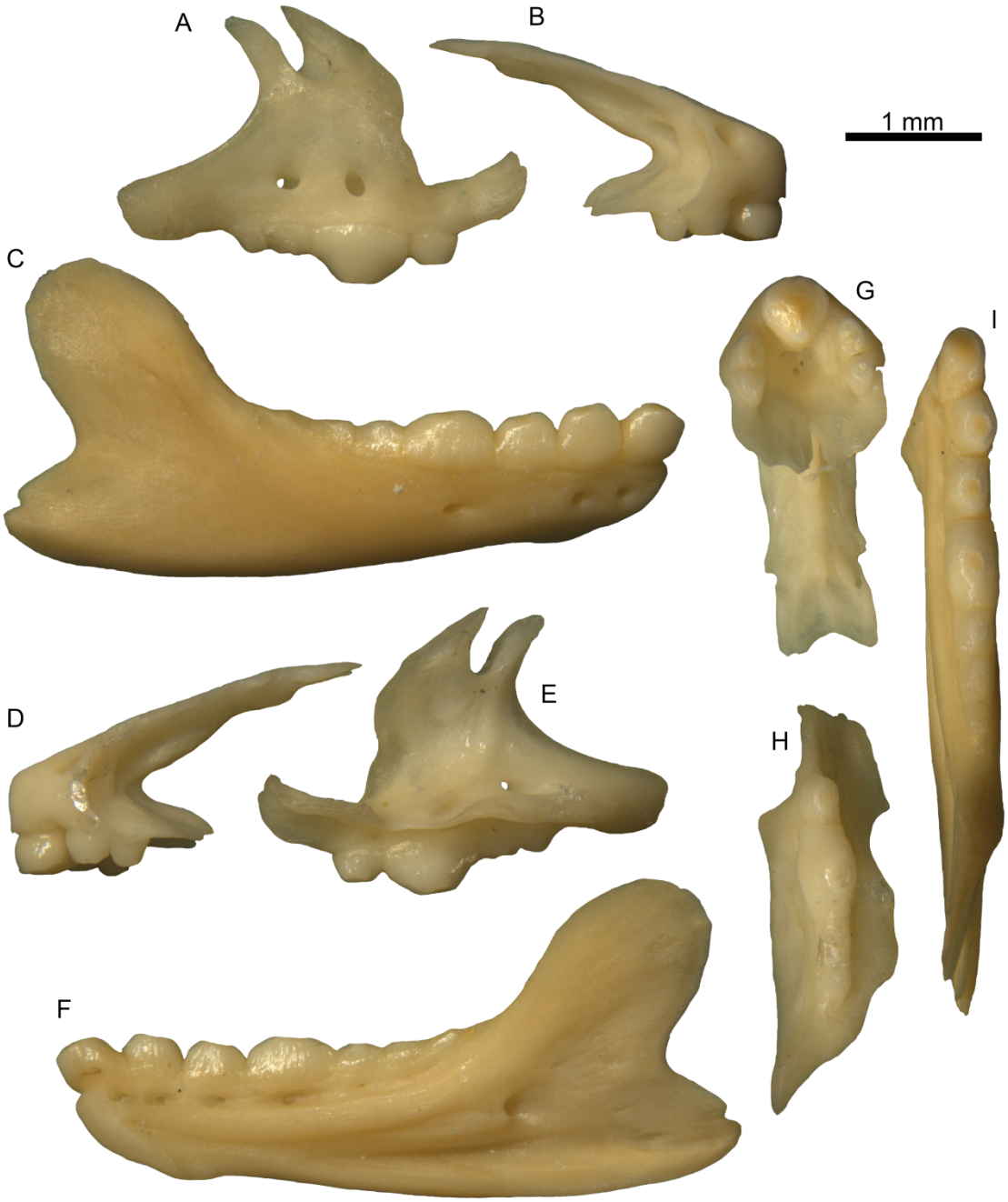

Figure 22. *Trogonophis wiegmanni*, specimen SMF-PH 566. Premaxilla (B, D, G), right maxilla (A, E, H), and right mandible (C, F, I) in right lateral (A), labial (B–C), left lateral (D), medial (E–F), and occlusal (G–I) views.

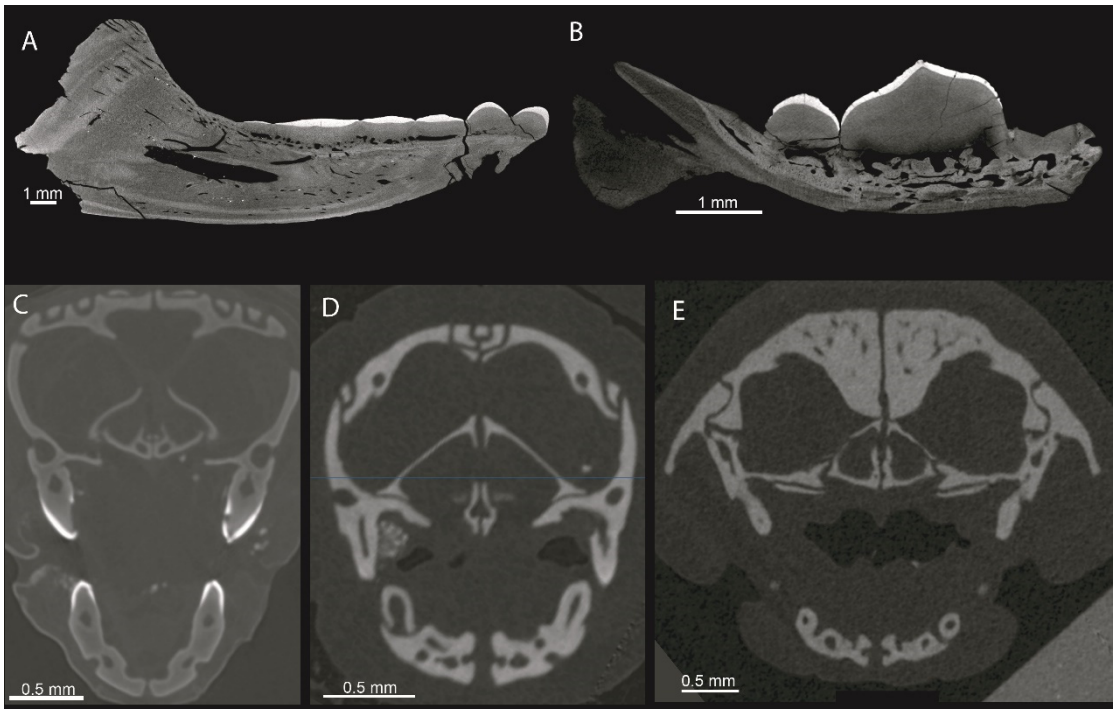

Figure 23. The profound enamel thickness in the teeth of Trogonophidae compared to other amphisbaenians. (A) Paratype dentary (ONM CBI-1-646) of ***Terastiodontosaurus marcelosanchezi*** gen. et sp. nov.; (B) holotype dentary (UM THR 407) of *Todrasaurus gheerbranti*; (C) *Trogonophis wiegmanni* (YPM HERR 6903), transverse section of snout; (D) *Zygaspis quadrifrons* (collection of A.H. uncat.), transverse section of snout; (E) *Monopeltis capensis* (collection of A.H. uncat.), transverse section of snout).

Figure 24. Life reconstruction of *Terastiodontosaurus marcelosanchezi* gen. et sp. nov. ready to prey on a large snail of the family Bulimulidae. Artwork by Jaime Chirinos.

Table 1. Unambiguous morphological synapomorphies (under acctran or deltran) of trogonophid clades inferred based on our phylogenetic analysis.

Clade	Character	Change	Description
Trogonophidae	10	0 → 1	Maxillary process of premaxilla extends lateral to level of palatine-maxilla suture
	17	1 → 0	Nasal descending lamina extends below level of nasal-maxilla suture
	26	1 → 0	Nasals abut or overlap frontals
	28	0 → 1	Frontals deeply notched to clasp a long and narrow caudal process of the nasals
	55	0 → 1	Parietal-supraoccipital opening closed
	59	1 → 2	Premaxillary process of maxilla extremely elongate, forming ventral and part of medial border of external naris
	66	0 → 2	Maxilla notched to receive a long, narrow process of the frontal
	67	0 → 1	Jugal process of maxilla strongly turned outward (flared in dorsal view)
	94	0 → 1	Stapedial shaft projects anterolaterally in ventral view
	107	1 → 0	Vomers do not overlap palatal shelf of maxilla behind posterior margin of opening for vomeronasal organ
	114	0 → 1	Vomers contacting for nearly or all of their length
	117	1 → 0	Palatine contact with braincase weak or absent
	120	0 → 1	Palatines with anterior contact only
	130	4 → 1	Ectopterygoid abuts posteromedial corner of maxilla, rather than interdigitating
	131	1 → 0	Fingerlike anterior process of ectopterygoid absent
	132	1 → 0	Maxillary process of ectopterygoid tapers or parallel-sided
	141	1 → 0	Posterior margin of supraoccipital straight to weakly incised in dorsal view
	152	3 → 1	Short basipterygoid process develops
	158	1 → 0	Occipital condyle convex and ball-shaped or only weakly divided
	174	1 → 0	Posterior margin of dentary lacks broad, U-shaped cutout extending to back of tooth-row
	205	0 → 1	Surangular foramen located along dentary-surangular suture
	219	0 → 1	Marginal teeth fused to each other
	224	1 → 2	Premaxillary tooth count decreases to 5
	225	1 → 0	Premaxillary teeth continuous with maxillary tooth-row
	230	2 → 1	Length of maxillary tooth row rises extends to anterior half of orbit
	237	0 → 2	Third tooth from back in dentary enlarged
Trogonophis **+ (*Terastiodontosaurus* gen. nov. + *Todrasaurus*)**	5	1 → 0	Dorsal foramina of premaxilla absent
	195	1 → 0	Anterior margin of coronoid process delimited by wall of bone anteriorly
	218	1 → 0	Teeth straight, or recurved only anteriorly
	228	1 → 0	Caniniform maxillary tooth absent
	309	0 → 1	Enamel on tooth crowns very thick
Terastiodontosaurus **gen. nov. +** ***Todrasaurus***	308	0 → 1	Hypertrophied dentary tooth at least 50% longer than adjacent teeth

Table 2. Morphometric data of specimens of *Trogonophis wiegmanni* and ***Terastiodontosaurus marcelosanchezi*** gen. et sp. nov.

Taxon	**Specimen Number**	**Maxilla length (mm)**	**Maxilla tooth count**	**Largest maxilla tooth length/ total tooth row length ratio**	**Skull length (mm)**	**Snout vent length (SVL) (mm)**	**Tail length (mm)**	**Skull / maxilla length ratio**	**Total length / maxilla length ratio**	**Total length (mm)**
Trogonophis wiegmanni	SMF-PH 565	3.23	4	-	-	134.4	9.9	-	44.7	144.3
Trogonophis wiegmanni	SMF-PH 566	3.4	4	0.44	-	-	-	-	-	-
Trogonophis wiegmanni	SMF-PH 567	3.32	4	0.47	11	156.4	13.4	3.31	51.1	169.8
Trogonophis wiegmanni	FMNH 109462	4.2	4	0.46	14.2	-	-	3.38	-	-
Trogonophis wiegmanni	YPM HERR 6903	2.16	3	0.51	6.94	-	-	3.21	-	-
Terastiodontosaurus marcelosanchezi gen. et sp. nov.	ONM CBI-1-645 (holotype)	16.3	3	0.52	**53.8 (estimated)**	-	-	-	-	**781 (estimated)**

Table 3. Measurements of the muscles of the dissected specimen of *Trogonophis wiegmanni* (MNHN-RA-1987.1895). Abbreviations: Add. = adductor; ext. = externus; m. = musculus; mand. = mandibulae; PCSA = physiological cross-sectional area; sup. = superficialis.

	Mass (g)	Fibre length (cm)	PCSA (cm^2)
m. depressor mandibulae	0.0042	0.15	0.03
m. cervicomandibularis	0.0636	0.36	0.17
m. add. mand. ext. sup. anterior	0.0024	0.27	0.01
m. add. mand. ext. sup. posterior	0.0278	0.27	0.10
m. add. mand. ext. medialis	0.0303	0.26	0.11
m. add. mand. externus profundus	0.0516	0.24	0.20
m. adductor mandibulae posterior	0.0042	0.17	0.02
m. pseudotemporalis superficialis	0.0146	0.27	0.05
m. pseudotemporalis profundus	0.0065	0.27	0.02
m. pterygoideus	0.006	0.11	0.05

SUPPORTING INFORMATION

Supplementary data is available at Zoological Journal of the Linnean Society Journal online. All data supporting these findings are included in this article and its online supporting information.

Supplementary text. List of characters of the phylogenetic analysis.

List of characters of the phylogenetic analysis

We deleted Longrich et al.'s (2015) character on geographic distribution (#308). AToL ("Assembling the Tree of Life") refers to Gauthier et al. (2012). Character order follows Longrich et al. (2015), and characters not otherwise labeled are from that work. New characters appear at the end.

1. Premaxilla, anterior margin of premaxilla rises steeply up (0); or anterior extension of premaxilla projects forward beyond oral margin (1).

2. Premaxilla, body of premaxilla rounded or keeled (0) or forming a transversely expanded, shovel-like shelf (1) (Kearney 2003: character 30); premaxillary shovel curled downward such that tip lies at the level of the oral margin of the premaxilla (2).

3. Premaxilla, body of premaxilla rounded or shovel-shaped (0); or forming a mediolaterally compressed, blade-like keel (1); or keel dorsoventrally expanded to form a tall, rounded blade (2).

4. Premaxilla, strongly hooked ventrally: absent (0) or present (1).

5. Premaxilla, dorsal foramina absent (0); two (1); or four (2). Kearney (2003: character 31).

6. Premaxilla, dorsal foramina pass through premaxilla (0); or foramina open along premaxilla-nasal suture (1).

7. Premaxilla, contact with frontals (when present): premaxillae extend posteriorly over frontals (0); or frontals extend anteriorly over premaxillae (1).

8. Premaxilla, palatal processes do not contact pterygoids (0) or posteriorly extended medial to first maxillary tooth (1) or extended to contact pterygoids (2). Kearney (2003: character 90).

9. [AToL Character 2]. Premaxilla palatal shelf: (0) not bifid posteriorly; (1) bifid posteriorly. Rieppel (1980).

10. [AToL Character 4]. Premaxilla maxillary process length relative to level of palatine - maxilla suture: (0) premaxilla medial to level of palatine - maxilla suture; (1) premaxilla extends lateral to level of palatine - maxilla suture.

11. [AToL Character 7]. Premaxilla body anterior ethmoidal foramina exit via: (0) external naris, (1) premaxilla notch; (2) premaxilla body.

12. [AToL Character 10]. Premaxilla internasal process length: (0) less than half nasal length; (1) more than half way to frontal between nasals; (2) nearly to, or articulates with, frontal. Kearney (2003).

13. [AToL Character 18]. Nasals anterior width: exceeds nasofrontal joint width (0), is subequal to nasofrontal joint width; Gauthier (1982) (1); less than nasofrontal joint width (2).

14. Nasals, with little or no anterior extension, nares open anterodorsally (0) nasals extend anteriorly, nares open anteriorly or slightly anteroventrally (1); nasals strongly extended anteriorly, nares open anteroventrally (2). Kearney (2003: character 37).

15. Nasals, abut or overlapped by premaxilla (0); or nasals overlap onto premaxilla (1).

16. Nasals, hook around maxillae in dorsal view to form an L-shaped articulation with maxillae: absent (0); or present (1).

17. [AToL Character 21]. Nasal descending lamina: absent (0); with descending lamina extending below level of nasal - maxilla suture (1).

18. [AToL Character 22]. Supranarial process in dorsal view: (0) present (1) reduced/absent.

19. Nasals, with frontals bounding a neurovascular foramen (0), neurovascular canal branching with numerous small foramina opening through the nasals (1).

20. [AToL Character 23]. Nasal - maxilla suture in cross section anteriorly: maxilla overlaps nasal (0); nasal partly overlaps maxilla dorsally (1); nasal abuts maxilla (2); nasal underlaps maxilla to floor of narial chamber (3).

21. [AToL Character 24]. Nasals ventral contact beneath premaxillary internasal process: (0) broad contact below; (1) near apex only if at all.

22. [AToL Character 25]. Nasals dorsal contact over premaxilla internasal process: no contact (0); in contact over apex (1); broadly in contact (2).

23. [AToL Character 28]. Nasal length relative to frontal length: (0) nasals shorter than frontals; (1) nasals longer than frontals.

24. Frontals, interior cancellous (0) or dense and avascular (1).

25. [AToL Character 36]. Frontals: (0) paired; (1) fused.

26. Frontal, contact with nasals: nasals abut or overlap frontals (0) or frontals extend anteriorly to overlap nasals (1).

27. Frontals, anterolateral processes weakly developed or absent (0) or elongate, slender anterolateral processes embracing nasals (1).

28. Frontals, deeply notched to clasp a long and narrow caudal process of the nasals: absent (0) or present (1).

29. Frontals, flat or weakly convex dorsally (0), or strong transverse arching (1), or peaked, with a strong midline ridge (2). Kearney (2003: character 25).

30. Frontals, dorsal surface pierced by frontal foramina: absent (0) or present (1).

31. Frontals, weakly deflected relative to parietals (0) strongly deflected by ≥30º or more (1). Kearney (2003: character 24).

32. [AToL Character 37] Frontal - maxilla suture: (0) frontal separated from maxilla by nasal - prefrontal contact; (1) frontal contacts maxilla, separating nasal from prefrontal. Gauthier (1982).

33. [AToL Character 38] Frontal subolfactory processes: (0) absent; (1) arch beneath brain but do not contact; (2) arch beneath brain to articulate on ventral midline; (3) arch beneath brain and fuse on ventral midline. Pregill et al. (1986).

34. [AToL Character 39] Frontal subolfactory process depth from skull roof to palatine: (0) 25-35%; (1) 42-53%; (2) 58-68%; (3) 75-85%; 4) >89%. Gauthier (1982).

35. Frontals, do not wall off brain-case anteriorly (0) or frontals partially enclose brain-case anteriorly, such that there is only a narrow anterior opening between them (1).

36. [AToL Character 40]. Frontal subolfactory process - parasphenoid suture: (0) absent; (1) present. Lee (1997).

37. [AToL Character 55]. Frontoparietal suture: (0) separate; (1) fused. Kearney (2003).

38. [AToL Character 56]. Frontoparietal suture interdigitation: frontal overlaps parietal dorsally (0); lightly interdigitate or simple abutment (1); moderate interdigitation (2); strong interdigitation (3); deeply interdigitate 4). Estes et al. (1988).

39. Frontal-parietal contact; parietals abut or overlap frontals laterally (0), frontals extend back over parietals (1), frontals with hypertrophied wings covering lateral surface of brain-case (2).

40. [AToL 62]. Postfrontal: present (0); absent (1); fused to postorbital (2); fused to frontal (3). Estes et al. (1988).

41. [AToL 67]. Postfrontal supratemporal shelf: absent (0); present as thin shelf extending over anterodorsal corner of supratemporal fenestra (1); extending posteriorly further than laterally across upper temporal fenestra (2); to occlude upper temporal fenestra (3). Estes et al. (1988).

42. [AToL 68]. Postorbital: (0) present; (1) absent. Estes et al. (1988).

43. Parietal, abuts or with limited underlap of frontals (0) or extensive anterior projection underlying frontals (1).

44. Parietal, dorsal surface straight in lateral view (0) or anterior margin inflected downward in lateral view (1).

45. [AToL 90]. Parietal temporal muscles originate: dorsally on parietal table and supratemporal process of parietal (0); ventrally on parietal table and dorsally on supratemporal process (1); ventrally on parietal table and supratemporal process (2). Gauthier (1982).

46. [AToL 93]. Parietal sagittal crest: absent (0); present (1); projecting dorsally (2). Etheridge and de Queiroz (1988).

47. Parietal, supratemporal fossae and parietal sagittal ridge do not extend to frontoparietal suture (0) or parietal sagittal ridge extends to frontoparietal suture (1).

48. Parietal, paired muscle attachments at the anterior end of the supratemporal fossae: absent (0) or present (1).

49. Parietal ventrolateral crest absent or rudimentary (0) well-developed crest running posterolaterally from orbit (1) present and extending posteriorly onto alar process of prootic (2). Kearney (2003: character 61) uses a version of this character.

50. [AToL 99]. Parietal extent over brain-case in dorsal view: does not cover occiput (0), covers nearly all of occiput (1), Estes et al. (1988); with emarginate lateral fossae (2). Lang (1991).

51. [AToL 104]. Parietal foramen: present (0); absent (1). Estes et al. (1988).

52. Parietal, horseshoe-shaped muscle scars atop parietal sagittal crest: absent (0) or present (1).

53. Parietal, sagittal crest of parietal with a prominent boss for muscle attachment: absent (0) or present (1). Kearney (2003: character 52).

54. Parietal dorsal foramina: absent (0) or present (1).

55. Parietal: opening between parietal and supraoccipital, sometimes reduced to a narrow foramen (0) or parietal-supraoccipital opening closed (1).

56. [AToL 101]. Parietal supratemporal process length: well-developed (0), reduced, less than 25% of parietal width (1), Estes et al. (1988); absent (2). Tchernov et al. (2000).

57. [AToL 102]. Parietal supratemporal process orientation: directed laterally (0); directed posterolaterally (1); directed posteriorly (2).

58. [AToL 109]. Parietal - prootic contact: absent (0); contact at apex of alar process (1); extensive conformable contact (2); ventral process of parietal overlaps prootic alar process laterally (3). Lee (1998).

59. Maxilla, premaxillary process short, ventrolateral border of external naris (0) or premaxillary process extends anteriorly, forms ventral border of external naris (1), or premaxillary process extremely elongate, forms ventral and part of medial border of external naris (2).

60. Maxilla, anterolateral process contributing to rostral shovel: absent (0), present and projecting anteriorly (1), present and extending onto anterolateral surface of maxilla (2), present and extending caudally across the lateral surface of the maxilla for the full length of the tooth-row (3). A different version of this character was used by Kearney (2003: character 69).

61. Maxilla, anterior of facial process with distinct concavity bounded by a dorsal lip ('dimple'): absent (0) or present (1). (Smith 2009b).

62. Maxilla, palatal shelves weakly developed (0) or broad and projecting medially to contribute to a secondary palate (1).

63. Maxilla, palatal shelves confluent with dental gutter (0) or teeth bounded medially by prominent dental gutter and medial palatal ridge of maxilla (1).

64. [AToL 114] Maxilla facial process length/maxilla length: 10-20% (0); 16-23% (1); 25-36% (2); 38-55% (3); >56% (4). Gauthier (1982).

65. [AToL 116] Maxilla facial process apical surface faces: laterally (0), dorsolaterally (1), anterodorsally (2); large, triangular, dorsally directed surface sharply set off from nearly vertical external surface of facial process (3).

66. Maxilla, abuts or overlaps skull roof elements (0) or notched to receive a triangular process of the pre frontal (1), or notched to receive a long, narrow process of the frontal (2)

67. Maxilla, jugal process projects posteriorly in line with tooth-row (0) or strongly turned outward such that the jugal processes are distinctly flared in dorsal view (1).

68. [AToL 124] Maxilla posterior process to mid-orbit or further (0) anterior half of orbit (1).

69. Maxilla, posterior process of palatal shelf weakly developed or absent (0) or elongate and extending posteriorly between ectopterygoid and palatine (1). Kearney (2003: character 94).

70. Rostrum elongate relative to brain-case, premaxilla+nasal ≥45% of skull length (0), or rostrum shortened <45% skull length (1) or rostrum extremely abbreviated ≤33% skull length (2).

71. [AToL 129]. Prefrontal posterior extent along orbital margin: terminates in anterior half of orbit (0); extends to mid-orbit (1); extends posterior to mid-orbit (2). Estes et al. (1988).

72. Prefrontal broadly separated from parietal (0) extends posteriorly to level of frontoparietal suture (1) laps over parietal (2).

73. [AToL 126]. Prefrontal reduction: not reduced (0); reduced (1); absent (2). Kearney (2003).

74. [AToL 127]. Prefrontal broadly overlaps frontal posterodorsally: absent (0); present (1).

75. [AToL 128]. Prefrontal orbitonasal margin in x-section: slopes ventrolaterally (0); vertical (1); slopes ventromedially (2); extends beneath subolfactory processes (3); extends to near contact with its opposite on midline (4).

76. [AToL 137]. Lacrimal: (0); absent (1). Estes et al. (1988).

77. [AToL 142]. Jugal absent: (0) present; (1) absent. Estes et al. (1988).

78. [AToL 152]. Jugal postorbital ramus development: complete bony postorbital bar (0); incomplete bony postorbital bar (1); bony postorbital bar absent (2). Estes et al. (1988).

79. [AToL 143]. Jugal extent anteriorly with respect to tooth row: jugal broadly overlaps level of posterior maxillary tooth row (0); jugal does not reach anterior to level of the last maxillary tooth (1); jugal fails to reach most posterior maxillary tooth (2).

80. [AToL 144]. Jugal anterior extent: broadly separated from prefrontal (0); reaches level of prefrontal (1).

81. [AToL 149]. Jugal lateral exposure below orbit: absent (0); partly exposed above orbital margin of maxilla (1); entirely exposed above orbital margin of maxilla (2). Estes et al. (1988).

82. [AToL 155]. Jugal posterior process: complete lower temporal bar (0); reduced to a discrete bony posterior process (1); Gauthier et al. (1988); absent (2), Benton (1984).

83. [AToL 159]. Squamosal: present (0), absent (1). Estes et al. (1988).

84. [AToL 166]. Supratemporal: (0) present; (1) absent. Estes et al. (1988).

85. [AToL 501]. Quadrate suprastapedial process: absent (0); present (1). Lee (1998), Tchernov (2000).

86. [AToL 180]. Quadrate lateral conch: present (0); absent (1). Benton (1984).

87. Quadrate articulates with brain-case above the level of the occipital condyle (0), or quadrate articulates with brain-case at or below the level of the occipital condyle (1).

88. Quadrate, anterior inclination of quadrate shaft >45º from the vertical (0) anteriorly inclined by ≥45º (1).

89. Quadrate articular condyles lie roughly at level of the maxillary tooth-row (0) or well below the level of the maxillary teeth (1).

90. Quadrates placed posteriorly, articulating posterior to stapedial shaft (0) stapes (0) or articulate anteriorly, articulating with brain-case laterally or anteriorly relative to the stapedial shaft (1).

91. Quadrate foramen present (0) or absent (1).

92. Quadrate, anterior wing large and well-developed (0) rudimentary or absent (1).

93. [AToL 191]. Stapedial shaft: long and slender (0); short and thick (1). Lee (1998).

94. Stapes, stapedial shaft projects laterally in ventral view (0), or stapedial shaft projects anterolaterally in ventral view (1).

95. Stapes, stapedial shaft does not contact quadrate (0) or stapedial shaft contacts posterior surface of quadrate (1).

96. [AToL 193]. Stapedial footplate: does not fill fenestra ovalis (0); fills fenestra ovalis (1). Lee (1998).

97. Stapes, anterior edge of stapedial footplate with broad articulation with anterior edge of fenestra ovalis: absent (0) or present (1).

98. Stapedial footplate small (0) enlarged (1) hypertrophied (2) Kearney (2003: character 85) previously used a different version of this character.

99. Stapedial footplate subcircular or elliptical (0), taller than wide (1), highly asymmetrical, expanded posteriorly and triangular-ovate to triangular (2).

100. [AToL 194]. Fenestra ovalis orientation: opens directly laterally (0); opens anterolaterally (1); opens ventrolaterally (2); opens posterolaterally (3). Gauthier et al. (1988).

101. Fenestra ovalis, broadly exposed in lateral view (0) or partly obscured by down-growth of paroccipital process as far as the stapedial shaft of the stapes (1) or largely/entirely obscured by down-growth of the paroccipital processes (2).

102. Extracolumella unossified (0) or ossified (1). Kearney (2003: character 83).

103. Extracolumella short, not extending far anterior to quadrate (0) or elongate and projecting almost to or past the back of the dentary tooth-row (1) Kearney (2003: character 82).

104. Extracolumella narrow anteriorly (0) expanded anteriorly, at least twice as deep anteriorly as posteriorly (1).

105. Extracolumella: widely separated from quadrate (0) or extracolumella lies along ventrolateral aspect of quadrate, passing through a broad, shallow groove on the posterolateral surface of the quadrate (1).

106. [AToL 212]. Vomer fusion: absent (0); partial (1); fully fused (2). Estes et al. (1988).

107. [AToL 215]. Vomer (when looking at skull in ventral view) overlaps (dorsally) the palatal shelf of the maxilla behind posterior margin of opening of vomeronasal organ: absent (0); present (1).

108. Vomer, lateral process hypertrophied and winglike: absent (0) or present (1).

109. [AToL 216]. Vomer: does not establish any sutural contact with the palatal shelf of the maxilla behind the incisura Jacobsoni (0); establishes narrow contact with the palatal shelf of the maxilla behind the incisura Jacobsoni (1); establishes broad contact with the palatal shelf of the maxilla along the entire length of the lateral margin of vomer (2). Rieppel et al. (2008).

110. [AToL 220]. Vomeronasal nerve exit: dorsal to vomer (0); via canals dorsally on vomer (1); via foramen at back end of vomer (2); via sieve-like arrangement of foramina through back of vomer (3). Rieppel et al. (2008).

111. [AToL 221]. Vomer degree underlap of palatine: just at tips (0); extending posteriorly to level of maxilla - ectopterygoid first contact (1). Kearney (2003).

112. [AToL 222]. Vomer ventral longitudinal ridges: absent (0); (1) long and converge toward midline, well-developed below vomeronasal nerve exit from septomaxilla (1); short parasagittal ridges anteriorly on vomer at level of vomeronasal duct opening (2); discrete canals anteriorly on vomer delimited by lateral ridges and median ridge (3).

113. Vomers, posterior ends of vomers lie medial to maxillary tooth-row (0), or posterior ends of vomers extending posteriorly beyond maxillary tooth-row (1).

114. Vomers, separated posteriorly (0) or contacting for nearly or all of their length (1).

115. Vomers, articulate with palatines for their full length (0) or posterior ends of vomers free, do not articulate with palatines (1).

116. Palatines, vomerine processes overlap vomers, or fit into a broad, U-shaped groove in vomers (0), or ridge on vomers fits into narrow groove in vomers (1) or deep slot in vomers to receive palatine anterior process (2).

117. Palatines, contact with brain-case weakly developed or absent (0) or palatines broadly contacting brain-case (1).

118. Palatine, narrow contact with palatal shelf of maxilla (0), or anteroposteriorly extensive contact between maxillary process of palatine and palatal shelf of maxilla (1).

119. Palatines, medial edge of palatine curls outward to form a lip below the choanal fossa: absent (0) or present (1).

120. [AToL 231]. Palatines: separated (0); anterior contact only (1); contact extends to midpoint, or beyond (2). Lee (1998).

121. Palatine, tab-like process of palatine projecting medially into choana: absent (0) or present (1).

122. Palatines, participate in a large suborbital fenestra (0) suborbital fenestra reduced or absent (1). Replaces [AToL 271].

123. [AToL 258]. Pterygoid separation on midline: pterygoids narrowly separated for most of their length 0); broad at base, narrow anteriorly (1) broad at base, less narrow anteriorly (2); broad throughout length (3). Estes et al. (1988).

124. [AToL 259]. Palatine ramus of the pterygoid: contacts vomer (0); does not contact vomer (1). Gauthier et al. (1988).

125. [AToL 261]. Lateral process of palatal ramus of pterygoid: absent (0); present, a lateral process of palatal ramus developed along lateral border of palatine (1). Wu et al. (1996).

126. [AToL 264]. Quadrate ramus of pterygoid short and small, tightly wrapping around posteromedial (ventromedial if quadrate horizontally oriented) surface of quadrate: absent (0); present (1). Wu et al. (1996).

127. [AToL 267]. Pterygoid teeth: present (0); absent (1). Pregill et al. (1986).

128. Pterygoid, does not contact maxilla (0) or extends anteriorly to contact jugal process of maxilla (1).

129. Pterygoid, dorsal ridge weakly developed or absent (0) prominent dorsal ridge (1).

130. [AToL 275]. Ectopterygoid - maxilla suture: ectopterygoid lies dorsally along supradental shelf of maxilla (0); ectopterygoid abuts posteromedial corner of maxilla (1); ectopterygoid with slot laterally clasping maxilla (2), ectopterygoid overlapping maxilla more ventrally than dorsally (3); interdigitating suture, with maxilla at least partly overlapping ectopterygoid dorsally (4) Smith (2009b).

We rescored *Trogonophis wiegmanni* and *Diplometopon zarudnyi* as state 1 (from "?"). They have simplified the more complex articulation (state 4) found in amphisbaenians exclusive of Rhineuridae.

131. Ectopterygoid with elongate, finger-like anterior process inserting into slot in maxillary shelf: absent (0) or present (1).

132. [AToL 276]. Ectopterygoid maxillary process shape in dorsal view: tapers or parallel-sided (0); widens anteriorly (1); to more than 3 times wider anteriorly relative to ectopterygoid shaft (2).

133. [AToL 281]. Ectopterygoid - palatine ventral articulation: palatine - maxilla contact excludes ectopterygoid (0); ectopterygoid anterior process largely separates palatine from maxilla posteriorly (1).

134. [AToL 283]. Ectopterygoid posterior process: prominent (0); small lateral knob (1); absent (2).

135. [AToL 286]. Ectopterygoid: does not contact prefrontal (0); contacts prefrontal at base of orbit (1).

136. [AToL 290]. Epipterygoid: (0) present; (1) absent. Estes et al. (1988).

137. Ectopterygoid dorsal ridge: absent (0) or present (1).

138. Supraoccipital, ascending process capped by an accessory ossification fitting into socket in parietal: present (0) ossification absent or fused (1).

139. [AToL 299]. Supraoccipital origin of temporal muscles: restricted to parietal (0); spread onto supraoccipital contacting nuchal crest in roughly T-shaped outline (1); spread onto supraoccipital to form Y-shaped crest (2); temporal muscles spread onto brain-case dorsally, but sagittal and nuchal crests join to form roughly anchor-shaped outline (3).

140. Supraoccipital, prominent supraoccipital crest projecting caudally over occiput: absent (0) or present (1). Kearney (2003: character 109).

141. Supraoccipital: posterior margin straight to weakly incised in dorsal view (0), deeply incised by a U- or V-shaped notch (1).

142. [AToL 307]. Crista prootica (ridge on lateral surface of the prootic, overhanging facial foramen): well-developed lateral flange (0); reduced to weak ridge (1); absent (2). Presch (1988).

143. [AToL 311]. Crista interfenestralis: prominent (0); reduced (1) Rieppel (1981); absent (2). Rieppel (1984b).

144. [AToL 312]. Crista tuberalis: prominent (0); reduced (1); absent (2). Rieppel (1984b).

145. [AToL 316]. Orbitosphenoid: absent (0); present (1); expanded to floor the brain-case (2). Wu et al. (1996).

146. [AToL 318]. Orbitosphenoid: paired (0); single (fused ventrally) (1).

147. [AToL 320]. Optic foramen: not fully enclosed by bone (0); enclosed partly or entirely by frontals (1); entirely within orbitosphenoid (2); entirely within parietal (3). Wu et al. (1996).

148. [AToL 321]. Trigeminal foramen or foramina: anterior margin not enclosed in bone (0); anterior margin enclosed by descending flange of parietal (1); anterior margin enclosed by orbitosphenoid (2); enclosed by prootic (3). Wu et al. (1996).

149. [AToL 324]. Dorsum sella shape in longitudinal cross-section: crista sellaris forms posterior wall, usually low and vertically disposed with more or less anterior slope (0); dorsum sella poorly differentiated, with, at most, shallow fossa with low crista sellaris (1), (Rieppel 1979a); enclosed in distinct fossa, a cup-like depression walled laterally and ventrally by the basisphenoid and anteriorly by the parasphenoid rostrum (2); completely enclosed tube-like dorsum sella (3).

150. Parabasisphenoid, cultriform process: narrow (0) broad and flooring brain-case (1).

151. Cultriform process, lies atop palatines (0) or projects down between palatines (1) or projects down between palatines to contact vomers (2).

152. Basipterygoid process: long (0), short (1), absent, but basipterygoid articulation retained (2), basipterygoid articulation lost (3).

153. [AToL 334]. Basipterygoid process: not expanded at distal end (0); distal end expanded (1). Lee (1998).

154. Basipterygoid processes, orientation: directed anterolaterally (0) or directed anteriorly, articulation between basipterygoid processes and pterygoid at right angles to long axis of skull (1).

155. [AToL 337]. Vidian canal caudal opening: within basisphenoid (0); anterior margin at basisphenoid-prootic suture (1); entirely within prootic (2); the dibamid-amphisbaenian condition (3).

156. [AToL 340]. Apophyseal ossification (Element "X") caps basal tubera: absent (0); present (1); huge (2).

157. [AToL 341]. Occipital condyle: posterior surface of condyle straight in ventral view (0); posterior surface of condyle concave in ventral view (1). Lee (1998).

158. Occipital condyle, convex and ball-shaped or weakly divided to form a C-shaped biconvex joint (0) or strongly divided with a broad cylindrical articular surface separating two lateral condyles, forming a spool-shaped roller joint (1). Kearney (2003: character 106.2).

159. [AToL 344]. Medial aperture of the recessus scala tympani (MARST): between basioccipital and opisthotic (0); entirely in opisthotic (1).

160. [AToL 348]. Vagus (= jugular in other amniotes) foramen far from MARST: with hypoglossal foramina lying below and between them medially (0); vagus foramen close to MARST, with hypoglossal foramina extending posterior to vagus (1).

161. [AToL 349]. Hypoglossal (XII) foramina exit(s) relative to vagus (X-XI) foramen on external surface of brain-case: hypoglossal foramina separated from vagus (= jugular) foramen (0); at least one hypoglossal foramen emerges from the same fossa as the vagus foramen (1); only one hypoglossal foramen still exits separately from the vagus foramen fossa (2); all three hypoglossals emerge from the same fossa as the vagus foramen (3).

162. [AToL 350]. LARST (lateral aperture of recessus scalae tympani): open (0); small (1), Rieppel (1981); closed (2). Rieppel (1984a).

163. [AToL 351]. Perilymphatic foramen: faces ventrally (0); faces medially (1); faces laterally (2); faces posteriorly (3). Rieppel (1979a, 1979b, 1985).

164. Dentary, long and slender (0) or dentary short and deep, depth of dentary at back of tooth row ≥ 33% of tooth-row length (1).

165. Dentary, symphysis primarily developed above Meckel's groove (0) or with extensive development of a symphyseal facet extending caudally below Meckel's groove (1). Longrich et al. (2012).

166. Dentary, shape of modified dentary symphyseal articulation: dorsal and ventral symphyseal facets long and narrow, symphyseal articulation V-shaped (0); dorsal and ventral facets short and broad and with little space between them, symphyseal articulation C-shaped (1); dorsal facet reduced and ventral facet extended posteriorly, symphyseal facets 7-shaped (2) UN.

167. Dentary, width of ventral symphyseal facet: broad, well-developed ventral symphyseal facet (0) or narrow ventral symphyseal facet (1).

168. Dentary, shape of Meckel's groove: straight or curving (0); or straight posteriorly and then distinctly kinking up at the region of the symphysis, groove 'L' shaped or hockey-stick shaped (1).

169. Dentary, mandibular foramen opens anteriorly (0); around level of last dentary tooth (1); well posterior to last tooth (2).

The character matrix, but not character list (text or in Nexus file) included a character state 2. Based on Longrich et al.'s (2015) scoring, we believe that state 1 is when the mandibular foramen opens around the level of the last tooth, and state 2 is when it opens well behind that point.

170. [AToL 361]. Number of mental foramina on lateral surface of dentary: 0 (0); 1 (1); 2 (2); 3 (3); 4 or more (4). Lee (1998).

171. Dentary, posterolateral surface bearing broad, shallow fossa for adductor muscles: absent (0), or present (1). Longrich et al. (2012).

172. [AToL 364]. Dentary coronoid process posterior termination: below (or anterior) to level of coronoid apex (0); just behind level of coronoid apex (1); well posterior to level of coronoid apex (2).

We rescored *Trogonophis wiegmanni* with state 0 (from "?").

173. Dentary, articulation with angular: angular appressed to medial surface of dentary (0) or dentary with long, narrow anteroposterior groove to receive ridge of angular (1).

174. Dentary, posterior margin with a broad, U-shaped cutout extending to the back of the tooth-row: absent (0) or present (1).

175. [AToL 367]. Dentary coronoid process posterodorsal extension: absent or with only small dorsal extension (0); large, and extending dorsally to overlap most of anterolateral surface of coronoid (1); extremely well-developed, covering almost entire lateral surface of coronoid (2) Estes et al. (1988).

We rescored *Todrasaurus gheerbranti* as state "1/2" (from state 1), as the broken dorsal margin and absence of coronoid make it impossible to be more precise.

176. [AToL 369]. Dentary angular process posterior termination: below (or anterior) level of coronoid apex (0); just posterior to coronoid apex (1); well posterior to level of coronoid apex (2); nearly to posterior surangular foramen (3).

177. [AToL 370]. Dentary angular process prominently bifid: absent (0); present (1).

178. Dentary, angular process with a second, accessory notch below primary angular notch: absent (0) or present (1).

179. [AToL 372]. Dentary restricts Meckel's canal: does not restrict or enclose Meckelian canal (0); lower dentary border of Meckel's canal folds up to approach closely upper border to restrict canal (1); upper and lower borders form sutural contact anterior to dentary (2); Meckel's canal closed and fused anterior to splenial (3). Etheridge and de Queiroz (1988).

180. Dentary, posteroventral margin lies ventrolateral to splenial (0); or posterolateral margin of dentary curls up around anterior edge of splenial (1); or posterolateral margin of dentary curls up around splenial for the full length of the dentary-splenial contact (2).

181. Dentary, contact with coronoid anterolateral process: coronoid forms simple overlapping contact with dentary (0) or dentary with a distinct recess or groove to receive coronoid anterolateral process (1).

182. Splenial, separate from angular (0) splenial fused to angular (1).

It is likely that *Terastiodontosaurus marcelosanchezi* shows state 0, given the clearly distinct articulation facets, but in the absence of the elements in question, we score it with "?".

183. [AToL 375]. Splenial anterior extent: 1/3 (or less) length relative to dentary tooth row (0); about 1/2 (1); about 2/3 (2); 3/4 (or more) (3).

184. [AToL 379]. Splenial anterior inferior alveolar foramen position relative to anterior mylohyoid foramen: anterodorsal (0); dorsal to posterodorsal (1).

185. Splenial articulates with subdental shelf (0) or splenial does not articulate with subdental shelf (1).

186. Splenial contacts anteromedial process of coronoid (0) or splenial does not contact anteromedial process of coronoid (1). Modified from [AToL 200].

187. Splenial, anterior mylohyoid foramen present (0) or absent (1).

188. Splenial, anterior inferior alveolar foramen present (0) or absent (1).

189. Posterior mylohyoid foramen present (0) or absent (1).

190. [AToL 381]. Angular posterior extent: reaches mandibular condyle (0); does not reach mandibular condyle (1). Gauthier et al. (1988).

191. [AToL 383]. Angular medial exposure: broad (0); reduced (1); narrow (2).

192. [AToL 385]. Posterior mylohyoid foramen position relative to coronoid apex: below (0); posterior (1); anterior (2).

193. [AToL 387]. Coronoid eminence composition: formed by both surangular and coronoid (0); formed exclusively by coronoid (1); formed exclusively by surangular (2). Gauthier et al. (1988).

194. Coronoid eminence: triangular in lateral view and tapering to a point (0) or broad and rounded in lateral view (1).

195. Coronoid, adductor fossa of coronoid process delimited by a wall of bone anteriorly (0), or anterior wall reduced/absent (1).

We rescored *Todrasaurus gheerbranti* and *Trogonophis wiegmanni* as state 0 (from "?" and state 1, respectively).

196. Coronoid, anterior margin of coronoid process slopes anteroventrally in medial view (0) or rises steeply up, anterior margin roughly vertical (1).

The matrix appears to mix up states 0 and 1, compared to the character description and illustration above. We scored *Terastiodontosaurus marcelosanchezi* and rescored *Todrasaurus gheerbranti* (from state "?") with state 1, like amphisbaenians exclusive of Rhineuridae.

197. [AToL 388]. Coronoid anteromedial process fits into sulcus beneath tooth-bearing border of dentary (at or behind end of tooth row): absent (0); present (1); and wraps around ventral margin of dentary tooth-bearing border at apex posteriorly (2). (Smith 2009a).

We rescored *Todrasaurus gheerbranti* with state 0 (from state "?").

198. [AToL 390]. Coronoid - surangular articulation: coronoid restricted to medial aspect of mandible (0); coronoid extends onto dorsal surface of surangular (1); coronoid arches over dorsal margin of mandible to reach lateral face of surangular (3). Estes et al. (1988).

199. [AToL 391]. Anteromedial process of coronoid: present (0); absent (1). Lee (1998).

200. Coronoid anteromedial process with narrow contact with dentary (0) broad and tongue-shaped process, with extensive overlap of dentary (1).

201. [AToL 393]. Posteromedial process of coronoid: absent (0); present (1). Lee (1998).

202. [AToL 394]. Anterolateral dentary process of coronoid: absent (0); present (1); overlaps dentary past level of tooth row (2).

203. Coronoid medial surface bearing a distinct vertical ridge (0) reduced or absent (1).

204. [AToL 396]. Surangular inserts into dentary lateral to the intramandibular septum, entering the intramandibular canal (which houses the alveolar branch of the inferior alveolar nerve, according to Oelrich 1956): absent (0); present slightly (1); present deeply (2). Gauthier (1982).

205. Surangular foramen, position: posterior to dentary-surangular contact (0) located along dentary-surangular border (1).

206. [AToL 398]. Adductor fossa: faces dorsomedially, medial wall below lateral wall (0); faces dorsally, medial/lateral walls same height (1) Lee (1998); no distinct medial wall at all (2); faces dorsolaterally, lateral wall below medial wall (3).

207. [AToL 399]. Surangular adductor fossa on external face of mandible: shallow and extends ventrally no more than half way down (0); deep and extends ventrally more than half way down (1). Gauthier (1984).

208. [AToL 400]. Surangular dorsal margin: nearly horizontal, rising somewhat toward the coronoid, anterodorsal edge set below level of tooth crowns (0); rises steeply

anterodorsally to coronoid, with apex reaching above level of tooth crowns (1). Lee (1998).

209. Articular, quadrate articular cotyle (glenoid) shallow (0) or strongly convex and C-shaped in lateral view (1).

210. Articular, quadrate articular cotyle (glenoid) with a straight or convex anterior margin (0) or anterior margin with a V-shaped notch in posterior view (1).

211. Articular, glenoid symmetrical (0) or strongly offset, with medial extension of glenoid (1) or with hypertrophied medial extension of glenoid (2).

212. Articular, quadrate articular cotyle (glenoid) directed posterodorsally in lateral view (0) directly posteriorly (1).

213. Retroarticular process, length: elongate, length exceeding anteroposterior diameter of glenoid (0), or short, length less than or equal to diameter of glenoid (1), or rudimentary/absent (2).

214. Retroarticular process projects posteriorly or slightly posteroventral (0); posteroventral (1); ventral (2). Kearney (2003: 123) used a different version of this character.

215. [AToL 401]. Prearticular and surangular fused in adult: separate (0); fused (1).

216. [AToL 403]. Prearticular crest: absent (0); present (1).

217. Tooth implantation pleurodont, with teeth at the middle of the tooth-row extending at least halfway down the inner surface of the dentary (0), or tooth implantation subacrodont to acrodont, teeth extending less than halfway down dentary (1). Modified from Longrich et al. (2012).

218. Teeth straight, or recurved anteriorly (0) or tips of crowns recurved along tooth rows (1).

219. [AToL 424]. Fusion of marginal teeth: unfused to each other (0); fused to each other (1).

Given available evidence, it does not seem appropriate to describe the teeth of *Trogonophis wiegmanni* as “fused.” Indeed, the posterior ones are closely appressed, but “cleavage planes between the individual teeth can be seen upon careful examination” (Gans 1960: 163). Yet, in the absence of histological study of these or other trogonophid teeth, we preferred to rescore *Todrasaurus gheerbranti* as state 1, which continues to reflect to close apposition of teeth in all Trogonophidae.

220. [AToL 427]. Marginal tooth spacing: crowns closely spaced (0); crowns separated by large gaps (1). Lee (1998).

221. Parietal, tapers posteriorly so that posterolateral edges form a distinct V in dorsal view: absent (0) or present (1).

222. [AToL 434]. Cusps on posterior teeth: unicuspid (0); bicuspid (1); tricuspid (2).

223. Median premaxillary tooth: subequal in size to other teeth (0); or distinctly larger than adjacent premaxillary teeth (1). Modified from [AToL 414]; Lee (1998).

224. Premaxillary teeth, number: 9 or more (0), 7 (1), 5 (2), 3 (3), 1 (4).

225. Premaxillary teeth, continuous with maxillary tooth-row (0) or inset, with diastema separating premaxillary and maxillary teeth (1). Kearney (2003: character 118).

226. Premaxillary tooth arc broad (0) strong angling of premaxillary tooth-rows, forming angle of 120º or less (1), or very strong angle between tooth-rows, 90º or less.

227. Maxillary teeth, number: 8 or more (0); 7 (1); 6 (2); 5 (3); 4 (4); 3 (5); 6 (2).

228. Caniniform maxillary tooth: absent (0); present (1).

229. Position of caniniform maxillary tooth: tooth 1 (0); or tooth 2 (1).

230. [AToL 418]. Maxilla tooth row length: to or behind mid-orbit (0); anterior to mid-orbit (1); anterior to orbit (2).

231. Dentary tooth count: ≥10 (0); 9 (1); 8 (2); 7 (3); 6 (4); 5 (5); 4 (6).

The matrix includes a state 6 for two taxa, *Rhineura floridana* and *Todrasaurus gheerbranti*. As the former has 4 maxillary teeth, we take this to be the definition of state 4 in Longrich et al. (2015). The latter is known only from the incomplete holotype dentary, so we consider the tooth count to be uncertain and rescored it as "?".

232. Dentary teeth project dorsally or hooked posteriorly (0); anterior dentary teeth procumbent (1).

233. Anterior dentary tooth smaller than second dentary tooth in size (0), subequal to second dentary tooth in size or distinctly larger than second dentary tooth (1)

234. Caniniform dentary tooth: absent (0); present (1).

235. Position of caniniform tooth: tooth 2 (0); tooth 3 (1); tooth 4 (2).

236. Anterior dentary teeth distinctly enlarged relative to posterior dentary teeth: absent (0) or present (1). Kearney (2003: character 129).

237. Penultimate tooth similar in size to last tooth (0); distinctly enlarged relative to preceding and following teeth (1); third tooth from back enlarged (2); fourth tooth from back enlarged (3).

We assume this refers to the dentary. We scored *Todrasaurus gheerbranti* and rescored *Trogonophis wiegmanni* (from state 0) as state 2.

238. Hypertrophied posteriormost dentary tooth: absent (0) or present (1).

239. [AToL 442]. Free epibranchials (= second epibranchial): absent (0); present (1). Gauthier et al. (1988).

240. [AToL 447]. Second ceratobranchial: shorter than first ceratobranchial (0); nearly equal to or longer than first ceratobranchial (1). Etheridge and de Queiroz (1988).

241. [AToL 449]. Large, wing-like hyoid cornu: absent (0); present (1). Kluge (1987).

242. [AToL 450]. Hyoid cornu: less than the length of the epihyal (0); greater than or equal to the length of the epihyal (1). Presch (1988).

243. [AToL 451]. Epihyal: meets hyoid cornu at (or near) its distal end (0); meets hyoid cornu along its body (1).

244. [AToL 452]. Epihyal: expansion or elaboration at proximal end absent (0); simple expansion at proximal end present (1); hook-like elaboration at proximal end present (2); lateral flange at proximal end present (3); medial flange at proximal end present. Estes et al. (1988).

245. [AToL 455]. Presacral vertebrae number increase I: 24 or fewer (0); 25 (1); 26 (2); 27 (3); 28 (4) or more. Estes et al. (1988).

246. [AToL 456]. Presacral vertebrae number increase II: less than or equal to 32 presacrals (0); 33-39 (1); 50-55 (2); 61-84 (3); 89 or more (4).

247. [AToL 457]. Presacral vertebrae number increase III: less than 104 (0); 118-132 (1); 144-156 (2); 168-180 (3); 184 or more (4). Lee and Scanlon (2002).

248. [AToL 459]. Cervical vertebra number reduction: six or more (0); five (1); four (2); three (3); two (4). Estes et al. (1988).

249. [AToL 462]. Cervical rib ossified portion shape: widens distally, at least in last cervical (0); tapers distally (1).

250. [AToL 463]. Cervical ribs start on vertebra number: 2 (0); 3 (1); 4 (2); 5 (3); 6 4). Estes et al. (1988).

251. [AToL 468]. Zygosphene-zygantrum accessory intervertebral articulations: absent (0); dorsolateral facing continuous facet just up edge of neural arch (1), Gauthier et al. (1988); lateral facing tall facet up neural arch to top of neural canal (2); separate facet set on distinct pedicle and facing ventrolaterally (3). Estes et al. (1988).

252. [AToL 470]. Caudal autotomic septum position relative to caudal rib: within caudal rib (0); anterior to caudal rib (1); posterior to caudal rib (2); absent (3). Estes et al. (1988).

253. [AToL 475]. Caudal haemal arch (intercentrum) position: intercentral, pedicles feeble/absent (0); contacting mainly condyle but also distinct pedicles beneath preceding centrum (1); mainly contacting pedicles on preceding centrum but still bordering condyle (2); well forward of condyle on preceding centrum (3).

254. [AToL 480]. Sternum: present (0); absent (1). Lee (1998).

255. [AToL 481]. Sternal fontanelle: absent (0); present (1). Estes et al. (1988).

256. [AToL 483]. Number of rib attachment points to sternum (including attachment of xiphisternum): 5 (0); 4 (1); 3 (2); 2 or fewer (3). Gauthier et al. (1986).

257. [AToL 486]. Number of xiphisternal rib attachment points: 0 (0); 1 (1); 2 (2); 3 (3); 4 (4).

258. [AToL 488]. Scapulocoracoid: large (0); reduced (1); absent (2). Lee (1998).

259. [AToL 489]. Scapula: short and wide (0); elongate and thin (1). Grismer (1988).

260. [AToL 493.] Scapulocoracoid emargination: absent (0); present (1). Gauthier et al. (1988).

261. [AToL 495]. Anterior (primary) coracoid emargination (fenestra): absent (0); present (1). Pregill et al. (1986).

262. [AToL 497]. Coracoid size: enlarged, extending anteriorly to level of clavicles (0); not enlarged, not extending anteriorly to level of clavicles (1).

263. [AToL 499]. Clavicle: present (0); absent (1). Estes et al. (1988).

264. [AToL 500]. Clavicle: no notch or fenestration present (0); notch present (1); fenestration present (2). Etheridge and de Queiroz (1988).

265. [AToL 501] Clavicle: rod-like (0); greatly expanded proximally (1). Gauthier (1982).

266. [AToL 502]. Clavicular angulation: simple curved rod, following contour of scapulocoracoid (0); strongly angulated, curving anteriorly away from scapulocoracoid (1). Estes et al. (1988).

267. [AToL 503]. Distal clavicle articulation: with scapula (0); with suprascapula (1); no distal articulation (2). Gauthier et al. (1988).

268. [AToL 504]. Medial contact of clavicles: clavicles do not meet on midline (0); clavicles meet on midline (1).

269. [AToL 505]. Interclavicle: present (0); absent (1). Estes et al. (1988).

270. [AToL 510]. Pubis: present (0); absent (1). Lee (1998).

271. [AToL 516]. Ischium: present (0); absent (1). Lee (1998).

272. [AToL 517]. Ischial tubercle: present (0); absent, or continuous with hypoischial cartilage (1). Estes et al. (1988).

273. [AToL 518]. Hypoischium: well-developed (0); vestigial (1); absent (2). Lee (2000).

274. [AToL 521]. Iliac tubercle: present (0); absent (1). Lee (1998).

275. [AToL 524]. Pelvic elements (ilium, ischium, pubis): in close sutural contact throughout postnatal ontogeny and co-ossified into a single pelvic bone late in postnatal ontogeny (0) Gauthier et al. (1988); distinct elements weakly united in non-sutural contacts (1) Lee (1998).

276. [AToL 528]. Proximal forelimb long bones (humerus, radius and ulna): (0) present; (1) absent. Lee (1998).

277. [AToL 529]. Ratio of radius/ulna to humerus: 0.50–0.61 (0); 0.62–0.97 (1); 0.98–1.10 (2).

280. [AToL 530]. Ectepicondylar foramen: present (0); absent (1). Estes et al. (1988).

279. [AToL 531]. Ulnar patella: present (0); absent (1).

280. Ulna, olecranon process on proximal epiphysis: (0) prominent; (1) short or absent. Gauthier et al. (1988).

281. [AToL 534]. Styloid process of radius: absent (0); present on posterolateral surface of distal epiphysis (1). Gauthier et al. (1988).

282. [AToL 535]. Carpal intermedium: large (0); small (1); absent (2). Gauthier et al. (1988).

283. [AToL 542]: Reduction in phalangeal counts in manus digits II-IV: 3, 4, 5 (0); reduced to three in digits III and IV (1); reduced to four in digit IV (2); reduced to three in digit III and four in digit IV (3).

284. [AToL 544]: Hyperphalangy in manus: absent (0); present in more than one digit (1); present only in digit 1 (2); present only in digit 5 (3). Bell (1997).

285. [AToL 546]. Penultimate phalanges in hand: shorter than or equal to antepenultimate (0); longer than antepenultimate (1).

286. [AToL 547]. Sesamoids dorsal to distal heads of penultimate phalanges (manus): (0) present; (1) absent.

287. [AToL 548]. Femur: present (0); absent (1). Lee (1998).

288. [AToL 549]. Femur: curved in dorsoventral plane (0); not curved in dorsoventral plane (1). Lee (1998).

289. [AToL 550]. Internal trochanter of femur: well-developed as a prominent, distinct head (0); poorly developed or absent (1). Estes et al. (1988).

290. [AToL 572]. Dermal skull bone ornamentation: smooth (0); lightly rugose about frontoparietal suture (1); present over dorsum (2); present on jugal postorbital bar (3). Estes et al. (1988).

291. [AToL 573]. Palpebral osteoderm below supraorbital scales (and their osteoderms): absent (0); present (1). Pregill et al. (1986).

292. Sclerotic ring, ossicles present and forming a ring (0) or absent (1). Kearney (2003: character 12); Longrich et al. (2012).

293. [AToL 586]. Interorbital septum: present (0); absent (1). Hallermann (1998).

294. Otooccipitals, vestibule and statolithic masses enlarged: absent (0); or present (1).

295. [AToL 590]. Tongue tip notching, as percentage of tongue length: no notch (0); less than 10% (1); 10-20% (2); 20-40% (3); >45% (4). Schwenk (1988).

296. [AToL 593]. Hindtongue epithelium: discrete papilla (filamentous or scale-like) (0); transverse plicae confined to lateral margins of posterior lobes (1); transverse plicae extend across hindtongue (2); and into the anterior half of the tongue (3). Schwenk (1988).

297. [AToL 602]. Tongue width across posterior notch/maximum tongue length: 50-60% (0); 40-44% (1); 30- 35% (2); 22-25% (3); less than 12% (4). Schwenk (1988).

298. [AToL 607]. Rectus abdominis muscles: not attached to belly skin (0); attached to hinges between ventral transverse scale rows (1). Bhullar (2009).

299. [AToL 608]. Ulnar nerve pathway: superficial to limb muscles (0); deep to limb muscles (1). (Jullien 1972).

300. Eyes, well-developed (0) or eyes and orbits highly reduced (1). Kearney (2003: character 10).

301. Eyelids, present (0) or absent, eyes covered by scale (1). Kearney (2003: character 11).

302. External ears present (0) absent (1). Kearney (2003: character 13).

303. Snout scale, polygonal (0) transversely expanded (1) dorsoventrally expanded (1).

304. Head scales, separate (0); or fused to form a dorsal shield (1).

305. Scales arranged in evenly-spaced rings around the body (annuli): absent (0); or present (1). Kearney (2003).

306. Pectoral scales similar in size to other scales (0); enlarged (1). Kearney (2003: character 4).

307. Tail long and tapered (0); fat and blunt (1).

308 (Novum). Where present, hypertrophied dentary tooth slightly to moderately larger than adjacent teeth (0), at least 60% longer (anteroposteriorly) than adjacent teeth (1).

309 (Novum). Enamel on tooth crowns thin (0); or thick (1).

Amongst available CT scans, only *Trogonophis wiegmanni* amongst extant taxa showed state 1. It would be worth studying *Oligodontosaurus* with CT scans, as the enamel caps are heavily diagenetically discolored, indicating something unusual might occur there.

310 (Novum). Premaxillary diastema, gap between median and first paired premaxillary teeth: (0) similar in size to gap between other marginal teeth, or (1) much larger than gap between other marginal teeth (diastema present).

References

Augé, M., Rage, J.-C., 2006. Herpetofaunas from the Upper Paleocene and Lower Eocene of Morocco. Annales de Paléontologie 92, 235–253.

Benton, M.J. 1984. The relationships and early evolution of the Diapsida. In). Symposia of the Zoological Society of London. Cambridge University Press, pp. 575–596.

Estes, R., de Queiroz, K., Gauthier, J., 1988. Phylogenetic relationships within Squamata. Phylogenetic relationships of the lizard families. Stanford University Press, pp. 119–281.

Etheridge, R., de Queiroz, K. 1988. Phylogeny of Iguanidae. In Estes, R. and Pregill, G. (Eds). Phylogenetic Relationships of the Lizard Families: Essays Commemorating Charles L. Camp. Stanford University Press, pp. 283–367.

Gauthier, J., Kearney, M., Maisano, J.A., Rieppel, O., Behlke, A., 2012. Assembling the squamate tree of life: perspectives from the phenotype and the fossil record. Bulletin Yale Peabody Museum 53, 3–308.

Gauthier, J.A., 1982. Fossil xenosaurid and anguid lizards from the early Eocene Wasatch Formation, southeast Wyoming, and a revision of Anguioidea. Contributions to Geology, University of Wyoming 21, 17–54.
Gauthier, J.A., Estes, R.D., de Queiroz, K. 1988. A phylogenetic analysis of Lepidosauromorpha. In Estes, R. and Pregill, G. (Eds). Phylogenetic Relationships of the Lizard Families: Essays Commemorating Charles L.Camp. Stanford University Press, pp. 15–98.
Grismer, L.L., 1988. Phylogeny, taxonomy, classification, and biogeography of eublepharid geckos. Phylogenetic relationships of the lizard families. Pp. 369–469.
Kearney, M., 2003. Systematics of the Amphisbaenia (Lepidosauria: Squamata) based on morphological evidence from Recent and fossil forms. Herpetological Monographs 17, 1–74.
Kluge, A.G., 1987. Cladistic relationships in the Gekkonoidea (Squamata, Sauria). Miscellaneous Publications of the Museum of Zoology, University of Michigan,173, 1–54.
Lang, M., 1991. Generic relationships within Cordyliformes (Reptilia: Squamata). Bulletin de l'Institut Royal des Sciences Naturelles de Belgique, Biologie 61,121–188.
Lee, M.S., 1997. The phylogeny of varanoid lizards and the affinities of snakes. Philosophical Transactions of the Royal Society of London B: Biological Sciences 352, 53–91.
Lee, M.S.Y., 1998. Convergent evolution and character correlation in burrowing reptiles: towards a resolution of squamate relationships. Biological Journal of the Linnean Society 65, 369–453.
Lee, M.S.Y., Scanlon, J.D., 2002. Snake phylogeny based on osteology, soft anatomy and ecology. Biological Reviews 77, 333–401.
Longrich, N.R., Bhullar, B.-A.S., Gauthier, J.A., 2012. A transitional snake from the Late Cretaceous Period of North America. Nature 488, 205–208.
Longrich, N.R., Vinther, J., Pyron, R.A., Pisani, D., Gauthier, J.A., 2015. Biogeography of worm lizards (Amphisbaenia) driven by end-Cretaceous mass extinction. Proceedings of the Royal Society B 282, 20143034.
Pregill, G.K., Gauthier, J.A., Greene, H.W., 1986. The evolution of helodermatid squamates, with description of a new taxon and an overview of Varanoidea. Transactions of the San Diego Society of Natural History 21, 167–202.
Presch, W., 1988. Phylogenetic relationships of the Scincomorpha. Phylogenetic relationships of the lizard families, pp. 471–492.
Rieppel, O., 1979a. The braincase of *Typhlops* and *Leptotyphlops* (Reptilia: Serpentes). Zoological Journal of the Linnean Society 65, 161–176.
Rieppel, O., 1979b. Classification of primitive snakes and the testability of phylogenetic theories. Biologisches Zentralblatt 98, 537–552.
Rieppel, O., 1980. The sound-transmitting apparatus in primitive snakes and its phylogenetic significance. Zoomorphology 96, 45–62.
Rieppel, O., 1981. The skull and the jaw adductor musculature in some burrowing scincomorph lizards of the genera *Acontias*, *Typhlosaurus* and *Feylinia*. Journal of Zoology 195, 493–528.
Rieppel, O., 1984a. The cranial morphology of the fossorial lizard genus *Dibamus* with a consideration of its phylogenetic relationships. Journal of Zoology 204, 289–327.

Rieppel, O. 1984b. Miniaturization of the lizard skull: its functional and evolutionary implications. In). Symposia of the Zoological Society of London 52, 503–520.
Rieppel, O., 1985. The recessus scalae tympani and its bearing on the classification of reptiles. Journal of Herpetology 19, 373–384.
Rieppel, O., Gauthier, J., Maisano, J., 2008. Comparative morphology of the dermal palate in squamate reptiles, with comments on phylogenetic implications. Zoological Journal of the Linnean Society 152, 131–152.
Smith, K.T., 2009a. Eocene lizards of the clade *Geiseltaliellus* from Messel and Geiseltal, Germany, and the early radiation of Iguanidae (Reptilia: Squamata). Bulletin of the Peabody Museum of Natural History 50, 219–306.
Smith, K.T., 2009b. A new lizard assemblage from the earliest Eocene (Zone Wa0) of the Bighorn Basin, Wyoming, USA: Biogeography during the warmest interval of the Cenozoic. Journal of Systematic Palaeontology 7, 299–358.
Tchernov, E., Rieppel, O., Zaher, H., Polcyn, M.J., Jacobs, L.L., 2000. A fossil snake with limbs. Science 287, 2010–2012.
Wu, X.-c., Brinkman, D.B., Russell, A.P., 1996. *Sineoamphisbaena hexatabularis*, an amphisbaenian (Diapsida: Squamata) from the Upper Cretaceous redbeds at Bayan Mandahu (Inner Mongolia, People's Republic of China), and comments on the phylogenetic relationships of the Amphisbaenia. Canadian Journal of Earth Sciences 33, 541–577.

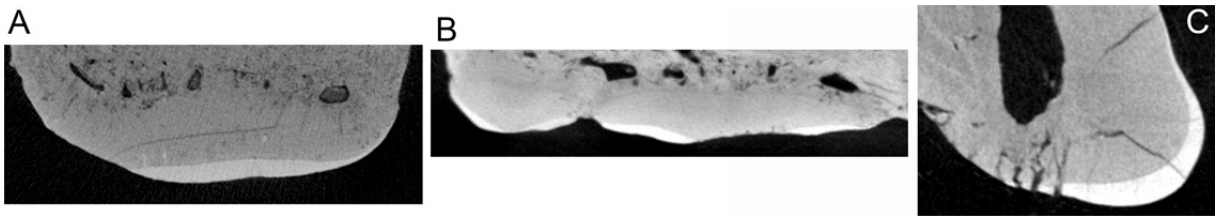

Figure S1. Additional examples of the enamel thickness in *Terastiodontosaurus marcelosanchezi* gen. et sp. nov.: (A) The largest tooth of the holotype maxilla ONM CBI-1-645; (B) Maxilla ONM CBI-1-649 (note also that in this specimen, there is part of the teeth with extreme thinness); (C) Premaxilla ONM CBI-1-711. Images not to the same scale.

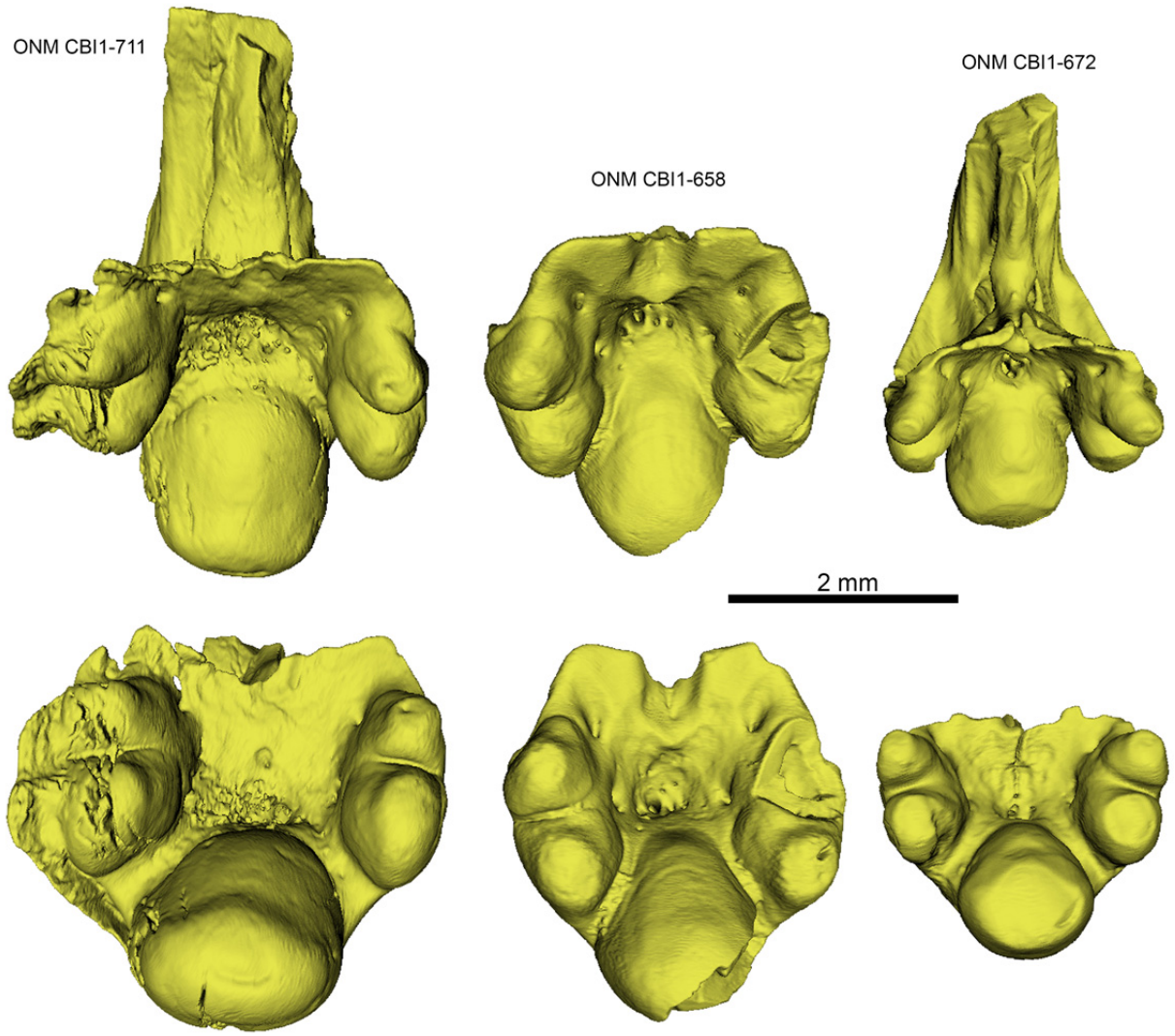

Figure S2. Size overview of three premaxillae of *Terastiodontosaurus marcelosanchezi* gen. et sp. nov. All specimens appear as 3D models and imaged in posterior view (upper row) and ventral view (lower row).

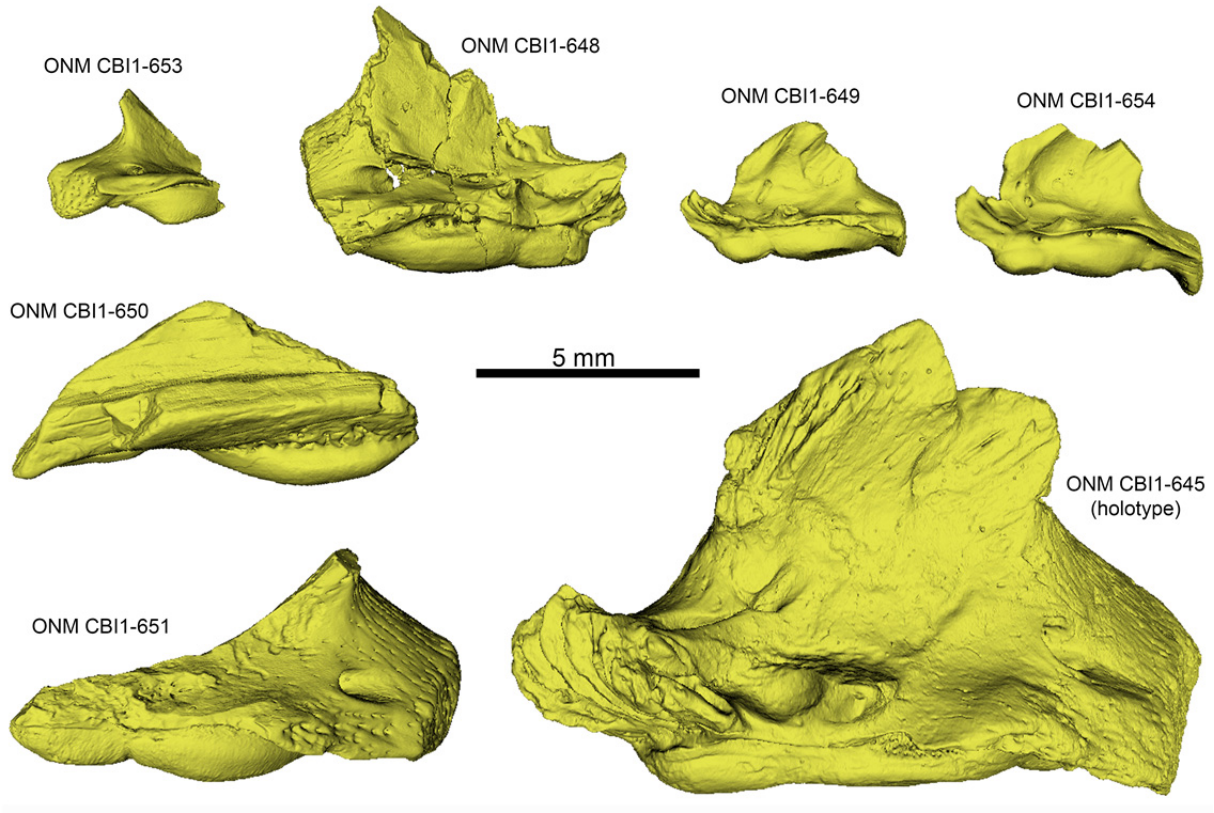

Figure S3. Size overview of various maxillae of *Terastiodontosaurus marcelosanchezi* gen. et sp. nov. All specimens appear as 3D models and imaged in medial view.

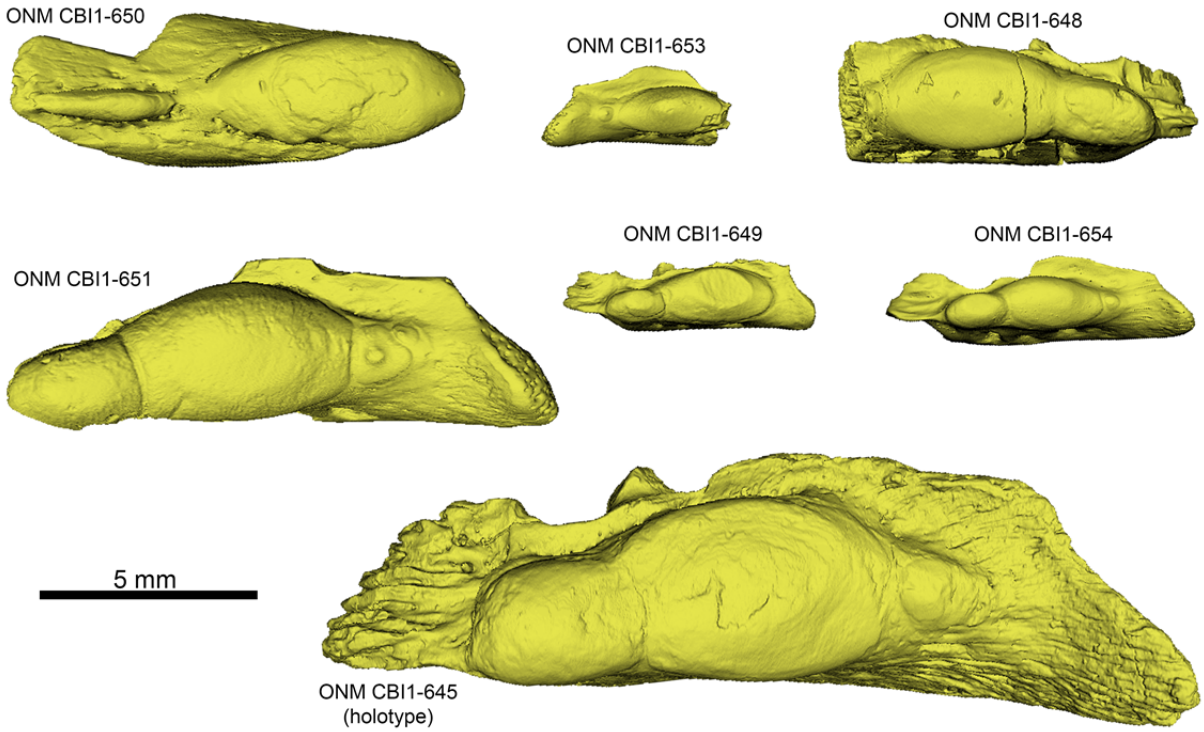

Figure S4. Size overview of various maxillae of *Terastiodontosaurus marcelosanchezi* gen. et sp. nov. All specimens appear as 3D models and imaged in ventral view.

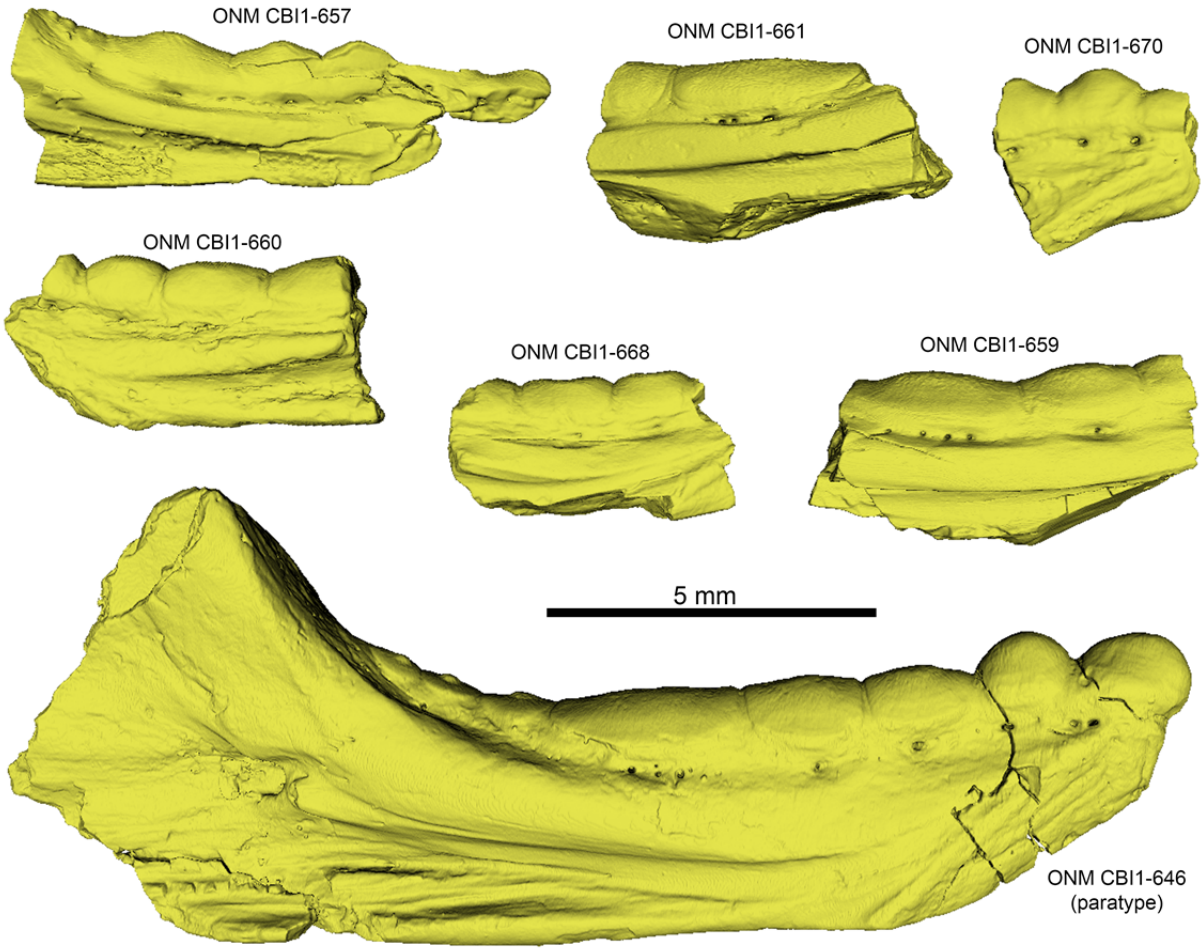

Figure S5. Size overview of various dentaries of *Terastiodontosaurus marcelosanchezi* gen. et sp. nov. All specimens appear as 3D models and imaged in medial view.

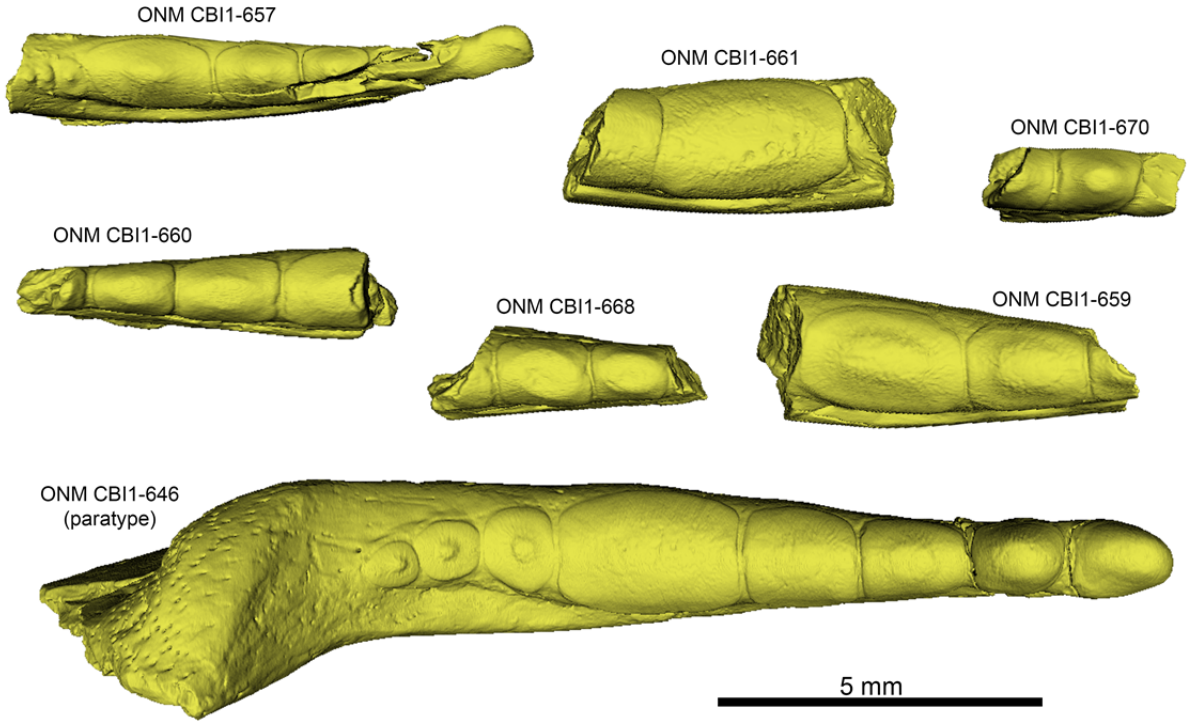

Figure S6. Size overview of various dentaries of *Terastiodontosaurus marcelosanchezi* gen. et sp. nov. All specimens appear as 3D models and imaged in dorsal view.

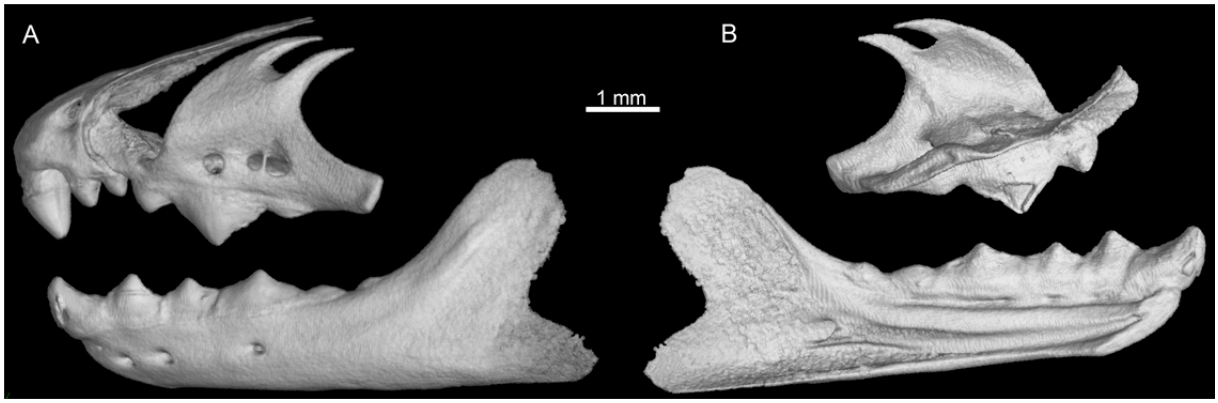

Figure S7. *Trogonophis wiegmanni* YPM HERR 6903. Premaxilla, left maxilla, and left mandible in labial (A) and medial (B) views.

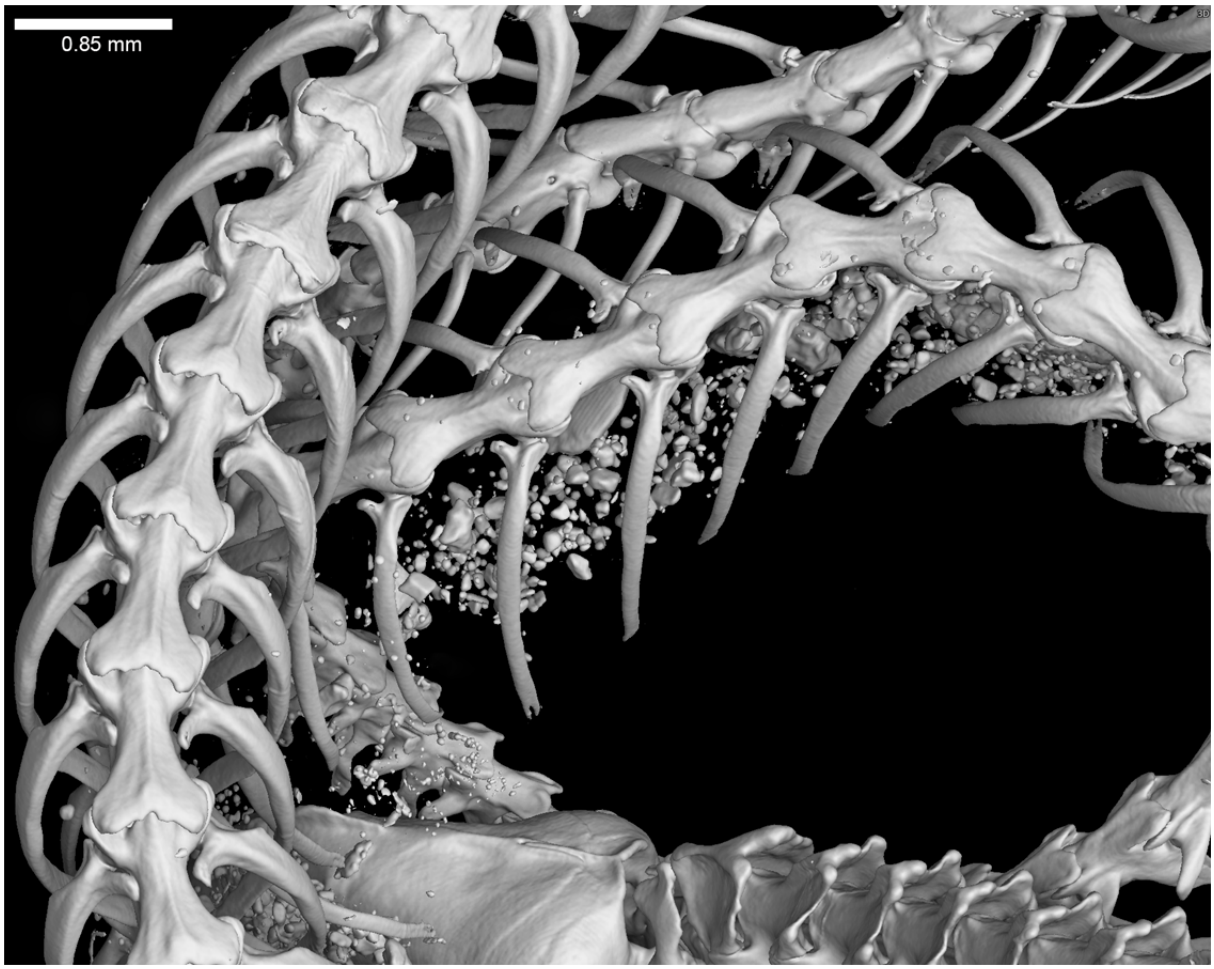

Figure S8. Vertebrae of the amphisbaenid *Geocalamus acutus* (collection of A.H. uncat.). The vertebral string seen on the left (with denticulation) is part from the front one-half of the trunk, while the next string seen on the right (without denticulation) is part from the posterior one-half of the trunk.